

The Institute of Paper Science and Technology

Atlanta, Georgia

Doctor's Dissertation

**The Influence of Hemicelluloses on the Structure
of Bacterial Cellulose**

Karin Ingegerd Uhlin

March, 1990

THE INFLUENCE OF HEMICELLULOSES ON THE STRUCTURE OF
BACTERIAL CELLULOSE

A thesis submitted by

Karin Ingegerd Uhlin

M.S. 1985, The Royal Institute of Technology

Stockholm, Sweden

in partial fulfillment of the requirements
for the degree of Doctor of Philosophy from
the Institute of Paper Science and Technology
Atlanta, Georgia

Publication rights reserved by the
Institute of Paper Science and Technology

March, 1990

TABLE OF CONTENTS

	Page
ABSTRACT	1
INTRODUCTION	3
BACKGROUND	6
<i>Acetobacter xylinum</i>	6
Disruption of bacterial cellulose aggregation	7
Sorption of hemicelluloses and gums by cellulose	10
Xyloglucans	10
Xylans	12
Glucomannans	13
Gums	14
Cellulose polymorphism and molecular conformations	14
Cellulose I and II	15
Hierarchical organization of cellulose structures	16
Analysis techniques for probing structural levels of cellulose	18
The significance of a β -(1 \rightarrow 4)-linked polysaccharide backbone for sorption	19
The additives used in this thesis and their relation to plant cell walls	19
Xyloglucan	19
Xylan	22
Mannan	23
Carboxymethyl cellulose (CMC)	23
Thesis objective	23
Experimental plan	24

MATERIALS AND METHODS	26
The additives tested for their influences on bacterial cellulose	26
Carboxymethyl cellulose	26
Xyloglucan	26
Mannan	27
Isolation and purification	27
Xylan	30
Strains of <i>Acetobacter xylinum</i>	31
Growth medium	31
Inoculation procedures and incubation conditions	32
Preliminary work on incubation conditions	32
Incubation solution for resting cells	33
Cellulose products from resting cells	34
pH of resting cell medium and binding of xyloglucan to cellulose	35
Celluloses produced in xyloglucan-salicin and xanthan gum	36
Alkaline extraction of cellulose products	37
X-ray diffraction	38
Profile fitting of x-ray diffractograms	38
Raman spectroscopy	39
Conformational component resolution of Raman spectra	40
Specimens for transmission electron microscopy	40
Micrograph enhancement in the image analyzer	42
RESULTS	44
Characterization of mannan	44
Characterization of xylan	45

Appearance of the cellulose products in the production vessels	46
Alkaline extraction of cellulose products	46
X-ray diffraction and profile fitting	47
Peak full widths at half maximum (FWHM)	48
Peak positions	51
Peak intensities	52
Raman spectroscopy	53
Visual comparison of band resolution	59
Conformational component resolution of Raman spectra	59
Transmission electron microscopy	61
Appearance of bacterial cellulose fibrils	61
Fibril width measurements with an image analyzer	65
DISCUSSION	69
Trends of similarities between modified bacterial celluloses and higher plant celluloses	69
Comparison of the x-ray diffraction results	69
Comparison of the Raman spectroscopy results	72
Comparison of the electron microscopy results	73
Ratio of cellulose I_{α} to I_{β} tertiary structures	74
Cellulose aggregation alterations related to the additive structures	75
Polymer chemistry of additive solutions	77
Effect of isolation procedures on the cellulose aggregation patterns	78
Additives used in this study and interactions in cell walls	82
Profile fitting of x-ray diffractograms	84
Raman bands at 1152 and 1506 cm^{-1}	85
CONCLUSIONS	87

RECOMMENDATIONS	89
ACKNOWLEDGEMENTS	90
LITERATURE CITED	92
APPENDIX A: Liquid state ^{13}C NMR spectra	97
APPENDIX B: X-ray diffractograms and profile fitting results	101
APPENDIX C: Raman spectra	110
APPENDIX D: Conformational component resolution of Raman spectra	116
APPENDIX E: Photomicrographs of bacterial cellulose ribbons	119

Figure page numbers

Figure number	Caption	Page number
1	Schematic representation of conformations k_I and k_{II}	17
2	Fitted x-ray diffractogram profiles of celluloses	49
3	The experimental diffractogram of xyloglucan-cellulose extracted with 1.0 N NaOH, the fitted total profile, background, and residual, and the fitted profiles of the four individual peaks	50
4	Raman spectrum of control cellulose after the extraction with 0.1 N NaOH	54
5	Raman spectrum of CMC-cellulose after the extraction with 0.1 N NaOH	55
6	Raman spectrum of mannan-cellulose after the extraction with 0.1 N NaOH	56
7	Raman spectrum of xylan-cellulose after the extraction with 0.1 N NaOH	57
8	Raman spectrum of xyloglucan-cellulose after the extraction with 0.1 N NaOH	58
9	Micrographs of control cellulose, no. 2480 and 2536	62
10	Micrographs of cellulose produced in CMC	62
11	Micrographs of cellulose produced in mannan	63
12	Micrographs of cellulose produced in xylan	63
13	Micrographs of cellulose produced in xyloglucan	64
14	Fibril widths of bacterial celluloses produced in the presence of xylan, xyloglucan, mannan, and CMC	68
15	X-ray diffractogram of cotton (CF1) cellulose	71
16	X-ray diffractogram of ramie cellulose	71
17	X-ray diffractograms of control cellulose after the last extraction and xylan-celluloses after each extraction step	80
18	Raman spectra of control cellulose after the last extraction and xylan-celluloses after each extraction step	81
19	^{13}C NMR spectrum of mannan	98
20	^{13}C NMR spectrum of xylan	100
21-25	X-ray diffractograms	102-6
26-28	Fitted peak widths, positions, and intensities	107-9
29-33	Raman spectra	111-5
34-38	Photomicrographs of bacterial celluloses	119-23

Table page numbers

Table number	Caption	Page number
1	Cellulose derivatives tested for alteration of bacterial cellulose	20
2	Other compounds tested for alteration of bacterial cellulose	20
3	Binding of polysaccharides and xyloglucan to pea cellulose	21
4	Chemical composition of xyloglucan	27
5	Carbohydrate composition of crude mannan (CM)	44
6	Carbohydrate composition of xylan	45
7	Weights of celluloses after alkaline extractions	47
8	Peak widths (2θ -degrees): bacterial celluloses produced in the absence or presence of additives, after extraction with 1.0 N NaOH	51
9	Peak positions (2θ -degrees): bacterial celluloses produced in the absence or presence of additives, after extraction with 1.0 N NaOH	52
10	Peak intensities and relative intensities: bacterial celluloses produced in the absence or presence of additives, after extraction with 1.0 N NaOH	53
11	Conformational components of bacterial celluloses produced in absence or presence of additives, after the extraction with 0.1 N NaOH	61
12	Fibril widths (nm) of bacterial celluloses produced in absence or presence of additives, at different concentrations (% w/v) of the additives in the growth medium	66
13	X-ray data for cotton (CF1) and ramie celluloses	70
14	^{13}C NMR spectrum of mannan	97
15	^{13}C NMR spectrum of xylan	99
16	X-ray diffractograms in Appendix B	101
17	Raman spectra in Appendix C	110
18	Conformational components of bacterial celluloses	118

ABSTRACT

One assumption implicit in much research on cellulose structure is that the crystal structure of higher-plant celluloses is the same as that of relatively pure celluloses. Another assumption is that treatments which are necessary to isolate celluloses from native material will not alter the cellulose structure. The purpose of this thesis was to investigate the impact of hemicellulose-like polysaccharides on the crystallinity and morphology of nascent cellulose fibrils while they were aggregating, and the impact of isolation procedures on the aggregation pattern of cellulose.

The approach was to build a model system of cellulose and hemicellulose. The bacterium *Acetobacter xylinum* was the source of cellulose. Carboxymethyl cellulose (CMC) and the hemicelluloses mannan, xylan, and xyloglucan were used as additives in the bacterial growth medium. The celluloses produced in the presence of additives were extracted with sodium hydroxide solutions of increasing concentrations to observe the effect of isolation on the cellulose structure. The alterations of cellulose aggregation were evaluated *via* x-ray diffraction, Raman spectroscopy, and transmission electron microscopy. The analyses were quantified by resolution of the x-ray diffractograms and Raman spectra, and by image analysis of the photomicrographs.

Cellulose I was produced by *A. xylinum* in the presence of all additives. Compared with control cellulose, celluloses produced with additives had decreased degree of crystallinity, smaller crystallites, lower degree of orientation, narrower fibrils, and changed dimensions of the crystal unit cells. The influences of xylan and xyloglucan were stronger than those of

mannan and CMC. The patterns of aggregation and fibril widths of the bacterial celluloses produced with xylan and xyloglucan resemble those found in celluloses from higher plants. Furthermore, comparisons of x-ray diffractograms and Raman spectra from the extraction stages indicated changes in the aggregation patterns induced by the isolation of the celluloses.

The major contributions from this study are the proposals that 1) matrix polysaccharides in the cell walls of higher plants influence the aggregation of cellulose; and 2) the aggregation pattern of cellulose is determined, in part, by the process for isolation of the cellulose.

INTRODUCTION

The structures of cellulose have been the subject of numerous investigations. However, several assumptions have been implicit in many of these studies. One common assumption is that the aggregation pattern of cellulose is not influenced by other cell wall components present when the cellulose is produced. Another assumption is that removal of noncellulosic material during the isolation of cellulose will not alter the structure of cellulose. The objectives of this thesis were to study the influence of hemicelluloses and of isolation procedures on the structure of bacterial cellulose.

Bacterial cellulose has been used frequently in cellulose studies as a substitute for celluloses from higher plants, in part due to its high purity and crystallinity and also because of the problems encountered in producing cellulose *in vitro* with plant enzyme preparations. In the first study of the modification of bacterial cellulose, Ben-Hayyim and Ohad¹ found that the presence of carboxymethyl cellulose could delay the aggregation of cellulose synthesized by *Acetobacter xylinum*. Haigler and Brown²⁻⁴ investigated the effect of a wide variety of polysaccharides and other compounds on the bacterial cellulose structure. These researchers found that the bacterial cellulose responded in a variety of ways, depending on the characteristics of the disrupting agent.

In another study of bacterial cellulose⁵, newly-formed bacterial cellulose could easily be modified, whereas the degree of transformation was much lower when the cellulose was more mature. This result indicates that

cellulose may be more susceptible to chemical or physical influences by other compounds when the cellulose is newly polymerized.

On the basis of such studies, the question was posed in the present investigation as to how celluloses in plant cell walls respond, in terms of changes in aggregation pattern and morphology, to other compounds present during deposition. In plant cell walls, hemicelluloses are deposited simultaneously with cellulose⁶, and, therefore, are the focus of this study.

The assumption that removal of noncellulosics has no influence on cellulose structures is based upon the belief that higher-plant native-cellulose structures are identical to those of highly purified celluloses produced by bacteria or manufactured commercially. This disregards the fact that most isolation methods involve extraction with strong acid or base. As Preston⁷ has written, "It had been shown ... that the removal from a cell wall of pectic substances, hemicelluloses and lignin had no effect upon the x-ray diagram of the wall (so long as the extraction procedures were not so severe as materially to degrade the cellulose) except for some sharpening of the arcs such as would indicate a small increase in crystallite size." Other studies have demonstrated that wood pulps prepared by different processes display subtle but consistent spectral and diffractometric differences.⁸⁻¹⁰ Such discrepancies led to the second objective for this investigation.

To challenge these two assumptions, the approach was taken in this study to use the cellulose-producing bacterium *A. xylinum* as a model system of cellulose biosynthesis in cell walls of higher plants, excluding lignin and similar wood components. In order to simulate the environment in plant cell walls, hemicelluloses or other compounds could be added to the growth medium

while the cellulose was synthesized and aggregated. The basis for this study was the hypothesis that, depending on properties of the hemicellulose, it could interact with the aggregation, and not with the polymerization, of bacterial cellulose. To observe the effect of isolation procedures on the cellulose structure, the celluloses produced in the presence of hemicelluloses were subjected to alkaline extractions as simplified representations of standard laboratory isolation procedures.

BACKGROUND

Acetobacter xylinum

Acetic acid bacteria of the genus *Acetobacter* are important organisms in industrial use as well as in research. They have been used for the production of vinegar from wine, and for the production of gluconic acid, ketogluconic acids, and sorbose. Glucose is a common substrate, but many other simple carbohydrates, alcohols, or polyalcohols can be used as carbon sources. The oxidative pathways in the acetic acid bacteria have been important models for biochemical studies of fermentation. The cellulose-producing species of these acetic acid bacteria have been useful in research on cellulose biogenesis.¹¹

Vinegar was produced for centuries by natural fermentation without the nature of the process being understood. Gradually it was realized that living organisms were involved. The first systematic studies of acetic acid fermentation were carried out by Pasteur.¹² Brown¹³ was among the first to recognize cellulose formation by *A. xylinum*.

All strains of *A. xylinum* produce cellulose extracellularly in the form of flat, twisting ribbons. Each cell produces one ribbon which is associated with the surface of the bacterial cell.^{14,15} The ribbon is assembled from fibrils, which themselves consist of a number of glucan chains. The fibrils are in close association with a longitudinal row of pores in the bacterial cell membrane.¹⁶ The cellulose-synthesizing multienzyme complexes are thought to be imbedded in the outer membranes of the cells where the glucan chains are assembled for extrusion through the pores in the cell wall. When *A. xylinum* is incubated in liquid medium, the ribbons intertwine to form a thick,

leathery pellicle at the air-liquid interface on top of the growth medium.

It is not clear why *A. xylinum* produces cellulose. The pellicle is suggested to function as a floating platform to position these obligately aerobic organisms near the air-liquid interface.¹⁷ The pellicles have been shown to provide protection against UV-light, and against other microorganisms competing for the same source of nutrition by enhancing colonization of *A. xylinum*.¹⁸ One speculation is that cellulose synthesis is a mechanism for mobility, since the force from the polymerization and crystallization actually propels the cell forward.^{15,19} The production of cellulose may, on the other hand, be a remnant of metabolism without any direct function.

DISRUPTION OF BACTERIAL CELLULOSE AGGREGATION

The research on disruption of the bacterial cellulose ribbon assembly is aimed at deepening the understanding of the formation of cellulose fibrils and ribbons. The focus has been primarily on the morphology, and not the aggregation, of the bacterial cellulose. The disruption has been induced by compounds of two types: 1. Fluorescent brightening agents and direct dyes, and 2. polysaccharides.

Fluorescent Brightening Agent 28 (FBA 28 or Calcofluor) and direct dyes are compounds used for the whitening and coloring of cellulosic material. The structures of these compounds are similar and the important characteristics of the molecules are the planar and linear configurations. The molecules contain between four and six aromatic rings substituted with hydrophilic groups to increase the water-solubility. FBA 28 and most other brighteners are based on a diaminostilbene skeleton, whereas the common feature in most direct dyes is

one or more azo (N=N) groups.^{20,21}

The presence of fluorescent brightening agents and direct dyes modified the morphology of the bacterial cellulose. When FBA 28 was present in the incubation medium of *A. xylinum*, the cellulose synthesized was in the form of a sheet of nonfibrillar cellulose, instead of the normal ribbon.^{2,3} At lower concentrations of FBA 28, a band with fibrillar substructure was produced. The brightening agents and dyes prevented crystallization of the cellulose, as shown by electron diffraction.²² Both the sheet and band products lacked crystal patterns, but cellulose I was recovered when the altered celluloses were washed free of disrupting agent. Kai²³ supported these results in an x-ray study. The presence of direct dyes resulted in the formation of cellulose products similar to those from FBA 28. The magnitude of the effect of each of the direct dyes depended on the degree of linearity and planarity of each of the respective molecules.

Carboxymethyl cellulose and other cellulose derivatives have also been reported to alter the assembly of the bacterial cellulose ribbon.^{1,4} The presence of CMC in the growth medium delayed the formation of visible aggregates of bacterial cellulose.¹ Instead of ribbons, bundles of separate intertwining fibrils were synthesized in the presence of CMC.⁴ The cellulose produced in the presence of CMC was crystalline, indicating that the influence of CMC on the bacterial cellulose is different than the influence of brightening agents and dyes. In addition to CMC, many other polysaccharides have been tested for their effects on ribbon assembly, including a xylan (isolated from larch or oats?), a pectin (probably from citrus fruit), and a yeast mannan.⁴ Of these additives, only xylan disrupted the ribbon assembly.

When the crystallization of bacterial cellulose is delayed or prevented in the presence of CMC or FBA 28, the rate of cellulose synthesis increases.^{1,24} The presence of CMC in the system increased the cellulose polymerization by about 30%.¹ The incorporation of ¹⁴C-labeled glucose into bacterial cellulose showed that the polymerization of cellulose was increased by 200-400% in the presence of FBA 28.²⁴ The degree of polymerization of FBA 28-altered cellulose was comparable to control cellulose, as measured by viscosity.²

The inhibition of the crystallization, but not the polymerization, of bacterial cellulose indicates that polymerization and crystallization are sequential processes separated in time. Furthermore, the kinetic studies referred to above suggest that the crystallization is the rate-limiting step. Haigler, Benziman, and Brown have proposed a model of hierarchical cell-directed self-assembly of the cellulose ribbon based on these results.^{19,24} In this model, brightening agents and dyes interact with the ribbon assembly earlier in the assembly process than the polysaccharides do.

The separation of cellulose polymerization and crystallization is also shown in a study by Kai and Koseki.⁵ *A. xylinum* was incubated for either 5 or 30 minutes and the cellulose was treated with sodium hydroxide solutions of different concentrations. When cellulose from the 5-minute incubation was extracted with 10^{-4} N alkali, electron diffraction revealed a crystallinity typical of cellulose I. When alkali solutions of higher concentrations (2.5×10^{-4} to 2.5×10^{-3} N) were used for extraction of products from the 5-minute incubation, a cellulose II crystallinity was detected and the conversion was estimated to be 50 to 100%. The report does not mention if any noncrystalline cellulose was present before or after the alkaline treatments.

When the cellulose from the 30-minute incubation was extracted with 1.15 N alkali, about 75% of the material showed cellulose I crystallinity and the remaining material showed cellulose II crystallinity. The reverse ratio of cellulose I and II material was obtained when 2.4 N alkali was used. Such an increased resistance to alkali with a prolonged period of incubation indicates that nascent material has weaker bonds but that the bond strength increases drastically during about 30 minutes, thereby supporting the idea of time-separated polymerization and crystallization of bacterial cellulose.

Recently, pea xyloglucan has been shown to disrupt the assembly of the bacterial cellulose ribbon.²⁵ Fibrils of cellulose synthesized in the presence of xyloglucan had a smaller diameter than the control fibrils. The interference of xyloglucan was suggested to be similar to that of CMC. The interference would be at a level in the assembly process where the fibril formation was not influenced and the further assembly of fibrils to a ribbon was prevented.

SORPTION OF HEMICELLULOSES AND GUMS BY CELLULOSE

To complement the discussion of associations with bacterial cellulose in the preceding section, sorption by plant celluloses will be examined here.

Xyloglucans

Hayashi *et al.*²⁵ studied the sorption of ¹²⁵I-labeled pea xyloglucan by pea cellulose. The xyloglucan used in the study had a molecular weight of 3.3×10^5 Daltons, determined *via* gel filtration. They found that sorption equilibrium was reached within four hours at 40°C, showing saturation at

approximately 5 μg xyloglucan per 100 μg cellulose (5% w/w). Sorption was inhibited above pH 6; 50% inhibition was observed at pH 7.

In a study by Valent and Albersheim²⁶, ^{14}C -labeled seven- and nine-sugar fragments of sycamore xyloglucan were sorbed by cellulose powder. This sorption was induced by using aqueous ethanol or acetone as the medium. Equilibrium-sorption was studied after 2.5 hr and determined from the amounts of xyloglucan remaining in the supernatants. Increasing the temperature caused a decrease in sorption. Changing the pH between 2 and 7 in 60-65% solvent had no effect on the sorption of the sugar fragments by the cellulose.

Seed xyloglucan sorption by cotton linters, at constant pH and temperature, was studied by Molinarolo at IPC.²⁷ The molecular weight of the xyloglucan was 1.6×10^6 Daltons as determined with gel filtration. By colorimetric analysis of the supernatants, it was determined that sorption equilibrium was reached after approximately 24 hr at 25°C. The xyloglucan was sorbed in monolayers, with a maximum specific sorption of 3.9 mg xyloglucan per gram of cotton (0.39%). The cotton linters had a hydrodynamic specific surface area of 1.06 m^2/g . The xyloglucan branches were thought to interfere with any association between xyloglucan molecules, whereas the xyloglucan backbone could associate with the cellulose molecules.

The sorption of narrower molecular weight fractions of xyloglucan were also measured in the same study.²⁷ These three fractions had molecular weights of 2×10^5 , 7×10^5 , and 1.9×10^6 Daltons. The effect of molecular weight on the maximum specific sorption was insignificant over the range investigated.

The experimental conditions for these three studies were very different

in terms of cellulose substrates, temperatures, xyloglucans, etc., making it difficult to compare the xyloglucan sorption behaviors. Hayashi *et al.*²⁵ showed that pea cellulose sorbed 3.3 times as much pea xyloglucan as cotton fibers did, explaining in part the differences in the sorption behaviors.

Xylans

Sorptions of xylans by cellulose substrates have been investigated by several authors.^{25,28-30} Walker²⁸ studied the influence of uronic acid content on cotton linter sorption by partially reducing a spruce 4-O-methyl-glucurono-arabinoxylan. The sorption of unreduced xylan was 9.1 mg per gram of cotton linters. A 40% and 60% reduction of the acids increased the sorption to 12.0 and 16.1 mg xylan per gram of linters, respectively. The cotton linters had a specific surface of 1.3 m²/g. Clayton and Phelps²⁹ investigated the rate of sorption of birch xylan on α -cellulose (see also the next section about sorption of mannan). Both authors concluded that even a small number of uronic acid groups present on the xylan would reduce the sorption by cellulose.

In a study by Mora *et al.*³⁰, xylan was sorbed by a beaten kraft birch pulp and a reed cellulose. Gold-enzyme labeling of the native xylans showed an even distribution as a thin layer along the cellulose fibril, whereas the redeposited xylan had formed heavily labeled clusters. The association between xylan molecules was preferred over the cellulose-xylan association.

Hayashi *et al.*²⁵ compared the affinities of xylan and xyloglucan for cellulose. The presence of a larch xylan (in a 10-fold excess over xyloglucan) decreased the sorption of pea xyloglucan by a pea cellulose by

about 50%.

Glucomannans

In two early studies^{29,31}, mixtures of glucomannans and xylans were sorbed by cellulose. Most³¹ used four ¹⁴C-labeled fractions of slash pine for sorption by α -cellulose. Each fraction was a mixture of glucomannans and xylans. Sorption equilibrium was not reached within 10 days and the sorption was considered irreversible. The fractions with increased sorption rates had higher contents of mannose, lower uronic acid contents, and higher molecular weights. Clayton and Phelps²⁹ sorbed a ¹⁴C-labeled spruce glucomannan and a tritium-labeled birch xylan upon an α -cellulose, both individually and in a mixture. In both cases, the glucomannan was about twice as readily sorbed as the xylan, in spite of lower degree of polymerization and conformational similarity of the xylan chain with cellulose. In a mixture, the hemicelluloses competed for the sorption sites and the rate of sorption of both hemicelluloses was reduced.

The influence of acetyl groups on glucomannan sorbed by cotton linters was studied by Laffend and Swanson.³² A reserve form of acetylated glucomannan was isolated from orchid bulb flour, enzymatically degraded to the molecular weight of a pine glucomannan, and sorbed by cotton linters. The removal of the acetyl groups led to a decreased water-solubility, a higher rate of sorption, an earlier mass equilibrium, and a higher specific sorption. Monolayer sorption was theorized for the acetylated glucomannan with a maximal specific sorption of 7.5%. Deacetylated glucomannan, on the other hand, sorbed in ever-increasing amounts as its initial concentration was increased.

Gums

The sorption of gums by cellulose has been studied extensively because of their importance as beater additives and strength enhancers in papermaking. Russo and Thode³³ investigated the sorption of locust bean gum (a galactomannan, with a ratio of galactose to mannose of approximately 1:4) by a bleached sulfite pulp. The influence of the mannose-to-galactose ratio was studied by Dugal and Swanson³⁴ using a modified guar gum sorbed by a cotton comber pulp. Increasing the mannose-to-galactose ratio from an initial 1.49 to 2.82 improved the fiber bonding. Going beyond this optimum mannose-to-galactose ratio did not increase the strength properties and actually decreased them in some cases.

In summary, the sorption of hemicelluloses and gums by cellulose is a multifaceted and complex association. The amount sorbed and the sorption behavior of a polymer depend on parameters such as the polymer composition (including branching pattern, size, and functional groups), the adsorbent (e.g., surface area and charge), the solubility in the selected solvent, and the temperature.

CELLULOSE POLYMORPHISM AND MOLECULAR CONFORMATIONS

Cellulose has been known for a long time to appear in four polymorphs which are distinguishable by their different x-ray diffractogram patterns. The best characterized forms are cellulose I, or crystalline native cellulose, and cellulose II which can be produced from native cellulose by treatment with alkali. The two other polymorphs are cellulose III and cellulose IV.

Cellulose I and II

In the classical hypothesis of the structures of cellulose polymorphs, the major difference between cellulose I and II is a difference in polarity of the cellulose chains. The backbone conformations of the chains themselves are essentially identical. Cellulose I has parallel chains whereas cellulose II has alternating antiparallel chains. Evidence for the classical hypothesis is taken mainly from studies using x-ray diffraction followed by calculations of packing energies and conformations.³⁵⁻³⁸ Other authors claim that the complexity of the cellulose molecule and the relatively small number of reflections in a diffraction pattern make it inappropriate to solve the structures of cellulose based solely on x-ray diffraction data.^{39,40} In a comparison of different conformation models, the conclusions regarding one packing mode or another depend on the set of diffraction data used.⁴¹ By using more flexible constraints for the calculations, the conformation of cellulose II has been refined to a parallel chain model.⁴²

Another hypothesis was developed when spectroscopy became more widely used for cellulose characterizations. The techniques used are infrared and Raman spectroscopy and solid state ^{13}C nuclear magnetic resonance spectroscopy enhanced with cross-polarization and magic angle spinning (CP/MAS). Additional information from these techniques indicated that conformational differences of the heavy atoms carbon and oxygen in the cellulose chains are responsible for the cellulose I and II polymorphs. Atalla⁴³ concluded from Raman spectra, in combination with potential energy calculations, that only two stable conformations were allowed. More than one stable pattern of intermolecular hydrogen bonding has been found to be consistent with each conformation.⁴⁴

Hierarchical organization of cellulose structures

Atalla^{8,45} has proposed a hierarchical organization of cellulose structures, with different levels related to each other. The primary level of organization is the chemical pattern of covalent bonds, in this case β -(1 \rightarrow 4)-linked anhydroglucose units. The conformation of the anhydroglucose chains in space is the secondary level of organization. In the cellulose molecule, this level includes variations in the position of the C6 primary alcohol group, in the dihedral angles defining the glycosidic linkages, and in the internal dihedral angles defining the conformation of the pyranose rings. The arrangement of the glucan chains relative to each other is described by the tertiary level of organization. The divisions between the levels are not absolute because of an interdependence: the packing of chains depends on the shape of individual chain molecules, and the forces of intermolecular interactions determine in part the equilibrium conformation of individual chains.

The two conformations of crystalline cellulose deduced from Raman spectroscopy and energy calculations are examples of structures on the secondary level of organization. They are called k_I and k_{II} after their predominance in cellulose I and II, respectively.⁹ The corresponding form for the disordered portion of cellulose is represented by k_0 . Figure 1 shows schematics of the conformations proposed for k_I and k_{II} . The key difference between the conformations k_I and k_{II} is the presence in k_I of a bifurcated intramolecular hydrogen bond associated with every other glucosidic bond in addition to a simple hydrogen bond. k_{II} in contrast, has two simple hydrogen bonds per dimer.¹⁰ A corollary to this model is that adjacent anhydroglucose units are nonequivalent, and, thus, that the anhydrocellobiose is the

repeating unit in cellulose.

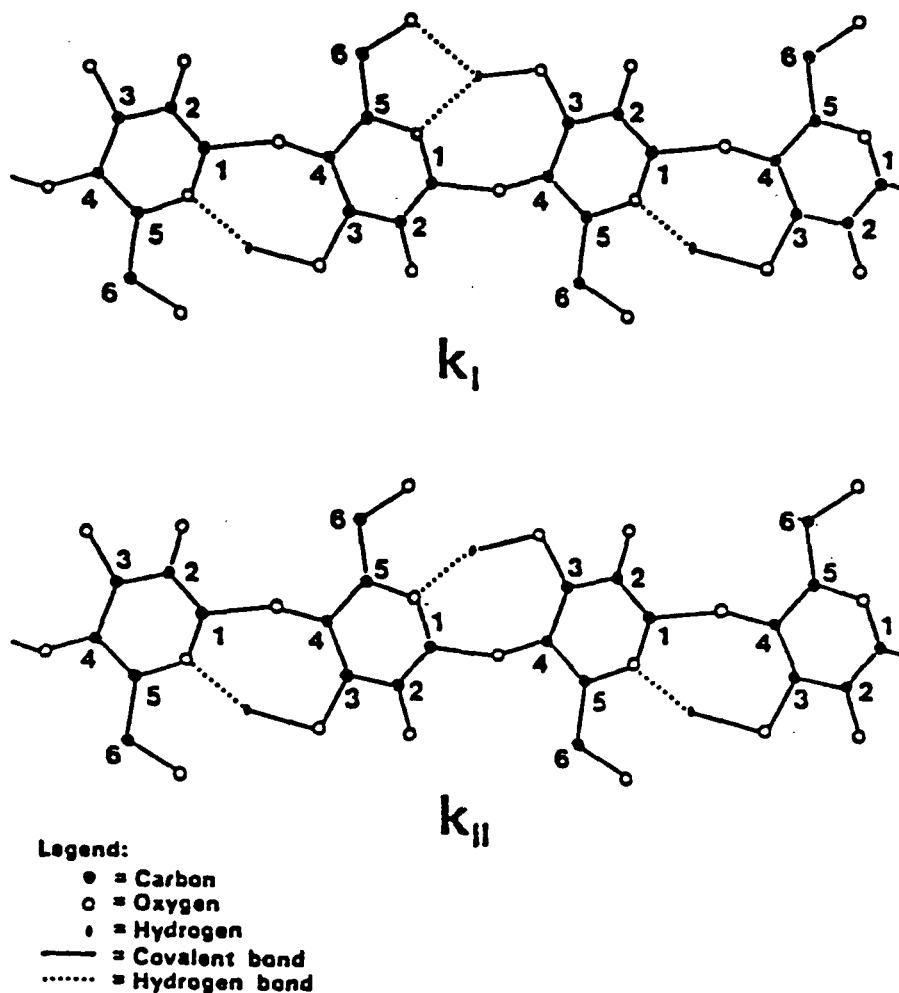


Figure 1. Schematic representation of conformations k_I and k_{II} (from reference 10).

In an early investigation of native celluloses from a variety of sources, it was found that the infrared spectra from algal and bacterial celluloses differed from those of regenerated (from cellulose III_I), ramie, and cotton celluloses.⁴⁶ Solid state ¹³C NMR has been used more recently for a

closer investigation of celluloses from these sources.^{47,48} Based on the NMR-studies, native celluloses are proposed to be composites of two distinct crystalline forms, I_α and I_β . These forms are examples of structures on the tertiary level. The two forms of cellulose I crystallinity have different intermolecular hydrogen bonding patterns, but the conformations of the heavy atoms are similar. The crystalline component of every native cellulose studied was a mixture of these two forms, but I_α was predominant in celluloses from bacteria and noncharophycean algae, and I_β was the major form in higher plant celluloses. Celluloses rich in I_α that have been subjected to acid hydrolysis¹⁰, steam annealing⁴⁹, or solid-state chemical transformation have a crystalline structure similar to the I_β -type, indicating that the I_β form is more stable or more resistant than the I_α form. Cellulose triacetate⁵⁰ and cellulose III_I⁵¹ were the intermediates in these solid-state transformations.

In a study of the solubility of celluloses in an amine-based solvent, it was found that mercerized cellulose (cellulose II) dissolved in this solvent, but regenerated cellulose II did not. The x-ray diffractogram patterns of the mercerized and regenerated celluloses indicated that the heavy atom lattices were similar, if not the same. It was suggested that the patterns of intermolecular hydrogen bonding are different in these two forms of cellulose II, similar to the crystalline cellulose forms I_α and I_β .⁴⁴

Analysis techniques for probing structural levels of cellulose.

Raman spectroscopy is primarily sensitive to the vibrations of the skeleton in the cellulose molecule and less sensitive to the packing of the molecules in a three-dimensional lattice. Raman spectroscopy is therefore a useful technique for probing the secondary level of organization. In

contrast, solid state ^{13}C NMR probes both the secondary level and the tertiary level. Measurements using high resolution enhancements of NMR are sensitive both to conformation of the molecules and to sites which are nonequivalent within the repeating unit of the molecule. X-ray and electron diffraction techniques are most sensitive to regularity in three dimensional lattices, and, therefore, probe at the tertiary level of structural organization.

THE SIGNIFICANCE OF A β -(1 \rightarrow 4)-LINKED POLYSACCHARIDE BACKBONE FOR SORPTION

The association between cellulose and polysaccharides with different backbone configurations has been tested in two studies.^{4,25} Tables 1 and 2 show the results of incubating bacterial cellulose in the presence of cellulose derivatives and other compounds. Of the bond types and configurations studied, only the polysaccharides with a β -(1 \rightarrow 4)-linked backbone are capable of disrupting the cellulose ribbon assembly. Hayashi *et al.*²⁵ studied the sorption of radioiodinated pea xyloglucan onto pea cellulose in the presence of a 10-fold excess of a variety of other polysaccharides. Only a xylan with a β -(1 \rightarrow 4)-linked backbone competed with the xyloglucan for the sorption sites, thereby decreasing the sorption of the xyloglucan (Table 3). The special backbone linkage was not the unique feature of the xylan in this study; it was also the only pentosan, and, together with pectin, the only polysaccharide with uronic acids.⁵²

THE ADDITIVES USED IN THIS THESIS AND THEIR RELATION TO PLANT CELL WALLS

Xyloglucan

Xyloglucans are found in immature and storage tissues in many plant

Table 1. Cellulose derivatives tested for alteration of bacterial cellulose.⁴

Additive	Source	Structural feature	Effect
carboxymethyl methyl	1 2	β -(1 \rightarrow 4)-, R=-CH ₂ COOH β -(1 \rightarrow 4)-, R=-CH ₃	loose coils of fibrils occasionally splayed, coherent but no twist
hydroxy-propylmethyl	2	β -(1 \rightarrow 4)-, R=-CH ₃ , -CH ₂ CH(CH ₃)OCH ₃ , or -CH ₂ CH(OH)CH ₃	coherent but no twist, occasionally splayed
hydroxyethyl	1	β -(1 \rightarrow 4)-, R=-CH ₂ CH ₂ OH or -CH ₂ CH ₂ OCH ₂ CH ₂ OH	coherent but no twist, or no alteration
hydroxypropyl	1	β -(1 \rightarrow 4)-, R=-CH ₂ CH(OH)CH ₃ or -CH ₂ CH(CH ₃)OCH ₂ CH(OH)CH ₃	no alteration, or co- herent but no twist

Sources: (1) Hercules Inc., Wilmington, DE; (2) Dow Chemical Co., Indianapolis, IN.

Table 2. Other compounds tested for alteration of bacterial cellulose.⁴

Additive	Source	Structural feature	Effect
xanthan gum	1	β -(1 \rightarrow 4)-, R=-6-O-Ac-Manp-(2,4)-GluA- β -(1 \rightarrow 4)-Manp-2,4-Pyruvate	no alteration
cellobiose	2	β -(1 \rightarrow 4)-Glup	coherent no twist, or no alteration
xylan	2	β -(1 \rightarrow 4)-Xylp	highly splayed fibrils
pectin	2	α -(1 \rightarrow 4)-GalA	slight alteration
starch	2	α -(1 \rightarrow 4)-Glup	no alteration
laminarin	2	β -(1 \rightarrow 3)-Glup	no alteration
mannan	2	α -(1 \rightarrow 6)-Manp	slight alteration
agar	3	alternating α -(1 \rightarrow 3)- and β -(1 \rightarrow 4)-bonds, >3 sulfated D/L galactans	no alteration
PEG	4	H(OCH ₂ CH ₂) _n OH	normal ribbons and bent and fractured ribbons
glycerol	-	HOCH ₂ CHOHCH ₂ OH	no alteration

Sources: (1) Kelco Div., Merck & Co., Clark, NJ; (2) Sigma Chem. Co., St. Louis, MO; (3) Wilson Diagnostics; (4) Fischer Scientific.

Table 3. Competitive binding of polysaccharides and xyloglucan to pea cellulose.²⁵

Additional polysaccharide	Relative binding activity of xyloglucan	Structural feature of other polysaccharide
None (only XG)	100%	-
Bacterial glucan	103%	β -(1 \rightarrow 2)-Glup
Laminarin	99%	β -(1 \rightarrow 3)-Glup
Pachyman	101%	β -(1 \rightarrow 3)-Glup
Pustulan	99%	β -(1 \rightarrow 6)-Glup
Lichenan	92%	mixed β -(1 \rightarrow 3)- and β -(1 \rightarrow 4)-Glup
Xylan	47%	β -(1 \rightarrow 4)-Xylp
Arabinogalactan	107%	β -(1 \rightarrow 3)-Galp
Pectin	108%	α -(1 \rightarrow 4)-GalA

species. Two different kinds of xyloglucans have been identified, those from seed walls and those from primary cell walls.

The seed xyloglucans function as reserve food for developing seeds and occur in large amounts (40-50%). They are generally easily isolated. Xyloglucans from different seed sources have similar repeating patterns and sugar composition. The repeating units are often hepta- to decasaccharides. D-glucose, D-xylose and D-galactose are the common sugars. Xyloglucan from seeds of tamarind (*Tamarindus indica*) has the sugar composition glucose, xylose, and galactose 4:3:1. The xyloglucan backbone is a β -(1 \rightarrow 4)-linked glucan substituted in the sixth position with α -xylose, either singly or with terminal galactose residues, linked β -(1 \rightarrow 2)- to the xylose.⁵³ The xyloglucan used in this thesis was isolated from tamarind seeds.

The other group of xyloglucans has been isolated from primary cell walls

of young plants. The levels of xyloglucan in primary walls are comparable to those of cellulose.⁵⁴ In contrast to the seed xyloglucans, the xyloglucans from cell walls are very hard to isolate; strong acid or alkali is required. Typical sources include pea stem⁵⁵, cotton⁵⁶, and suspension cultured cells of sycamore⁵⁷ and loblolly pine⁵⁸. Such cell-wall xyloglucans often contain terminal fucose units on the side chains in addition to glucose, xylose and galactose.

Much research has been devoted to understanding the functions of xyloglucan in cell walls. Xyloglucan is thought to be involved in the cell wall expansion necessary for cell growth.⁵⁹ It has been speculated that oligosaccharides from xyloglucan, especially a nonasaccharide, have biological activity.⁶⁰

Xylan

Angiosperms contain glucuronoxylan as the major hemicellulose (15-30% of dry wood). The bulk of the xylan is present in the secondary cell walls.⁶¹ The backbone of β -(1 \rightarrow 4)-xylose units has side chains of methylglucuronic acid units or acetyl groups. In birch, the unit next to the reducing xylose end group is a galacturonic acid, which is linked to a α -L-rhamnose, which, in turn, is connected to the xylan chain. Birch was the source for the xylan used in this thesis.

In gymnosperms, xylan constitutes 5-10% of the wood.⁶² It is similar to the xylan in angiosperms, but the xylan backbone is also substituted with α -L-arabino units. The xylan content is lowest in the middle layer of the secondary wall (S_2) and higher in the S_1 and S_3 layers.

Mannan

Mannans occur in gymnosperms in the form of a galactoglucomannan which constitutes about 20% of the wood. It has a main chain of alternating D-mannose and D-glucose units and side chains of D-galactose units and O-acetyl groups. Mannose-containing hemicelluloses are concentrated in the middle layer of the secondary cell wall.⁶³ Angiosperms are composed of 2-5% of β -(1 \rightarrow 4)-glucomannan.⁶²

Mannan homopolymers can be found in seeds such as ivory nut, which was the source of the mannan used in this thesis. The main chain is β -(1 \rightarrow 4)-linked mannose units substituted with galactose units.⁶⁴ There are indications that glucose is incorporated in the main chain and that some mannose units are α -linked.⁶⁵ A few (1 \rightarrow 6)-linkages presumably are also present.⁶⁶

Carboxymethyl cellulose (CMC)

CMC or cellulose gum is not a natural product of plants. It is an anionic, water-soluble cellulose carboxymethyl ether, produced by the reaction of alkali cellulose with sodium monochloroacetate.⁶⁷

THESIS OBJECTIVE

The main objective for this study was to qualitatively investigate the influence of β -(1 \rightarrow 4)-linked hemicellulose-like polysaccharides on the structure of cellulose synthesized by *Acetobacter xylinum*. The second objective was to investigate the influence of isolation procedures on the bacterial cellulose produced in the presence of these additives.

The objective was to study the influence on cellulose structure during the early stage of cellulose aggregation. The bacterium *Acetobacter xylinum*, rather than plant cells, was the producer of the cellulose, creating a model system of the cellulose biogenesis in plants which excluded lignin and other wood components. A plant cell-wall environment was simulated by having a hemicellulose present in the medium while the bacterial cellulose was synthesized and aggregated. The hemicellulose-like polysaccharides investigated were mannan, xylan, and xyloglucan. Carboxymethyl cellulose, a cellulose derivative, was included in this investigation to correlate this study with work previously reported in the literature.

The investigation was based on the hypothesis that the presence of hemicelluloses influences the aggregation, but not the polymerization, of cellulose. The mode of interaction depends on properties of the hemicellulose, such as chain length, branching, and electrical charges. The effects on aggregation may be expressed as changes in degree and nature of crystallinity, backbone conformation, and/or morphology. The anticipated alterations of the cellulose structure were evaluated via x-ray diffraction, Raman spectroscopy, and electron microscopy.

EXPERIMENTAL PLAN

The experimental work of this thesis consisted of three parts. The first part involved the discovery and preparation of suitable water-soluble polysaccharides for use as additives. It was essential that the additives were completely water-soluble to control the conditions for the aggregation of cellulose. A low molecular-weight fraction of mannan was isolated from ivory nut. Water-soluble xylan was prepared from a previously isolated birch xylan.

Carboxymethyl cellulose and xyloglucan were obtained in water-soluble forms.

In the second part of the experimental work, bulk samples of cellulose were produced in the presence of an additive. A method with resting nondividing cells was employed to prepare the cellulose bulk samples. The medium was stirred gently during incubation, allowing the additive to be mixed homogeneously. The cellulose-additive products were subjected to a series of alkali extractions to get an estimate of the strength of the association between the cellulose and additive. The second purpose of the series of extractions was to investigate the influence of isolation on the structure of cellulose. The cellulose samples were evaluated with x-ray diffraction and Raman spectroscopy. Profile fitting and conformational component resolution were performed on the diffractograms and Raman spectra, respectively, to further quantify the results.

The influence of the additives on the morphology of cellulose fibrils was investigated in the final part of the work. Specimens for transmission electron microscopy were prepared from bacterial cellulose fibrils produced in the presence of an additive. The dimensions of the fibrils were measured with the help of an image analyzer.

MATERIALS AND METHODS

THE ADDITIVES TESTED FOR THEIR INFLUENCES ON BACTERIAL CELLULOSE

In the routine experiments, the additives tested for their influences on bacterial cellulose were CMC, xyloglucan, mannan, and xylan. Each additive will be described in further detail in the following sections. In addition, xanthan gum and salicin were used in two experiments.

CARBOXYMETHYL CELLULOSE

Carboxymethyl cellulose (CMC) was of the purest food grade (7MF) supplied by Hercules, Inc. It was completely water-soluble and was used without further purification. The degree of polymerization was approximately 500, the molecular weight was 10^5 , and the degree of substitution was 0.65-0.85.⁶⁷ X-ray diffraction of CMC gave an amorphous pattern.

XYLOGLUCAN

Xyloglucan was kindly provided by Dr. S.L. Molinarolo.²⁷ The xyloglucan had been isolated from Tamarind seeds (*Tamarindus indica*) by hot-water extraction, and extensively characterized.

The molecular weight of the xyloglucan was determined to be 1.6×10^6 by size exclusion chromatography. Characterization of the xyloglucan identified 97% of the components (Table 4). Acetate and pyruvate groups could not be detected in the xyloglucan but the methoxyl content was 0.44%. X-ray diffraction showed the xyloglucan to be amorphous.

Table 4. Chemical composition of xyloglucan.²⁷

Nitrogen, %	<0.1
Carbohydrate Analysis, %	
Glucose	49.8
Galactose	15.4
Mannose	1.5
Xylose	28.8
Arabinose	1.4

Total carbohydrate, %	96.9
Ash, %	0.2

MANNAN

Finely ground ivory nut (*Phytelephas macrocarpa*) was obtained from Mr. J. Becher at IPC. A water-soluble fraction of mannan was isolated according to the following procedure.^{68,69}

Isolation and purification

The ivory nut flour (165 g) was extracted with chloroform-methanol (1:1, 2000 ml) in a Soxhlet apparatus for 12 hours. The extracted residue was air dried overnight. Repeated extractions yielded 159-163 g (96-99%).

Extracted ivory nut flour was bleached by adding the flour (56 or 100 g) to a warm (30°C) solution of sodium chlorite in water (250 g NaClO₂ in 2500 ml H₂O was used for 100 g nut flour). The temperature was raised to 35°C and glacial acetic acid (250 ml for 100 g nut flour) was added. The reaction flask was placed in a 30°C water bath for 24 hours. The bleached ivory nut flour was collected by centrifugation at low speed, and filtration of the

supernatants on a fine sintered-glass funnel. The solid phase was washed with water on the funnel until free from yellow liquor and then washed with methanol. The bleached ivory nut flour was dried *in vacuo* at 40°C to yield 51 g (91%) or 87-89 g (87-89%), respectively, of a white solid.

The filtrate of acid-chlorite liquor was decomposed before it was discarded, in order to reduce the odor of ClO_2 in the liquor. Aqueous sodium hydroxide solution was kept in the filtration flask to neutralize the chlorite liquor after it was separated from the bleached ivory nut flour.

Alkaline extraction of the ivory nut flour was the next step in the isolation procedure. The bleached flour (35 g) was placed in a solution of sodium hydroxide (700 g of 6.0% NaOH) and nitrogen gas was bubbled through the mixture for 30 minutes. The mixture was stored under refrigeration ($3\pm 1^\circ\text{C}$) for three days and was shaken occasionally. The mixture was centrifuged and the supernatants were filtered through a fine sintered-glass filter. The solids were washed three times with water by dispersing the pellets in distilled water (400-500 ml), centrifuging, and filtering, before the solid residue was discarded. The mannan was precipitated by adding four volumes of ethanol to the alkali filtrate and the three wash-waters. The precipitates were settled overnight at $3\pm 1^\circ\text{C}$ and were collected by filtration the next day (giving PEt1).

The combined precipitates (PEt1) were extracted four times with water and the mannan was again precipitated from the water with ethanol (added ethanol in four times the volume). The precipitates were settled overnight at $3\pm 1^\circ\text{C}$ and were collected by filtration the next day (giving PEt2). The precipitates were collected by filtration and extracted four times with water.

The water-extracts were combined and neutralized with ion exchange resin (Aldrich Amberlite IR 120+ washed with distilled water until no further change of pH), and freeze-dried to yield a white fluffy material (UnFCM). A portion of this material (UnFCM) was again fractionated by dispersing it in water and centrifuging. The supernatants were filtered through a fine sintered-glass funnel, and Millipore filters with 1.2 μm and 0.8 μm pore sizes. The filtrate was freeze-dried to yield crude mannan (CM) (3.7 g).

Salts were removed from the crude mannan (CM) by ultrafiltration. Portions of the crude mannan were dissolved in distilled water, and placed in an ultrafiltration cell of 200 or 400 ml volume. A membrane with molecular-weight cut-off of 500 was used (Amicon, YC05), and the cell was pressurized with nitrogen gas to 55 psi. The inorganic material and the smallest mannan oligomers were filtered through the membrane, leaving behind the higher oligomers of mannan in the cell. The filtration was continued until the conductivity of the filtrate had stabilized. This took approximately six days. The fraction retained in the cell was filtered through a fine sintered-glass funnel and Millipore filters with 1.2 μm and 0.8 μm pore sizes, and the filtrate was freeze-dried. The mannan was dissolved in water, centrifuged at 11,900g for 60 minutes, and freeze-dried to yield a water-soluble mannan (WSM1).

Another method for desalting the mannan was tested with improved results. (However, this method was not employed for the mannan added to the bacterial growth medium.) The crude mannan (CM) was extracted four times with aqueous ethanol (76%) and the ethanol was separated by centrifugation. The mannan pellets were dispersed in water, and the residual ethanol was removed *in vacuo*. The precipitate was separated by centrifugation, and the

supernatants were freeze-dried. The mannan was dissolved in distilled water and additional salts were removed by ultrafiltration for 1.5 days. The retained fraction was filtered through a fine sintered-glass funnel and Millipore filters with 1.2 μm and 0.8 μm pore sizes, and the filtrate was freeze-dried. The mannan was again dissolved, centrifuged at 26,800g for 60 minutes, and the supernatant was freeze-dried, yielding a water-soluble fraction of mannan as a white fluffy material (WSM2). The advantage of this second method of desalting was the time saved in the ultrafiltration step. Another advantage of the shorter dwell time was the decreased risk for contamination during ultrafiltration.

X-ray diffraction of the water-soluble mannan (WSM1) was performed. Liquid state ^{13}C NMR was performed by Spectral Data Services, Inc., Champaign, IL. Carbohydrate analysis was performed on the mannan by the IPC Analytical Department using the TAPPI method⁷⁰, and by the Analytical Department at the U.S.D.A. Forest Products Laboratory, Madison, WI. At FPL, a method (unpublished) was used where the carbohydrates were hydrolyzed with 72% H_2SO_4 , the acid solution was diluted, and the monomers were separated on a HPLC-column.

XYLAN

Xylan isolated from birch was kindly provided by Dr. N.S. Thompson. The xylan had been characterized earlier.⁷¹ In order to obtain a water-soluble fraction, the xylan was extracted with sodium hydroxide solution (102 ml of 0.01 N NaOH for 1.97 g xylan) overnight at $3 \pm 1^\circ\text{C}$. The xylan was centrifuged at 26,800g for 30 minutes. The pellets from centrifugation were dispersed in sodium hydroxide solution (80 ml of 0.01 N NaOH) and centrifuged at 26,800g

for 45 minutes. The pellets were again dispersed in sodium hydroxide solution (50 ml of 0.01 N NaOH) and centrifuged at 26,800g for 45 minutes. The combined supernatants were neutralized with ion exchange resin (Aldrich Amberlite IR 120+, washed with distilled water until no further change of pH), and freeze-dried. The freeze-dried material was extracted with water three times, with centrifugation and filtration of the supernatants through a fine sintered-glass funnel after each time. The filtrates were freeze-dried and the combined water-soluble products (WSX) yielded 1.15 g (58.3% of 1.97 g) of a white fluffy material.

Carbohydrate analysis of the xylan (WSX) was performed by the IPC Analytical Department using the TAPPI method.⁷⁰ Liquid state ¹³C NMR of xylan (WSX) dissolved in D₂O/NaOD was performed by Spectral Data Services, Inc., Champaign, IL, and by Dr. L.L. Landucci at the U.S.D.A. Forest Products Laboratory, Madison, WI, on xylan (WSX) dissolved in DMSO-d₆.

STRAINS OF *Acetobacter xylinum*

The strain of *Acetobacter xylinum* used in this study was kindly provided by Dr. C.H. Haigler. The strain was originally of *A. aceti* ss. *xylinum* from the American Type Culture Collection (ATCC 23769).²² It was a faster cellulose producer than a strain of *A. xylinum* used initially, which had been obtained directly from the American Type Culture Collection (ATCC 23769).

GROWTH MEDIUM

The medium developed by Hestrin⁷² was used for the production of bacterial cells. It consisted of 2.0% (w/v) D-glucose (Mallinckrodt), 0.5%

bactopeptone (Difco), 0.5% yeast extract (Difco), and 0.1% dibasic potassium phosphate (Baker). The pH was adjusted to 6.5 with hydrochloric acid. Solid medium was prepared by adding 1.5% (w/v) Bacto-agar (Difco) to the liquid medium before autoclaving. The medium was sterilized by autoclaving for 20 minutes at 120°C and 15 psi.

INOCULATION PROCEDURES AND INCUBATION CONDITIONS

Aliquots of 5 ml of growth medium were used in 4 dram (≈ 16 ml) screw-cap vials for culture storage and transfers. The aliquots were inoculated with colonies from solid medium or with 0.5 ml of cell suspension from a culture previously incubated. Petri dishes (100 x 10 mm) with 25 ml growth medium were used for growing cellulose pellicles and larger quantities of cells. The dishes were inoculated with 2-5 ml of cell suspension. The suspensions were prepared from cellulose pellicles which were shaken vigorously and squeezed with forceps before the desired volume of cell suspension was withdrawn from the medium. The vials and dishes were incubated at $28 \pm 1^\circ\text{C}$ for 24 hr to seven days.

In order to maintain a healthy and fast cellulose-producing culture, the culture was streaked periodically on solid medium in Petri dishes. Colonies growing high above the medium surface were selected for further inoculations. Large flat colonies developed occasionally in the strain. These types of colonies formed a soft pellicle.

PRELIMINARY WORK ON INCUBATION CONDITIONS

Initially, the influence of additives was studied using static

conditions of incubation. The incubation lasted for three to seven days. Cellulose pellicles were formed on these static cultures and the yield of cellulose was usually good. However, no effect on the cellulose structure could be detected. Because the production of new cellulose occurs on the upper surface of the pellicle¹⁷, the possibility that the additive would be depleted in the immediate surrounding of productive bacterial cells was a concern. To provide for a more homogeneous growth environment, the method using resting cells in shaking cultures was adopted.

INCUBATION SOLUTION FOR RESTING CELLS

The procedure and incubation solutions for resting cell production of cellulose followed Haigler⁷³ and Benziman⁷⁴. The incubation medium for resting cells was 50 mM phosphate buffer with 2% (w/v) D-glucose. Equal volumes of 50 mM monobasic (MCB) and dibasic (Baker) potassium phosphate solutions were mixed, and the pH was adjusted to 6.8-7.0 with hydrochloric acid or sodium hydroxide. The buffer was sterilized by autoclaving for 20 minutes at 120°C and 15 psi before glucose was added. The buffer turned bright yellow if glucose had been added before autoclaving.

The additive was dissolved in double concentration in buffer. Glucose was added in double concentration (4%) after the additive was dissolved and right before inoculation. The standard protocol for a resting-cell incubation consisted of six 125 ml Erlenmeyer flasks, each with 25 ml buffer containing additive and glucose in double concentrations before addition of an equal volume of cell suspension. To prevent the additives from being metabolized, an excess of glucose was used in the buffer. The final concentration of glucose was 2% instead of 40 mM which is commonly used in the literature. The

final concentrations of the additives were 0.05%, 0.1%, 0.4% or 0.8%, after adding the cell suspensions.

CELLULOSE PRODUCTS FROM RESTING CELLS

Each cellulose sample was prepared from the bacterial cells collected from nine Petri dishes which had been incubated for 36 hr. The cultures used to inoculate the nine Petri dishes had been transferred not more than three times after being selected and picked from a solid medium. The pellicles were gently placed in a big beaker and soaked in four changes of cold phosphate buffer (50 mM) for 20-30 minutes each time until the yellowish color of the growth medium had disappeared. The pellicles were kept at +2°C between changes of buffer. The pellicles were carefully blotted on paper towels between each change in order to remove additional medium.

When the growth medium had been removed, the cells were dislodged from the pellicles by shaking the pellicles vigorously in an Erlenmeyer flask. Liquid with additional cells was squeezed out of the pellicles with the help of forceps. The liquids from the shaking and squeezing were combined and filtered through two layers of wet cheese cloth to retain any cellulose remaining with the cells. The cell suspension was kept on ice, especially after the filtration, to halt the cellulose production. The cell suspension was diluted with phosphate buffer to 150 ml and divided among the six Erlenmeyer flasks with dissolved additive, giving a final volume of 50 ml of buffer and cell suspension in each flask. The flasks with resting cells were incubated for 3 hr at 28°C and were gently shaken at 50 rpm. The cellulose product was collected by centrifugation at 11,900g, 45 minutes at 15°C, and then washed twice by dispersing the cellulose product in distilled water and

centrifuging for 35 minutes before freeze-drying. Repeated preparations yielded 4-8 mg control cellulose (6 preparations), 6-180 mg of CMC-cellulose (3 preparations, 1x0.1%, 1x0.4%, and 1x0.8%), 8-12 mg of xyloglucan-cellulose (7 preparations, 3x0.1%, 3x0.4%, and 1x0.8%), 7-10 mg of xylan-cellulose (4 preparations, 1x0.05% and 3x0.1%), and 5-11 mg of mannan-cellulose (4 preparations, 1x0.05% and 3x0.1%). Raman spectra and x-ray diffractograms were recorded on the freeze-dried cellulose samples.

The amount of cellulose produced by resting cells was very small. It appeared that the cells quit producing cellulose after two to three hours. Experiments were performed in which small volumes of the growth medium were left in the cellulose pellicles providing a possibility for the cells to divide. This certainly promoted a higher yield of cellulose. However, the Raman spectra and x-ray diffractogram of the product indicated that cellulose I was not the exclusive product, and the method was therefore abandoned.

pH of resting cell medium and binding of xyloglucan to cellulose

Hayashi *et al.*²⁵ has reported that pea cellulose binds 40-50% more pea xyloglucan at pH 5 than at pH 7. In order to determine if the effect of xyloglucan on bacterial cellulose structure was influenced by pH, a sample was prepared in phosphate buffer of pH 5 and xyloglucan (0.1%). The x-ray diffractogram was recorded after washing the sample with water and freeze-drying. Comparison of diffractograms of the samples prepared at pH 5 and pH 7 showed no noticeable difference.

The synthesis of cellulose in *A. xylinum* is accompanied by the formation of organic acids; acetic acid from ethanol, gluconic acid from glucose, etc.,

and the pH in the medium is thereby reduced.¹¹ In this experiment, the pH decreased from pH 5 to 3.9 during the incubation period of 3 hr. In another sample preparation (with 0.05% mannan in the medium) the pH decreased from pH 6.8 to 6.5.

Celluloses produced in xyloglucan-salicin and xanthan gum

The resting cell method was used to produce cellulose samples from a medium containing xanthan gum (from Sigma) and a mixture of xyloglucan and salicin (courtesy of Dr. I.A. Pearl). All three compounds were used in concentrations of 0.1%. Xanthan gum is produced by the bacterium *Xanthomonas campestris*. This polysaccharide has a β -(1 \rightarrow 4)-D-glucose backbone.⁷⁵ Every other glucose in the main chain has a side chain consisting of an acetyl-D-mannose unit, a potassium D-glucuronate unit, and a terminal D-mannose unit of which about half contain a pyruvate unit. Xanthan gum was tested as an additive because of its structural similarities with CMC. The x-ray diffraction pattern of the cellulose product from xanthan gum showed the effect of xanthan gum to be very similar to the effect of CMC.

The second set of additives (xyloglucan and salicin) was tested for any synergistic effect of a hemicellulose and a lignin-precursor type additive. Salicin, or 2-(hydroxymethyl)phenyl- β -D-glucopyranoside, is structurally related to the β -glucosides of the lignin precursors; they are water-soluble and thought to be involved in the lignification of plant cell walls. The cellulose from xyloglucan-salicin gave an x-ray diffraction pattern very similar to the cellulose from xyloglucan. The Raman spectrum did not have any intense bands in the region corresponding to conjugated or aromatic C-C, C-H or C-OH bonds (1595 to 1650 cm^{-1}) indicating that the salicin was probably

removed during the washing of the cellulose product.

ALKALINE EXTRACTION OF CELLULOSE PRODUCTS

A series of extractions with sodium hydroxide was performed on cellulose samples produced by resting cells in the presence of 0% or 0.1% of CMC, mannan, xylan, or xyloglucan. The five samples were extracted once with distilled water, centrifuged, and freeze-dried. X-ray diffractograms and Raman spectra were recorded on these samples before the alkaline extractions. The celluloses were then extracted with alkali according to the following procedure: The cellulose pellets were wetted with three drops of distilled water for 10-15 minutes in plastic centrifuge tubes. Sodium hydroxide solution (8.0 ml) was added, and the celluloses were dispersed with a Pasteur pipet and stirred occasionally during the 8-9 hr extraction period. The celluloses were pelleted by centrifugation at 4,300g, 60 minutes at 15°C, in a Sorvall high speed centrifuge. The celluloses were washed twice with about 35 ml distilled water, centrifuged after each wash at 26,800g for 60-90 minutes, and freeze-dried. The extractions were performed with 0.01 N NaOH, 0.1 N NaOH, and 1.0 N NaOH diluted from an Acculute solution. X-ray diffractograms and Raman spectra were recorded after each extraction.

Before the series of alkaline extractions was performed, two sets of preliminary experiments were conducted. Three control samples were extracted with 1.0 N NaOH. One sample of cellulose produced in the presence of 0.1% xyloglucan was extracted first with 0.1% NH_4OH and then with 1.0 N NaOH. The extraction was performed with ammonium hydroxide instead of sodium hydroxide because the ammonium hydroxide could be removed by evaporation. However, the concentration of ammonium hydroxide in solution could be changing because of

its volatility. Therefore, the subsequent extractions were performed exclusively with sodium hydroxide. The Raman spectrum of the extracted xyloglucan-cellulose and the x-ray diffractograms of all extracted samples were very similar to the spectrum and diffractograms of corresponding samples in the alkaline extraction series.

X-RAY DIFFRACTION

X-ray diffractograms were recorded on a Philips powder diffractometer (APD 3720) using CuK_α radiation filtered with a crystal monochromator. The samples were analyzed as pellets pressed at about 800 psi. The pellets were analyzed on a low background holder. The radiation was generated using conditions of 45 kV and 40 mA. The diffractograms were recorded from 5 to 30 degrees 2θ . The step size was 0.02 degrees and the count time 1.00 second, giving a scanning rate of 1.2 degrees of 2θ per minute.

PROFILE FITTING OF X-RAY DIFFRACTOGRAMS

The x-ray diffractograms were resolved into individual peaks using a profile-fitting computer program obtained from Philips.⁷⁶ This resolution model fitted profiles to the experimental diffraction profile by iteration, using a nonlinear least-squares algorithm. Four peaks were used in the fitting of each diffractogram, three peaks for the cellulose crystalline peaks (101, $10\bar{1}$, and 002 peaks) and one peak accounting for the amorphous background of the diffractogram. The step size in the fitting was 0.04 degrees which, being twice the size of the scanning step, was by default the smallest step possible.

Results from a profile fitting included a fitted total profile for the diffractogram, profiles for the resolved peaks, a fitted background, and a residual indicating the accuracy of the fit. In addition, the full width at half maximum (FWHM), the intensity, and the position were obtained for each fitted peak. The peak width was measured at half maximum intensity of the fitted individual peaks which had been corrected for the background intensity.

RAMAN SPECTROSCOPY

The Raman system was a Jobin Yvon Ramanor HG2S monochromator with 514.5 nm radiation of an argon ion laser (Spectra-Physics model 2025) as the excitation source. The incident laser power was 40-70 mW. The slit width was 400 μm . The samples were analyzed as pressed pellets and the scattered Raman emission was collected perpendicular to the excitation radiation. This instrumental set-up provided for a macro-mode acquisition of the Raman light from the samples which decreased effects attributable to orientation of the cellulose samples. The data acquisition system consisted of a photo multiplier detector (RCA C31034-A05) and a Tracor Northern TN-1500 digital signal analyzer. The scanning motor in the monochromator was computer controlled. The scan rate was 60 cm^{-1} per minute, and the scanning range was 250-3700 cm^{-1} . Multiple (15-25) scans were recorded for each spectrum to decrease distortion of the spectrum due to any drift in the laser power during a single scan. The samples were highly fluorescent in the region scanned, and the spectra were flattened to correct for contributions from the fluorescent background.

CONFORMATIONAL COMPONENT RESOLUTION OF RAMAN SPECTRA

The low frequency regions ($250\text{-}550\text{ cm}^{-1}$) of the Raman spectra were resolved into linear combinations of spectra representative of the conformations k_I , k_{II} and k_0 . The original Raman spectra of bacterial cellulose samples after the extractions with 0.01 N , 0.1 N , and 1.0 N NaOH were subjected to this resolution. The standard procedure of preparing the spectra for analysis included smoothing, flattening, and normalizing.⁷⁷ The spectra of celluloses extracted with 0.01 N NaOH were smoothed ten times. The spectra recorded after the second and third alkali extractions were smoothed five times because they had higher signal-to-noise ratios. The smoothed spectra were flattened in the $250\text{-}750\text{ cm}^{-1}$ region. The spectra were integrated between 250 and 550 cm^{-1} , and the integrated area was normalized to $600,000$ by multiplying the spectra with a correction factor.

The resolution of the spectra was accomplished by an iterative search procedure for the least-squares deviation of a linear combination of the spectra of standards from the experimental spectra. The computer program used for this search can be found in Appendix D. The reference spectrum used for k_I was of a bacterial cellulose pellicle purified by boiling in 1% NaOH for one hour. The spectrum of regenerated microcrystalline cotton cellulose (CF1) was the reference for k_{II} . For k_0 , the spectrum of ball-milled microcrystalline cotton cellulose was used as the standard.

SPECIMENS FOR TRANSMISSION ELECTRON MICROSCOPY

The procedure for preparation of specimens followed Haigler.^{19,73} Bacterial cellulose was produced directly on the grids by floating the grid

upside down in the incubation medium. The specimens were prepared by the following method: A cellulose pellicle was blotted on a paper towel to remove excess liquid. The remaining liquid with bacterial cells was squeezed out of the pellicle with forceps. The pellicle must be freshly produced (one or two days old) otherwise the cells did not produce cellulose as readily and elongated cells were formed. The cell suspension was centrifuged in a bench-top centrifuge and the supernatant was pipetted off, leaving about 0.5 ml liquid. The pellet of cells was stirred up and the cell suspension was stored on ice.

Beforehand, the additive had been dissolved in 50 mM phosphate buffer to a concentration of 0.8%, and glucose was added to a final concentration of 2%. This solution was mixed with appropriate volumes of 50 mM phosphate buffer containing 2% glucose to give incubation solutions of 0.1%, 0.4%, and 0.8% additive. Mannan did not dissolve in buffer but was dissolved in sterile H₂O, mixed with an equal volume of 100 mM phosphate buffer, and glucose was added to 2%. Drops of the mixtures were placed in a spot dish. Bacterial cells were attached to the grids by touching the coated side of a grid to the cell suspension. The grids were floated with the coated side down on the drops of additive mixture and incubated between 17 and 30 minutes at 28±1°C. The grids used for the specimens were 300 mesh copper grids that had been coated with Formvar and carbon.⁷⁸ After incubation, the grids were rinsed in sterile distilled water, and negatively stained with uranyl acetate (1% in H₂O) containing Bacitracin (Aldrich Chem. Co., 0.1 mg/ml) as a spreading agent. The grids were gently wiped on the backside and along the edge with a piece of filter paper, and air dried.

The grids were observed in a JEOL JEM-100CX II electron microscope

operating in the transmission mode, with an accelerating voltage of 80 kV. All grids were placed in the same specimen holder. Photomicrographs were taken at magnifications of 36,000, 48,000, and 72,000. The Kodak 4489 film plates used for micrographs were developed in Kodak developer D-19 (diluted 1:3) for 3 minutes.

MICROGRAPH ENHANCEMENT IN THE IMAGE ANALYZER

Twenty-six representative micrographs, containing many ribbons, were selected for further analyses. The selection consisted of five micrographs of the control samples, and, for each additive, two micrographs from the use of 0.1% additive, one micrograph from the use of 0.4% additive, and two micrographs from the use of 0.8% additive. One extra micrograph was selected from the use of 0.4% xyloglucan.

The micrographs were digitized, enhanced and enlarged using a Tracor Northern TN-8502 image analyzer equipped with a 1024x1024 high-resolution camera (DAGE-MTI model 81). The enhancement consisted of contrast sharpening with a seven-by-seven digital filter, and grey-scale contrast stretching which eliminated the extreme grey shades and optimized the grey scale.

After the enhancement, the numbers of fibrils in the ribbons were estimated. The widths of the ribbons and fibrils were measured on the monitor using the distance measurement function of the image analyzer, after suitable calibration. Each width was measured three times and averaged before further processing. The standard deviations of these measurements averaged 7%, and ranged from 0% to 25%.

The distance calibration was performed by digitizing micrographs of a

line grating replica and measuring the line spacing on the screen. These micrographs were taken at the same magnifications and with the specimen holder in the same position in the microscope as for the cellulose specimens. The line spacing on the grating replica was 462.9 nm (Polyscience, Inc. Warrington, PA).

RESULTS

CHARACTERIZATION OF MANNAN

The total carbohydrate content of the water-soluble mannan preparations ranged from 83 to 99%. The mannan that was extracted with ethanol to remove inorganics had the higher carbohydrate content. Mannose was the major species, constituting 77-91% of the carbohydrates. Galactose, glucose, xylose, and arabinose were all present to varying degrees. Table 5 shows the composition of the crude mannan fraction before the ultrafiltration step in the preparation of the water-soluble mannan used in the resting cell medium. The purified material was consumed in a faulty analysis, and the crude fraction was used in its stead. Except for the inorganic content, the samples were expected to have the same composition, therefore, the material not accounted for in Table 5 is primarily inorganics.

Table 5. Carbohydrate composition of crude mannan (CM).

	<u>Fraction of CM</u>	<u>Fraction of carbohydrates</u>
Glucose	0.4	0.5
Galactose	3.3	4.5
Mannose	66.5	90.5
Xylose	1.7	2.3
Arabinose	1.6	2.2
	----	-----
Total carbohydrate, %	73.5	100.0

X-ray diffraction showed the mannan to be crystalline, with reflection peaks indicating a mixture of mannan I and II.⁷⁹ In a liquid state ¹³C NMR

spectrum of the mannan (see Appendix A), the resonance peaks of the nonreducing C4 end group and of the C4 internal moiety were identified.^{80,81} Using the integrated intensities of these resonances, the average degree of polymerization (DP) of the water-soluble fraction of mannan was calculated to be 5.6. The response from the carbons in different positions in the molecule can be slightly different for such large molecules as penta- or hexa-saccharides which could result in an underestimation of the DP.

CHARACTERIZATION OF XYLAN

X-ray diffraction showed the water-soluble xylan to be amorphous. The carbohydrate composition of the xylan is shown in Table 6. The material not accounted for in Table 6 is likely to be uronic acids and ash.

Table 6. Carbohydrate composition of xylan.

	<u>Fraction of</u> <u>sample</u>	<u>Fraction of</u> <u>carbohydrates</u>
Glucose	0.7	0.9
Galactose	0.6	0.8
Mannose	1.5	2.0
Xylose	69.8	92.6
Arabinose	2.0	2.7
Ribose	0.4	0.5
Fucose	0.4	0.5
	----	-----
Total carbohydrate, %	75.4	100.0

Liquid state ^{13}C NMR in $\text{D}_2\text{O}/\text{NaOD}$ (see Appendix A) indicated that the xylan contained carboxylic acid carbons ($\delta=176.8$ ppm). The integrated peak areas from the C4 end group and internal moiety, respectively, gave an average DP of 8.2. The NMR-spectrum of xylan in DMSO-d_6 showed peaks at approximately

the same magnetic shifts as in the spectrum of xylan in $D_2O/NaOD$. The spectrum from $DMSO-d_6$ had a lower resolution of the peaks. The DP was estimated to 8.3 from the integrated peak areas of the C1 end groups in this spectrum. As with the ^{13}C NMR analysis of mannan, these values for xylan DP based on integration of ^{13}C NMR spectra may be underestimations. The DP_N of a birch xylan comparable to the original birch xylan was 215 as measured with osmometry.⁷¹ However, a liquid state ^{13}C NMR spectrum of the original xylan recorded in $D_2O/NaOD$ gave a DP of the same magnitude as the water-soluble xylan, suggesting nonlinear responses from the carbons in different positions.

APPEARANCE OF THE CELLULOSE PRODUCTS IN THE PRODUCTION VESSELS

When the control samples of cellulose were produced with the resting cell method, the cellulose was formed as a coherent aggregate in the medium. Cellulose produced in presence of an additive was dispersed throughout the medium as small flocculent particles. CMC at a concentration of 0.8% caused the medium to become almost clear even though cellulosic material was isolated later.

ALKALINE EXTRACTION OF CELLULOSE PRODUCTS

The series of extractions removed a large fraction of the cellulose samples. Table 7 shows the weights of the celluloses after the extractions. On average, only 17% of the starting material remained after the extractions. The smaller the sample was, the more difficult it was to isolate the material completely. Any difference in the final weights may therefore have been exaggerated.

Table 7. Weights of celluloses after alkaline extractions.

	Start mtrl (mg)	Wtr ext. (mg)	0.01 N (mg)	0.1 N (mg)	1.0 N NaOH (mg)
Control	8.3	5.4 65%	1.6 30%	1.1 79%	0.6 67%
CMC	5.7	5.4 95%	2.5 45%	1.9 79%	0.9 50%
Xyloglu	11.3	9.3 82%	4.2 45%	3.2 80%	2.1 64%
Xylan	10.5	9.3 89%	3.5 37%	2.3 68%	1.5 61%
Mannan	5.0	3.9 78%	1.3 32%	1.0 80%	0.7 88%

The percentages represent amounts of samples remaining after extractions compared to the weights before that extraction.

X-RAY DIFFRACTION AND PROFILE FITTING

The "old" terminology for the cellulose unit cell has been used throughout this thesis. With this notation, the planes of the anhydroglucose units lie in the *ab* plane and the axes of the cellobiose units are parallel to the *b* axis of the unit cell. In an x-ray diffractogram of cellulose I, the main diffractions are then called (101), (10 $\bar{1}$), and (002), using Miller indices based on this notation.

The x-ray diffractograms of bacterial cellulose samples were resolved into individual peaks using a profile-fitting computer program. The profile-fitting result of each diffractogram consisted of a fitted total profile, profiles for each of the resolved peaks, a fitted background, and a residual portion indicating the accuracy of the fit. A good fit was obtained when four peaks were used for the fitting. The fitting gave more stable results for the (101) and (002) peaks. The accuracy of the profile fitting will be addressed further in the Discussion section. For each fitted peak, the resolution also

gave the full width at half maximum (FWHM), the position, and the intensity. The information for the resolved peaks will be discussed in more detail in the following subsections.

Figure 2 shows the fitted diffractogram profiles of control cellulose and celluloses produced in presence of CMC, mannan, xylan, and xyloglucan, after the last extraction with 1.0 N NaOH. The result of fitting an x-ray diffractogram is shown in Figure 3, which contains the experimental diffractogram, the fitted total profile, background, and residual, together with the fitted profiles of the four individual peaks. The total profile equals the sum of the individual profiles and the background. (The original x-ray diffractograms after all extraction steps can be found in Appendix B.) Cellulose I was the dominant polymorph in all samples. In Figure 2, the diffractogram of the control sample has an appearance typical of a bacterial cellulose, with a separation of the (101) and (10 $\bar{1}$) peaks. The intensity of the (10 $\bar{1}$) peak in bacterial cellulose is about half of the intensity of the (101) peak. The diffractograms of cellulose produced in the presence of an additive were different because the intensities of the (101) and (10 $\bar{1}$) peaks were closer to equal. This difference in appearance was most noticeable in the diffractogram of cellulose produced in the presence of xylan or xyloglucan.

Peak Full Widths at Half Maximum (FWHM)

The peak width at half maximum is a measurement of the degree of crystallinity in a material. The diffractogram peaks are wider when the lateral dimensions of the cellulose crystallites are smaller. The widths of the fitted crystalline peaks are listed in Table 8 for control cellulose and

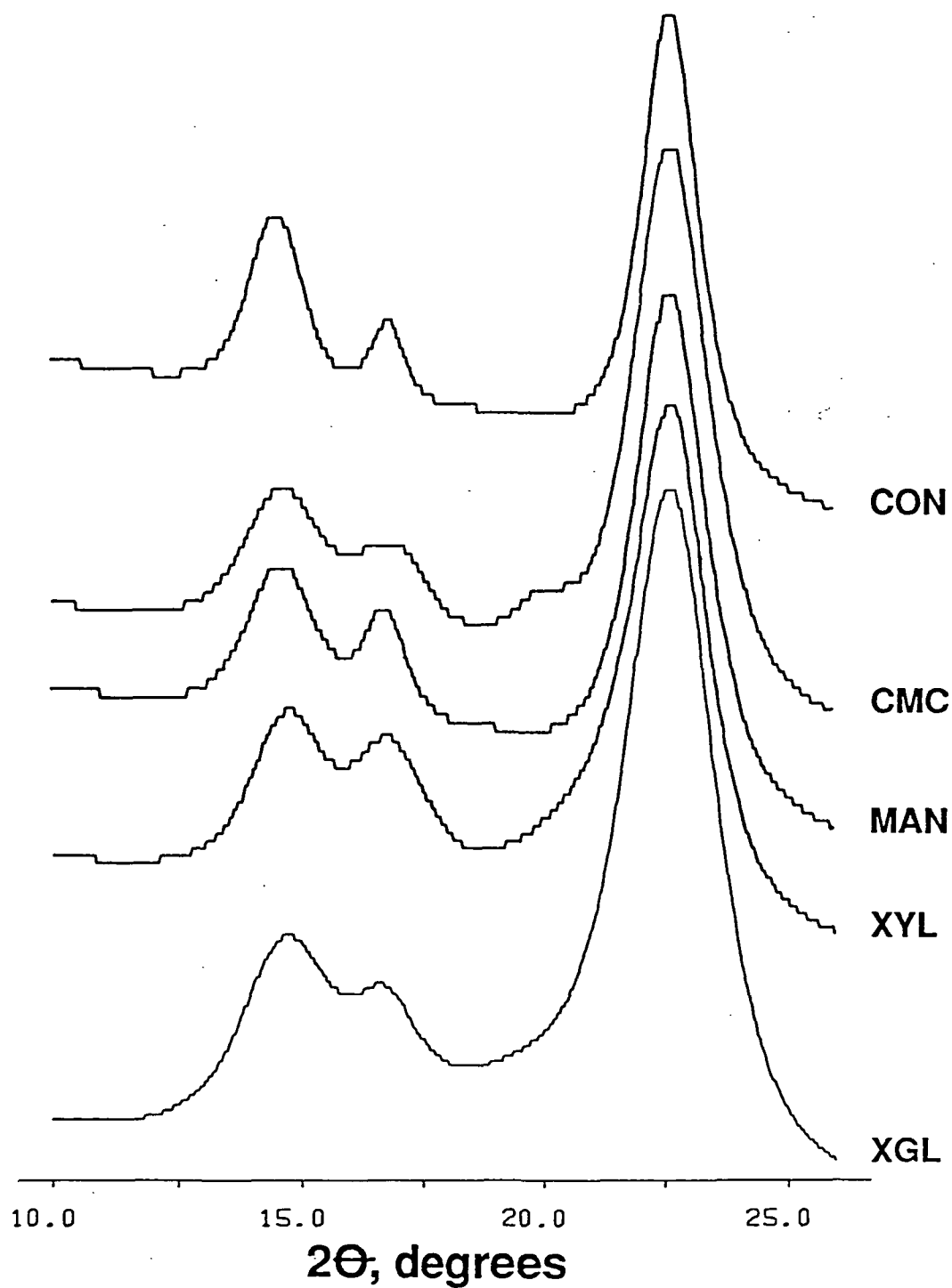


Figure 2. Fitted x-ray diffractogram profiles of celluloses. CON: Control cellulose without additive; CMC: Cellulose produced with CMC; MAN: Cellulose produced with mannan; XYL: Cellulose produced with xylan; XGL: Cellulose produced with xyloglucan.

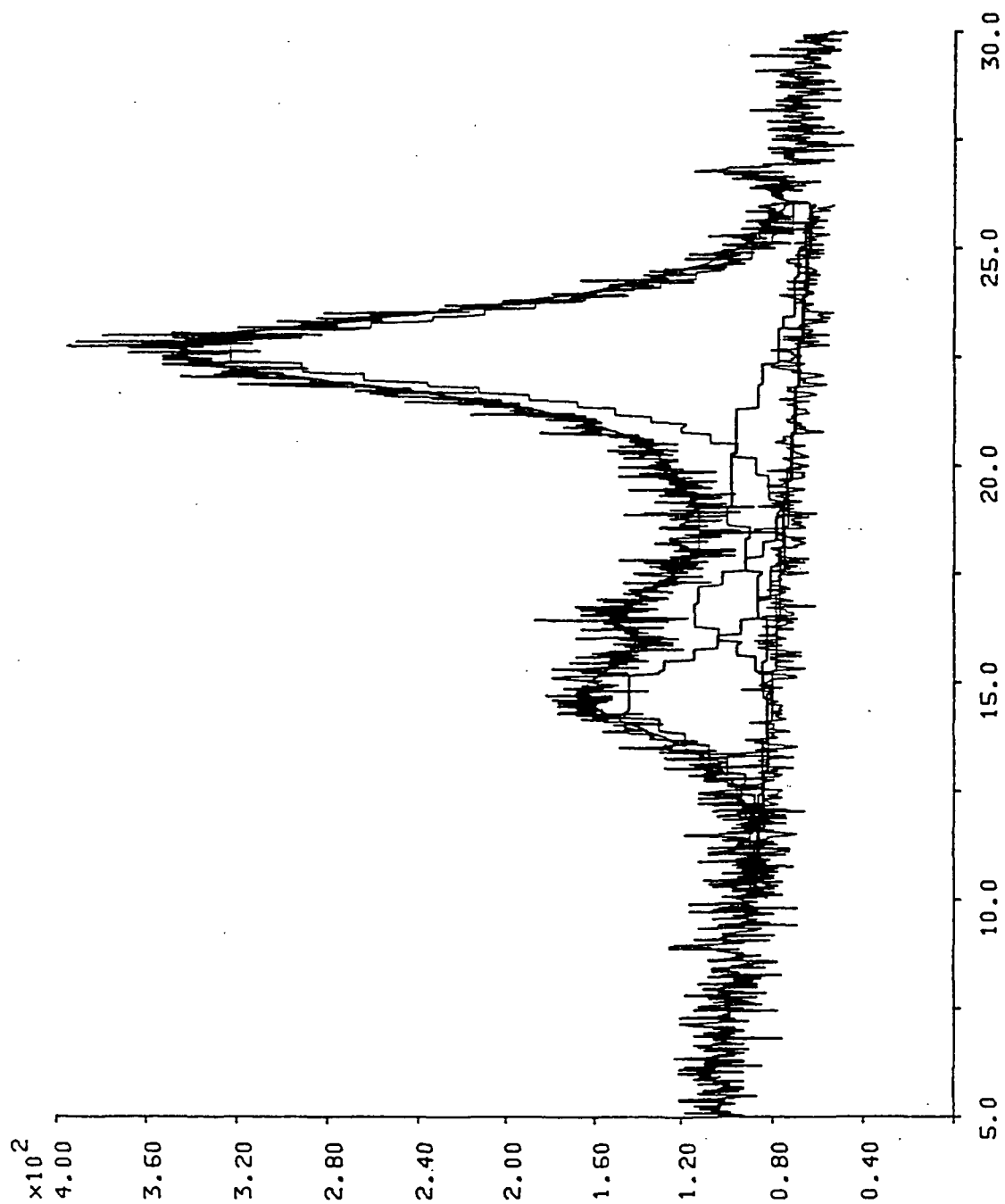


Figure 3. The experimental diffractogram of xyloglucan-cellulose extracted with 1.0 N NaOH, the fitted total profile, background, and residual, and the fitted profiles of the four individual peaks.

celluloses produced in the presence of xylan, xyloglucan, mannan, and CMC. (Appendix B contains the complete set of peak widths for all samples after each extraction step.)

Table 8. Peak widths (2θ -degrees): bacterial celluloses produced in the absence or presence of additives, after extraction with 1.0 N NaOH.

	CON	CMC	MAN	XYL	XGL
101	1.29	1.83	1.64	1.70	2.07
10 $\bar{1}$	0.82	2.03	1.04	1.89	1.73
002	1.32	1.77	1.64	1.67	2.07
Increase (%) [*]	-	38	26	30	60

^{*} Average of the increase in percent for the (101) and (002) peaks over a control sample.

CON: Control cellulose without additive; CMC: Cellulose produced with CMC; MAN: Cellulose produced with mannan; XYL: Cellulose produced with xylan; XGL: Cellulose produced with xyloglucan.

The presence of additives in the growth medium increased the peak widths of the bacterial cellulose, and, hence, reduced the crystallite size. Average values for the (101) and (002) peaks show that xyloglucan increased the widths most effectively when compared to the control. The differences attributable to influences of CMC, xylan, and mannan are of approximately the same magnitude and are smaller than the effect of xyloglucan.

Peak Positions

The positions of the fitted peaks in the diffractograms of control cellulose and celluloses produced in the presence of additives are summarized in Table 9, and the complete peak-position information can be found in Appendix B.

Table 9. Peak positions (2θ -degrees): bacterial celluloses produced in the absence or presence of additives, after extraction with 1.0 N NaOH.

	CON	CMC	MAN	XYL	XGL
101	14.52	14.62	14.62	14.67	14.65
$10\bar{1}$	16.81	16.91	16.72	16.77	16.69
002	22.67	22.66	22.67	22.61	22.59

CON: Control cellulose without additive; CMC: Cellulose produced with CMC; MAN: Cellulose produced with mannan; XYL: Cellulose produced with xylan; XGL: Cellulose produced with xyloglucan.

The presence of any of the additives shifted the position of the (101) peaks to higher values relative to the control sample. The position of the (002) peaks shifted to lower values when xylan and xyloglucan were present in the growth medium, and remained the same in the presence of CMC and mannan. The position of the ($10\bar{1}$) peaks shifted to lower values in the presence of xyloglucan, mannan, and xylan. CMC caused the position of this peak to shift to a higher value.

The additives influenced the cellulose aggregation pattern resulting in narrower ranges of the diffractogram peaks. The positions of the peaks in an x-ray diffractogram reflect the dimensions of the crystalline unit cell. When the peaks were closer together in the x-ray diffractograms, the angle between the *a* and *c* axes in the unit cell became closer to 90 degrees.⁸² Therefore, the *ac* plane perpendicular to the cell axis (*b*) changed from a diamond-shape to more of a rectangle.

Peak Intensities

Table 10 lists the fitted peak intensities from the diffractograms of

control cellulose and celluloses produced in the presence of additives (see Appendix B for the remaining data on peak intensities).

Table 10. Peak intensities and relative intensities: bacterial celluloses produced in the absence or presence of additives, after extraction with 1.0 N NaOH.

	CON	CMC	MAN	XYL	XGL
101 (cts)	34	29	29	38	77
10 $\bar{1}$ /101	0.44	0.72	0.69	0.87	0.60
002/101	2.50	3.93	3.21	3.05	3.51

CON: Control cellulose without additive; CMC: Cellulose produced with CMC; MAN: Cellulose produced with mannan; XYL: Cellulose produced with xylan; XGL: Cellulose produced with xyloglucan.

The intensities of the (10 $\bar{1}$) and (002) peaks were normalized against the (101) peak intensity. In bacterial cellulose, the intensity of the (10 $\bar{1}$) peak is approximately half of the (101) peak intensity. When additives were present in the growth medium, the intensities of the (101) and (10 $\bar{1}$) peaks changed and became more equal. Bacterial cellulose was highly oriented, as indicated by the nonequal intensities of the (101) and (10 $\bar{1}$) peaks, whereas the crystallites of celluloses produced in additives were more randomly oriented.

RAMAN SPECTROSCOPY

The Raman spectra of the control cellulose and celluloses produced in presence of CMC, mannan, xylan, and xyloglucan are shown in Figures 4-8. These spectra were recorded after the extraction with 0.1 N NaOH. In the low-frequency region of the spectra (250-600 cm^{-1}), the bands are primarily

Control Cellulose, 0.1 N NaOH

3875-115-4, 21 scans, smoothed 3 times

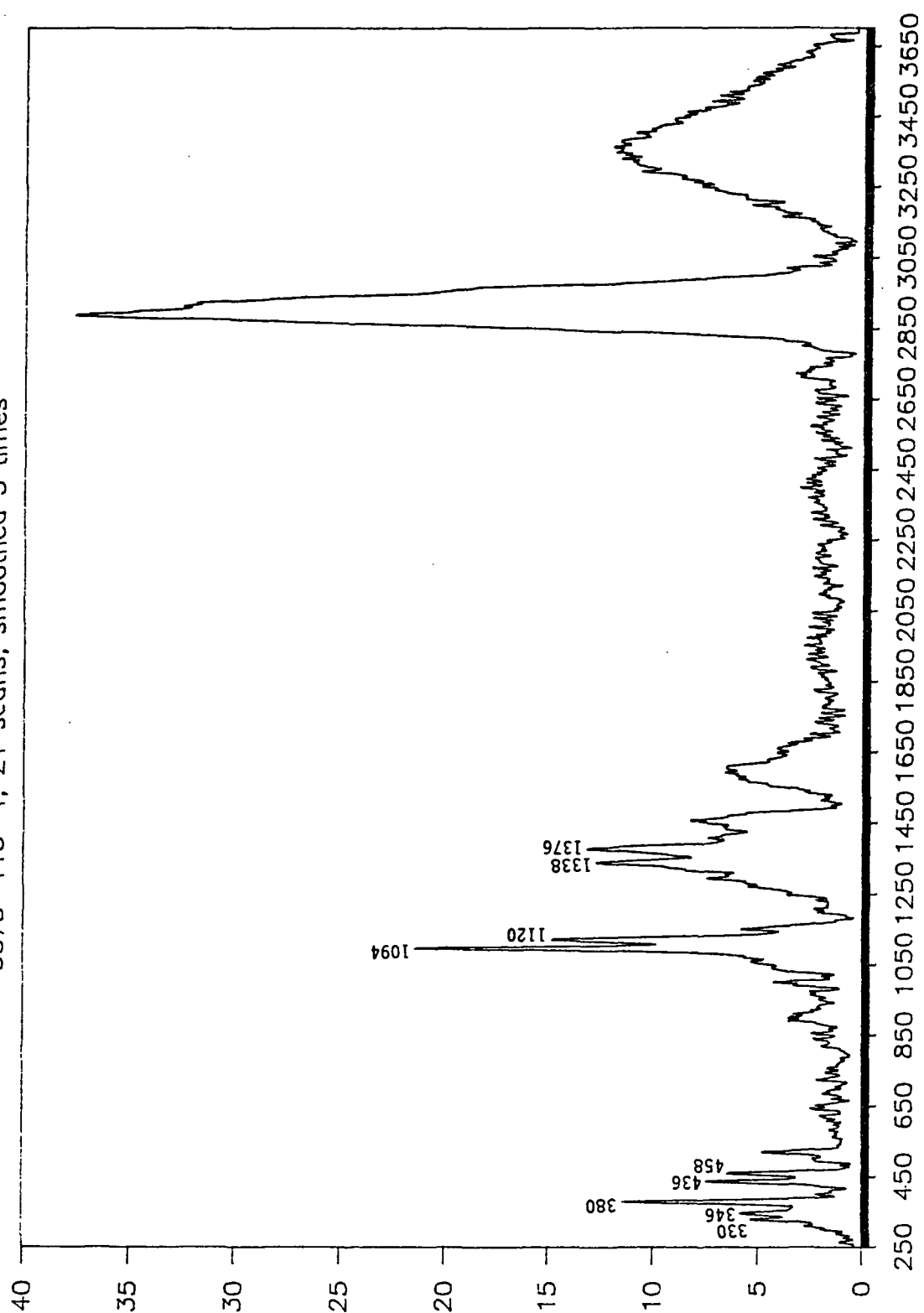


Figure 4. Raman spectrum of control cellulose after the extraction with 0.1 N NaOH.

CMC(0.1%)—Cellulose, 0.1 N NaOH

3875-115-1, 21 scans, smoothed 3 times

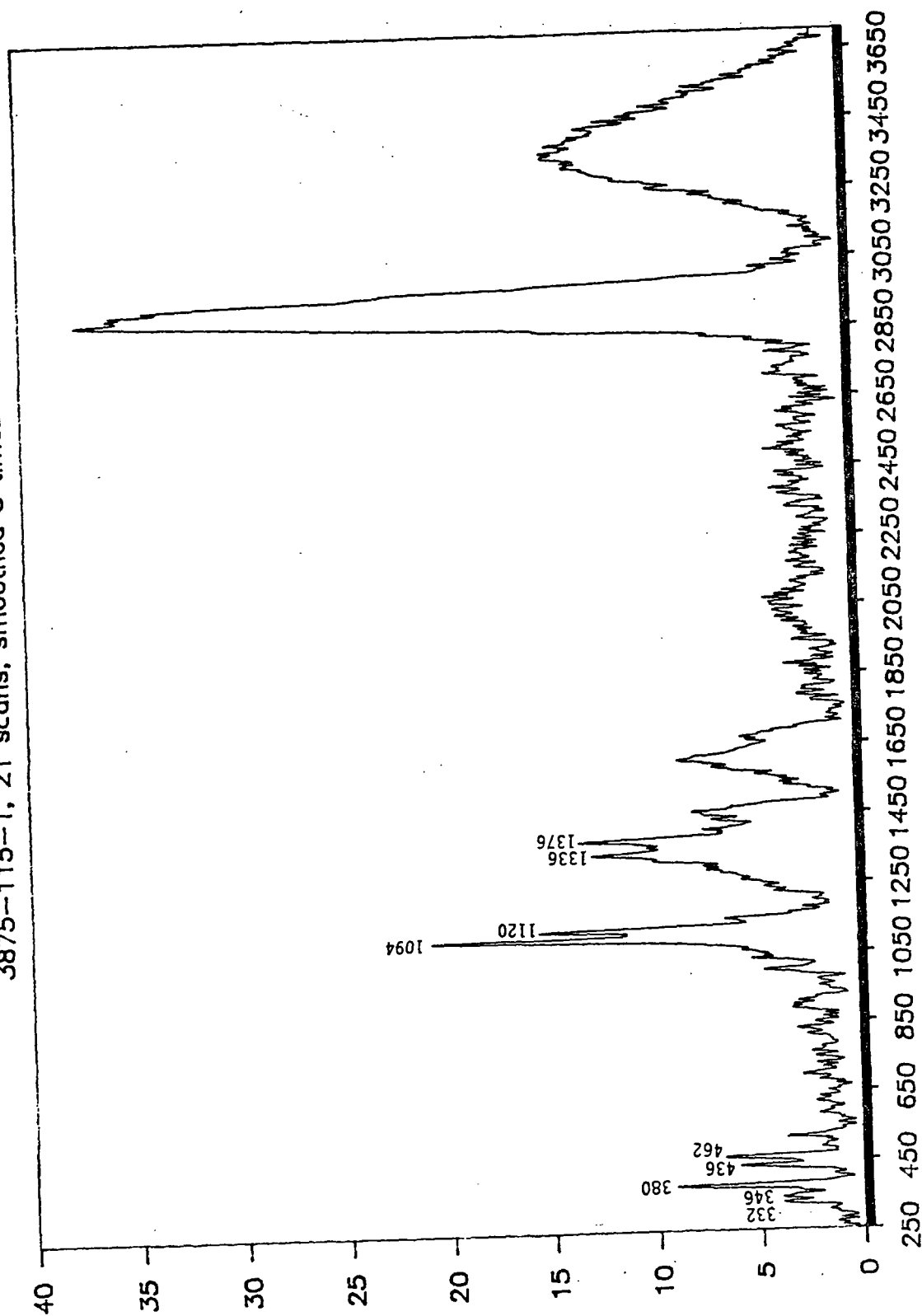


Figure 5. Raman spectrum of CMC-cellulose after the extraction with 0.1 N NaOH.

Mannan(0.1%)—Cellulose, 0.1 N NaOH

3875–115–5, 21 scans, smoothed 3 times

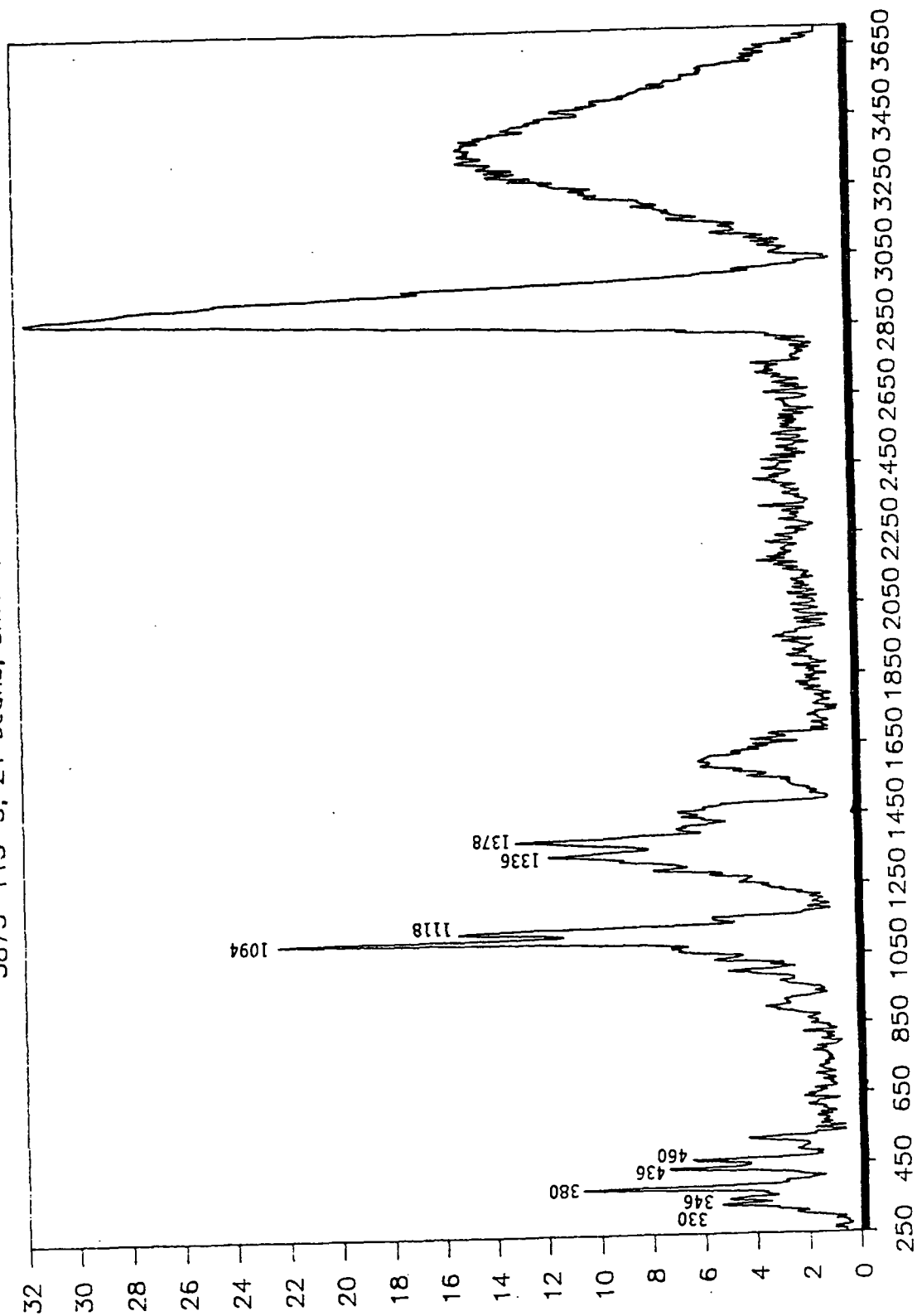


Figure 6. Raman spectrum of mannan-cellulose after the extraction with 0.1 N NaOH.

Xylan(0.1%)—Cellulose, 0.1 N NaOH

3875-115-3, 20 scans, smoothed 3 times

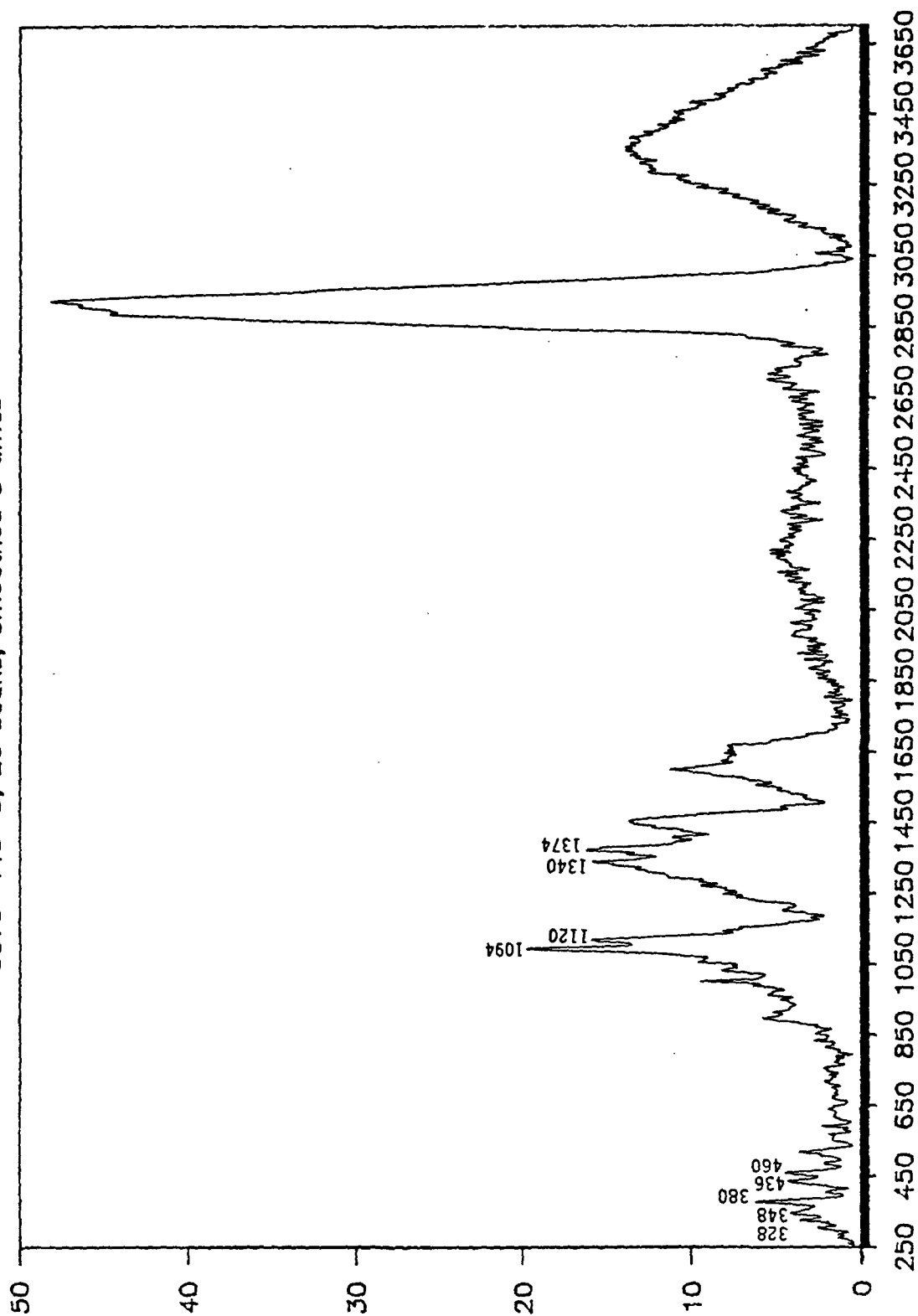


Figure 7. Raman spectrum of xylan-cellulose after the extraction with 0.1 N NaOH.

Xyloglucan(0.1%)—Cellulose, 0.1 N NaOH

3875–115–2, 21 scans, smoothed 3 times

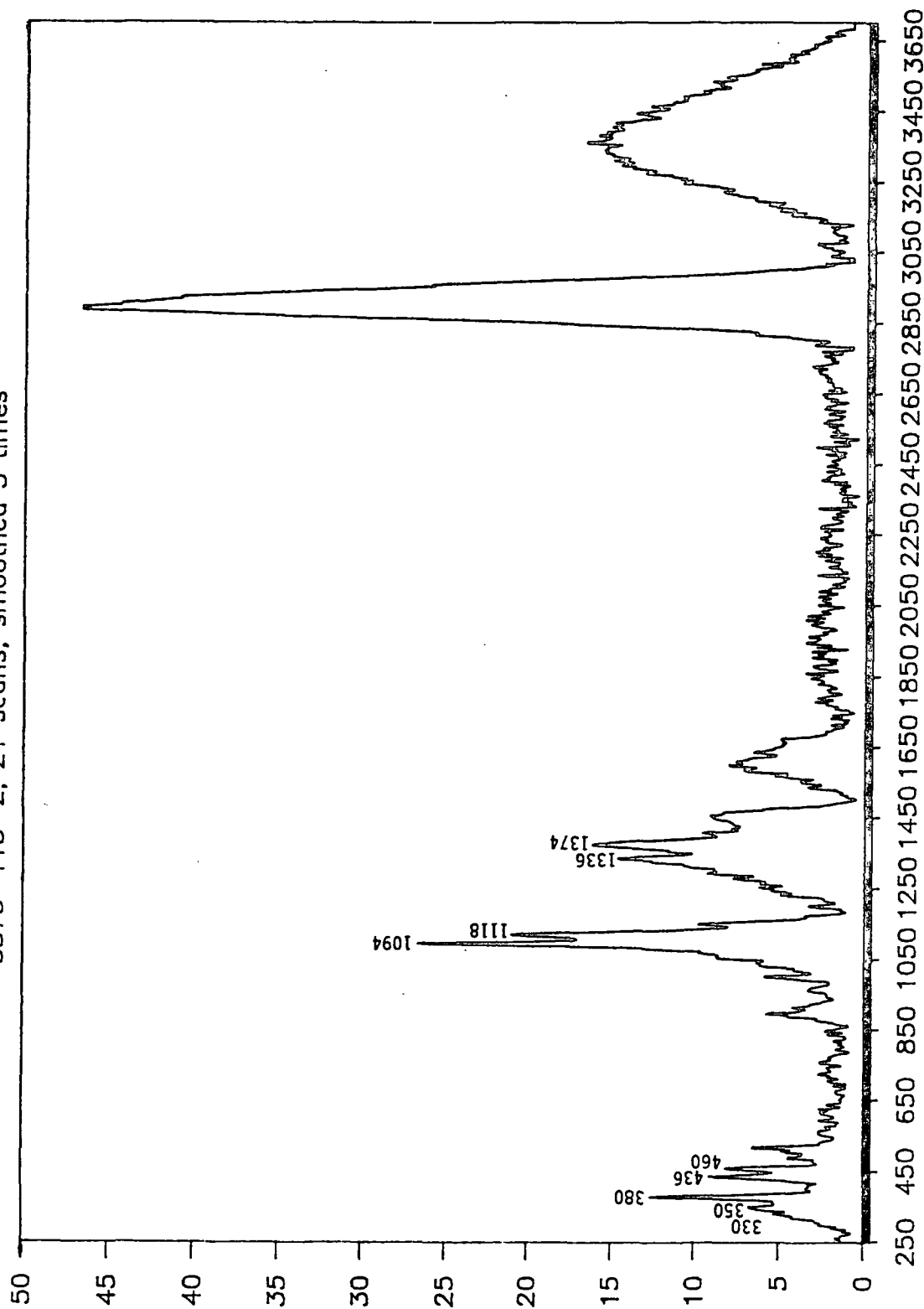


Figure 8. Raman spectrum of xyloglucan-cellulose after the extraction with 0.1 N NaOH.

sensitive to vibrations in the molecular skeleton. In all Raman spectra, the positions of the bands shifted very little, never more than $\pm 2 \text{ cm}^{-1}$. All the spectra in Figures 4-8 compare favorably with a cellulose I spectrum.

However, the ratio of intensities and the resolution of bands varied among the spectra. Appendix C contains the Raman spectra of the cellulose samples after each extraction step.

Visual comparison of band resolution

A comparison was made of the resolution of adjacent bands in the Raman spectra of samples after the extractions with 0.1 N and 1.0 N NaOH. The spectra were visually compared with respect to the resolution of pairs or triplets of bands after expansion of the $250\text{-}650 \text{ cm}^{-1}$ and $250\text{-}1700 \text{ cm}^{-1}$ regions. The bands used for these comparisons were at $330\text{-}346\text{-}380 \text{ cm}^{-1}$, $436\text{-}460 \text{ cm}^{-1}$, $1094\text{-}1120 \text{ cm}^{-1}$, and $1338\text{-}1376 \text{ cm}^{-1}$. The spectra of xyloglucan-cellulose had the bands least resolved, followed by the spectra of cellulose produced in the presence of xylan, CMC, and mannan. The control cellulose gave the spectrum with the best resolved bands. The sharper and more resolved bands are indications of larger sizes of the cellulose crystallites.⁸³ The molecules are in a more homogeneous environment when the crystallites are larger, therefore, the frequencies corresponding to the Raman bands have a more narrow distribution resulting in narrower bands.

Conformational component resolution of Raman spectra

The low frequency regions ($250\text{-}550 \text{ cm}^{-1}$) of the Raman spectra of the cellulose samples were resolved into spectra of k_I , k_{II} and k_0 , the conformational forms responsible for the polymorphs cellulose I, cellulose II,

and amorphous cellulose. Table 11 describes the fractions of the conformational components in the bacterial celluloses produced in the absence and presence of additives. (The component fractions of the bacterial celluloses after all the alkaline extractions can be found in Appendix D.) The conformational component resolution resulted in k_I -contents of the samples which were at three levels: the control sample had the highest amount of k_I ; celluloses produced in CMC or mannan had a medium content of k_I ; and celluloses produced in xylan or xyloglucan had the lowest content of k_I .

The conformational components given in Table 11 were based on spectra of the celluloses after the extractions with 0.1 N NaOH. The resolution of the samples after the extraction with 1.0 N NaOH gave lower fractions of the k_I and higher fractions of the k_0 conformations than after the preceding extraction with 0.1 N NaOH, which would imply that the degree of crystallinity was lower. However, the x-ray diffraction showed the amorphous fraction of these samples to be lower after the last extraction. One explanation for this discrepancy is that the degradation products possibly combined with the cellulose (see also in the Discussion section about Raman bands at 1152 and 1506 cm^{-1}). This could have led to a shift in the positions of the resonance bands in the low-frequency regions from the positions of the bands in k_I , in addition to the unknown bands at 1152 and 1506 cm^{-1} . Even small changes in the band positions can shift the fractions of the different conformations in a sample.

Table 11. Conformational components of bacterial celluloses produced in the absence or presence of additives, after the extraction with 0.1 N NaOH.

	CON	CMC	MAN	XYL	XGL
k_I	0.77 ± 0.03	0.69 ± 0.04	0.67 ± 0.02	0.51 ± 0.04	0.51 ± 0.03
k_{II}	0.04 ± 0.11	$-.12 \pm 0.12$	$-.06 \pm 0.08$	0.16 ± 0.13	0.03 ± 0.09
k_0	0.17 ± 0.10	0.41 ± 0.12	0.37 ± 0.08	0.30 ± 0.12	0.45 ± 0.09

CON: Control cellulose without additive; CMC: Cellulose produced with CMC; MAN: Cellulose produced with mannan; XYL: Cellulose produced with xylan; XGL: Cellulose produced with xyloglucan.

TRANSMISSION ELECTRON MICROSCOPY

Appearance of bacterial cellulose fibrils

Two photomicrographs of the control cellulose and celluloses produced in the presence of each additive are shown in Figures 9-13. The remaining micrographs which were used for the measurements of fibril widths can be found in Appendix E. Photomicrographs showed the normal cellulose ribbons to be flat and twisting (Figure 9). Some ribbons were very tightly twisted, whereas other ribbons had fibrils which were more splayed or separated from each other. The ribbons had a range of widths, varying from 40 to 150 nm. Enlarging the micrographs using an image analyzer made it possible to estimate the number of fibrils in a ribbon. This was easier at higher concentrations of additive when the fibrils were more widely splayed; it was more difficult to distinguish the subunits in micrographs of the control samples. The ribbons consisted of about 15 fibrils and ranged between 5 and 25 fibrils. The distance between twists varied significantly; the distances between two twists measured typically within the range of 0.3 μm to 0.8 μm .



Figure 9. Micrographs of control cellulose, no. 2480 and 2536; scale bar: $0.3\ \mu\text{m}$, X48,000.



Figure 10. Micrographs of cellulose produced in 0.1% CMC; no. 2448 and 2449; scale bar: $0.3\ \mu\text{m}$, X48,000.

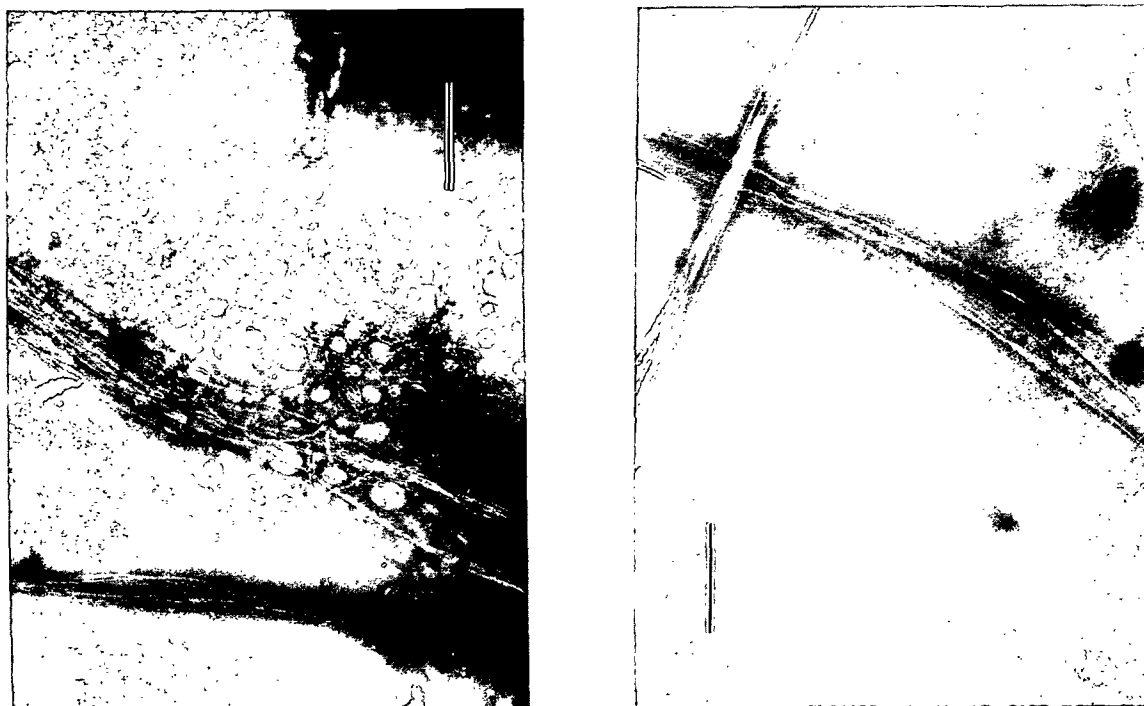


Figure 11. Micrographs of cellulose produced in mannan; no. 2481: 0.1% mannan, no. 2490: 0.8% mannan; scale bar: 0.2 μm , X72,000.

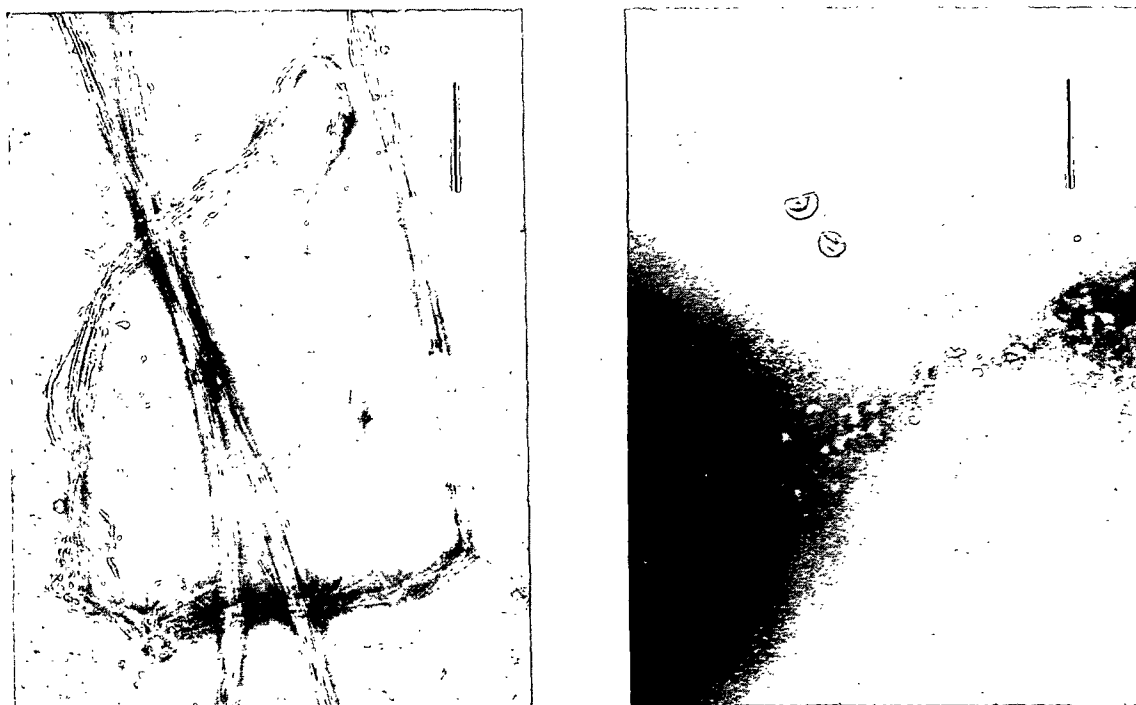


Figure 12. Micrographs of cellulose produced in xylan; no. 2454: 0.8% xylan, no. 2470: 0.1% xylan; scale bar: 0.3 μm , X48,000.

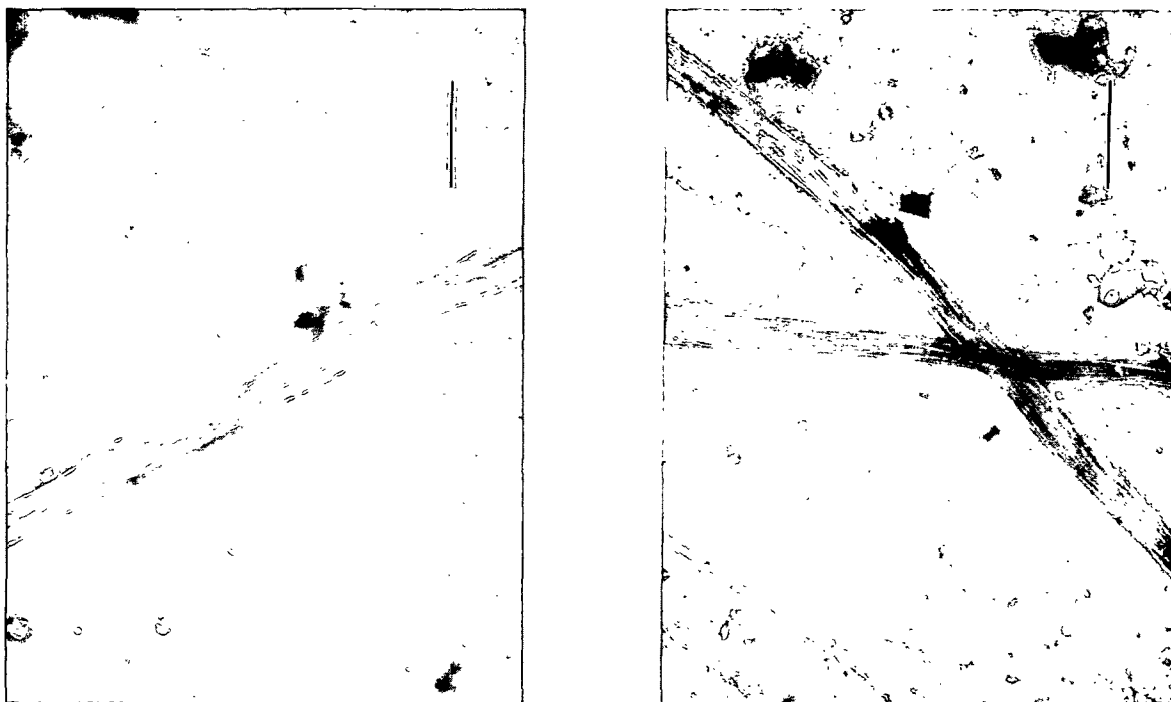


Figure 13. Micrographs of cellulose produced in 0.4% xyloglucan; no. 2419 and 2532; scale bar: 0.3 μm , X48,000.

Ribbons produced in the presence of CMC at all concentrations (0.1%, 0.4%, 0.8%) looked very similar to normal ribbons but were slightly more splayed (Figure 10).

Mannan caused the ribbons to separate but they still had more of a flat twisting appearance (Figure 11).

Xylan at 0.1% and 0.4% addition levels caused a separation of the fibrils. At 0.8% addition level, the fibrils in most cases formed a coherent bundle rather than a flat ribbon (Figure 12, no. 2454). The bundles were wavy and not twisting like the ribbons. In some instances, fuzzy fine fibrils were produced at a low addition level of xylan (Figure 12, no. 2470).

Figure 13 shows photomicrographs of cellulose produced in the presence of xyloglucan. The presence of xyloglucan splayed the ribbons. Nontwisting coherent bundles were also formed at all addition levels.

The micrographs of specimens produced in the presence of xylan and mannan also contained what looked like short fibrils. The widths of these shorter fibrils were comparable with the fibrils in the ribbons, 4 and 5 nm, respectively. The lengths of the short fibrils produced in the presence of xylan were roughly 36 nm. On the micrographs of specimens produced in the presence of mannan, the fibrils were considerably longer and averaged about 217 nm. The origin of these shorter fibrils was uncertain. One possibility is that the presence of hemicellulose caused pieces of cellulose fibril to break off. Another explanation of the short fibrils is that they were aggregates of hemicellulose. In one study of redeposition of xylan onto cellulose, the xylan formed aggregates at the surface of the microfibrils.³⁰ It is feasible that uneven spots on the Formvar film covering the grids could act as nucleation sites for aggregation of the hemicellulose.

Fibril width measurements with an image analyzer

After the photomicrographs had been digitized, the widths of the fibrils were measured on the computer screen using a distance function in the image analyzer. All widths of the long fibrils were averaged for each additive and each addition level, and the widths were plotted against the addition levels (Figure 14). The fibril widths are summarized in Table 12. For each additive, the widths were also averaged for all fibrils over the concentration range. In the sample of control cellulose, averaging the fibril widths gave as a mean $5.9 \text{ nm} \pm 1.5 \text{ SD}$, which agrees with a bacterial fibril width of 5.3-

5.5 nm reported in the literature.⁸⁴

Table 12. Fibril widths (nm) of bacterial celluloses produced in the absence or presence of additives, at different concentrations (% w/v) of the additives in the growth medium.

	CON	CMC	MAN	XYL	XGL
0.0 %	5.9±1.5	-	-	-	-
0.1 %	-	6.0±1.5	3.2±0.4	4.4±1.2	4.1±1.1
0.4 %	-	4.7±0.9	2.8±0.3	3.8±0.6	4.7±1.1
0.8 %	-	5.6±1.6	3.4±0.5	3.6±0.6	5.2±1.2
Average	5.9±1.5	5.5±1.5	3.2±0.5	4.1±1.0	4.7±1.2
Number of fibrils for averaging	54	55	52	56	103
Magnification of micrographs	48,000	48,000	72,000	48,000 (36,000)	48,000

CON: Control cellulose without additive; CMC: Cellulose produced with CMC; MAN: Cellulose produced with mannan; XYL: Cellulose produced with xylan; XGL: Cellulose produced with xyloglucan.

The fibril widths decreased in the presence of the additives over the concentration range of 0.1-0.8% additive in the medium used in this study. The presence of xylan, xyloglucan, and CMC decreased the average fibril widths to 4.1 ± 1.0 nm, 4.7 ± 1.2 nm, and 5.5 ± 1.5 nm, respectively. The presence of mannan decreased the fibril width to an average of 3.2 ± 0.5 nm.

The photomicrographs were taken at the highest magnification where it was possible to obtain a focused image. This was determined in part by the thickness of the Formvar film coating the grids. The majority of the photomicrographs were taken at a magnification of 48,000; one micrograph of xylan-cellulose was taken at 36,000, and the photomicrographs of cellulose produced in the presence of mannan were taken at 72,000. The pixel sizes of the digitized images were 0.69, 1.02, and 1.31 nm at magnifications of 72,000,

48,000, and 36,000, respectively. The higher magnification of 72,000 is a likely explanation for the lower standard deviation of the average mannan-cellulose fibril width. The magnitude of the magnification should not have any impact on the fibril-width mean values.

The standard deviations obtained for some of the average fibril widths were of significant size; the largest was 28%. The standard deviations reflected variations from different sources such as variations in the width of one fibril, variations among fibrils in one ribbon or among ribbons at one addition level of a certain additive. No test of confidence limits were performed for the influences of the presence of an additive on the average fibril widths. As an estimation, a 95% confidence interval corresponds to 1.96σ (standard deviation) which would result in no significant difference between any of the cases where cellulose was produced in the absence or presence of an additive. In spite of the lack of significant difference on the 95%-confidence level, the presence of the additives xylan, xyloglucan, and mannan resulted in trends of decreasing fibril widths. On the other hand, the trend of influence from the presence of CMC was weaker.

The method of measuring cellulose ribbon subunits with a cursor on the computer monitor was rather crude and included sources of mechanical error and subjectivity. This can be seen in the rather large ranges of values obtained for the widths of the cellulose fibrils. However, considering that fibril measurements with errors ranging from 10 to 25% can be found in the literature^{2,14}, and that the data in this study are in the order of nanometers, the method can be considered satisfactory.

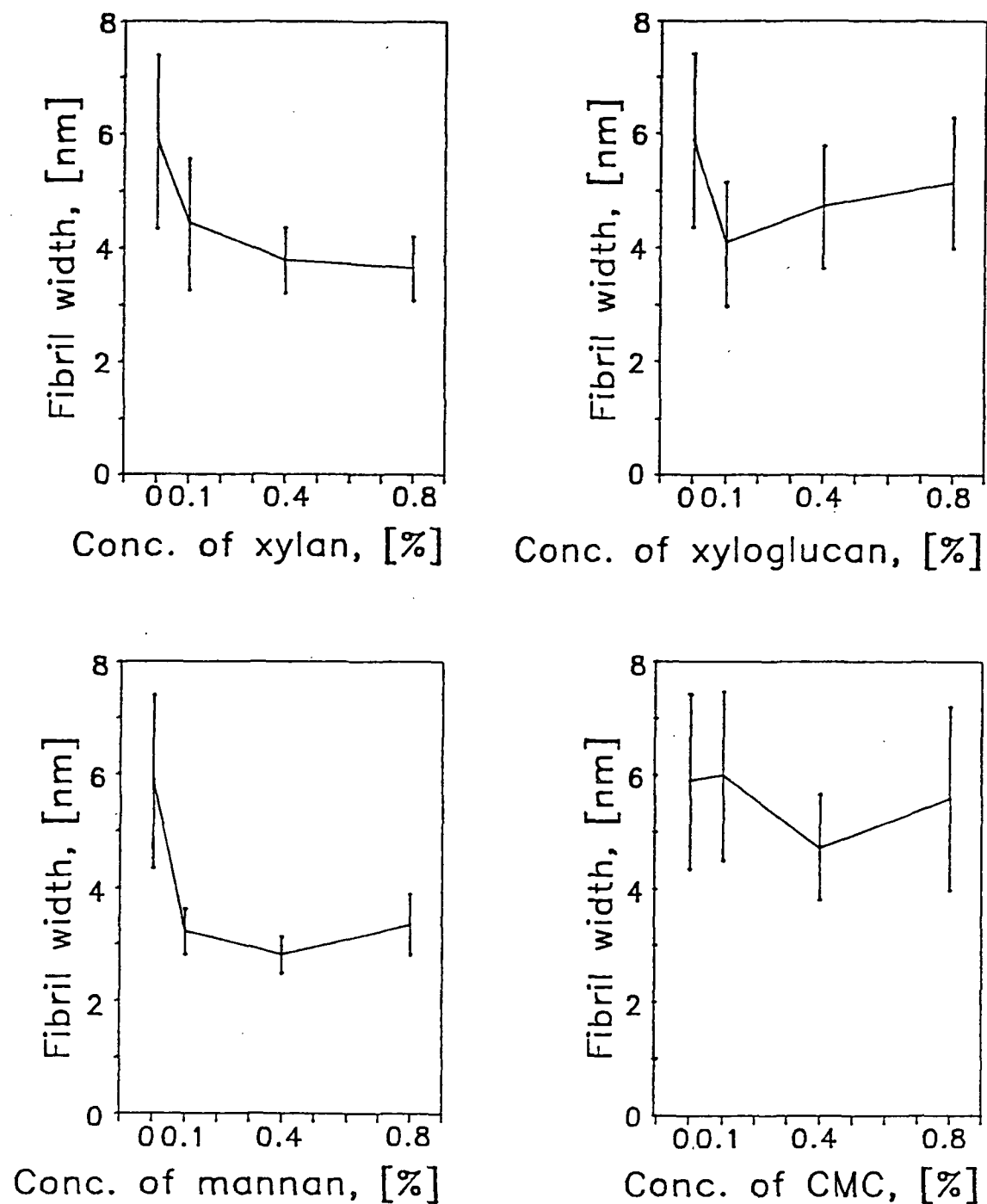


Figure 14. Fibril widths of bacterial celluloses produced in the presence of xylan (magnification of micrographs: 48,000 and 36,000), xyloglucan (X48,000), mannan (X72,000), and CMC (X48,000). The bars indicate plus-minus one standard deviation.

DISCUSSION

The influences on the aggregation pattern and morphology of bacterial cellulose were reported in the preceding section. Two implications of these results will be discussed in this section, namely the similarities between modified bacterial celluloses and celluloses from higher plants, and influences of the cellulose isolation on the aggregation pattern. Furthermore, the effect of the additives used in this study will be compared with hemicellulose-cellulose sorption in the literature. Finally, some aspects of profile fitting of x-ray diffractograms will be discussed, as will an unresolved problem with the source of two unknown Raman bands.

TRENDS OF SIMILARITIES BETWEEN MODIFIED BACTERIAL CELLULOSES AND HIGHER PLANT CELLULOSES

Comparison of the x-ray diffraction results

The celluloses from cotton and ramie were used as examples of celluloses from higher plants. The x-ray diffractograms of these celluloses are shown in Figures 15 and 16. These celluloses have a high crystallinity, but the appearances of the diffraction profiles are different from a typical bacterial cellulose which can be seen in Figure 2. The (101) and (10 $\bar{1}$) peaks are closer together in cotton and ramie celluloses than in bacterial cellulose, and the intensity ratios are different. Table 13 lists data from x-ray diffractograms of cotton and ramie celluloses.

Peak widths, positions, and intensity ratios of the bacterial cellulose samples were compared with the data from the higher plant celluloses, based on

Table 13. X-ray data for cotton (CF1) and ramie celluloses.

X-ray peaks:	101	10 $\bar{1}$	002
<u>Peak widths</u>			
Cotton	1.43	1.32	1.18
Ramie	1.42	1.48	1.40
<u>Peak positions</u>			
Cotton	14.77	16.39	22.58
Ramie	14.83	16.44	22.66
Avicel ⁸²	15.00	16.56	22.88
CF1 ⁸²	14.94	16.50	22.81
Ramie ⁸²	15.06	16.50	22.75
<u>Peak intensities</u>			
Cotton	729	0.90*I ₁₀₁	6.30*I ₁₀₁
Ramie	2044	0.92*I ₁₀₁	6.16*I ₁₀₁

The data from reference 82 are calculated with intensity functions for each peak. The other data are estimated from Figures 15 and 16.

information in Tables 8, 9, and 10 (pp. 51-53) and Table 13. Comparisons of the peak widths showed that, for all additives, their presence during incubation reduced the degree of crystallinity and the crystallite size below the magnitudes of both the control sample and the reference plant celluloses. The positions of (101) and (10 $\bar{1}$) peaks were shifted due to the influences of the additives, xylan and xyloglucan in particular, to approach the ranges of the cotton and ramie peak positions. The presence of xylan and xyloglucan shifted the (002) peak positions to lower values. This change is interpreted less readily because the information available on the (002) peak positions of cotton and ramie (Table 13) is inconsistent. Comparisons of the peak intensities revealed that the presence of the additives increased the (101) and (10 $\bar{1}$) intensity ratios toward the magnitudes found in cotton and ramie

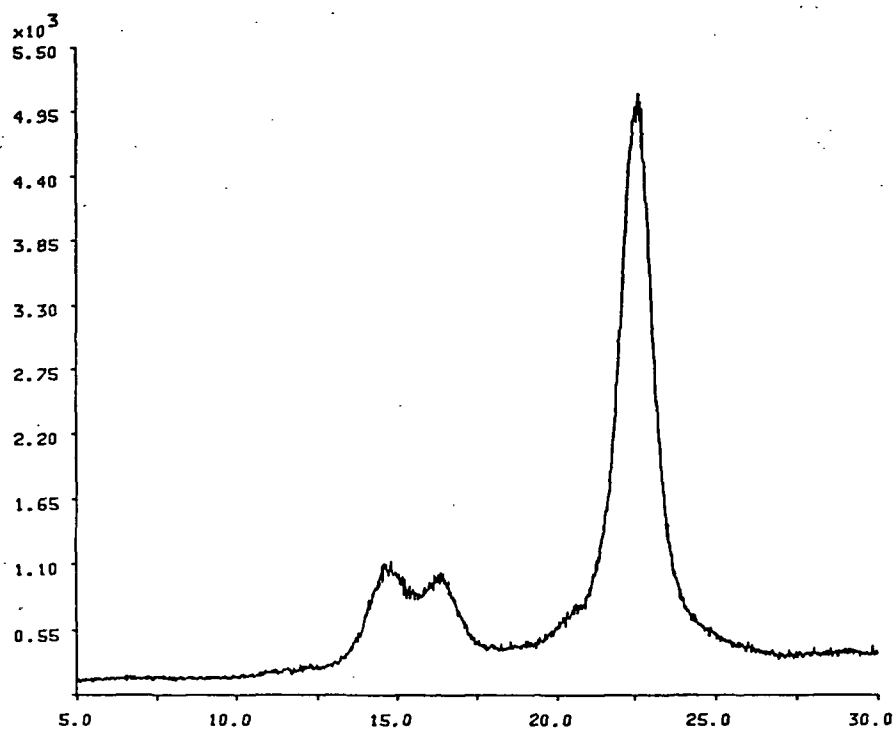


Figure 15. X-ray diffractogram of cotton (CF1) cellulose.⁸⁷

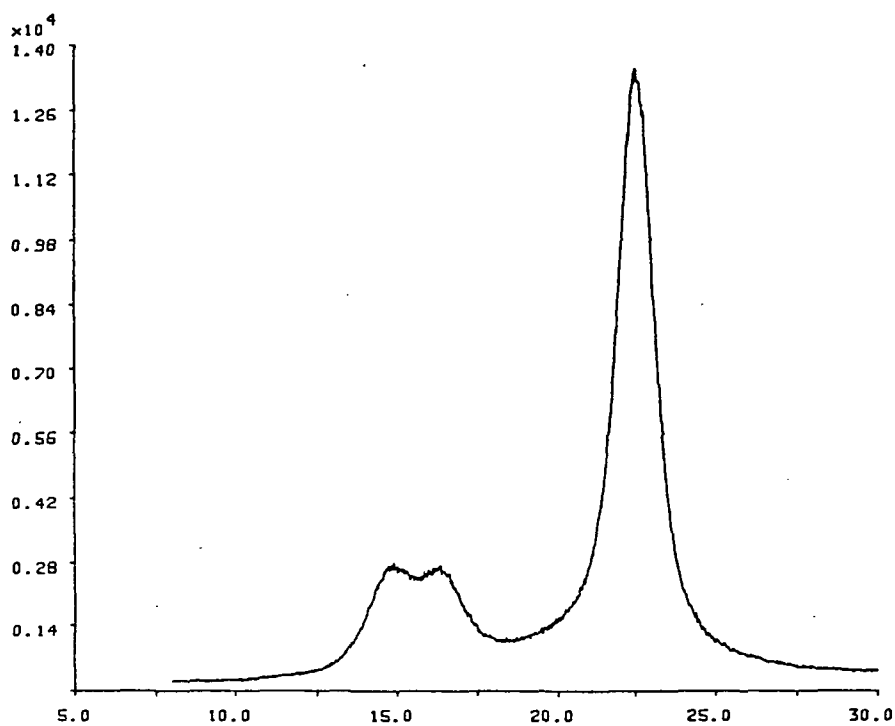


Figure 16. X-ray diffractogram of ramie cellulose.⁸³

celluloses. The ratio of 0.60 for xyloglucan (Table 10) is lower than expected and may be caused by a less accurate fit of this x-ray diffractogram because the intensity ratios of celluloses produced with xylan and xyloglucan after the 0.01 *N* NaOH and 0.1 *N* NaOH extractions are similar, which can be seen in Figure 28 in Appendix B.

In the case of all additives, their presence during incubation of bacterial cellulose has an effect on the peak widths, positions, and intensity ratios. The effects of xylan and xyloglucan are generally stronger than the effects of mannan and CMC, resulting in x-ray diffraction data that approach the data from x-ray diffractograms of ramie and cotton celluloses. This similarity can also be seen by comparing, in terms of the appearances, the x-ray diffractograms of the cotton and ramie (Figures 15 and 16) with the diffractograms of the celluloses modified by the presence of xylan or xyloglucan (Figure 2). The celluloses produced in the presence of xylan or xyloglucan no longer have the x-ray diffraction pattern of the typical bacterial cellulose but more closely resemble the pattern of higher plant celluloses.

Comparison of the Raman spectroscopy results

The Raman spectra of bacterial celluloses produced in the presence of an additive (Figures 4-8) were compared with Raman spectra of ramie fibers reported in the literature⁸⁵. The low frequency regions in the spectra of both ramie and xylan-cellulose have bands which are wider and less resolved than in a spectrum of control bacterial cellulose. The wider bands in the low frequency regions of the spectra of ramie cellulose and xylan-cellulose indicate that the cellulose crystallites are smaller in these celluloses than

in the control bacterial cellulose.⁸³ Therefore, the results of Raman spectroscopy support the results of x-ray diffraction that indicate celluloses produced in the presence of additives have decreased crystallite dimensions.

Comparison of the electron microscopy results

The fibril widths of bacterial cellulose decreased when additives were present in the growth medium (Table 12). The average width of fibrils in control cellulose was 5.9 nm. The presences of CMC, xyloglucan, xylan, and mannan decreased the average fibril width to 5.5, 4.7, 4.1, and 3.2 nm, respectively. This trend agrees with the lower values reported in the literature of fibril widths in higher plants, compared with widths of bacterial cellulose fibrils. Boylston⁸⁴ reported widths for bacterial cellulose fibrils of 5.3-5.5 nm, for cotton fibrils of 2.2-4.0 nm, and for ramie fibrils of 2.5-4.4 nm. The widths of fibrils in a conifer (*Pinus densiflora*) and a hardwood (*Populus euramericana*) are 2-5 nm as reported by Harada and Goto.⁸⁶

In summary, the results from x-ray diffraction, Raman spectroscopy, and electron microscopy all indicate that polysaccharides can have an impact on the pattern of aggregation of cellulose when they are present during cellulose production. The polysaccharides in this study which were most similar to hemicelluloses in plant cell walls had the largest impact on the structure of the cellulose. Furthermore, the changes were such that the bacterial celluloses were modified to resemble the aggregation patterns found in celluloses from higher plants. It follows, therefore, that hemicelluloses present in higher-plant cell walls may form part of the mechanisms controlling the patterns of aggregation among higher plant celluloses.

RATIO OF CELLULOSE I_α TO I_β TERTIARY STRUCTURES

It is tempting to draw the conclusion that the presence of the hemicellulose-like additives during the aggregation of bacterial cellulose changed the ratio of cellulose I_α to I_β because the x-ray diffractogram patterns and Raman spectra changed from a bacterial-type cellulose to a wood-type cellulose. (See Background-section on cellulose I_α and I_β , and hierarchical organization of cellulose structures). Cellulose I_α and I_β are tertiary structures that have been defined from analysis with solid state ^{13}C NMR. The forms I_α and I_β can also be distinguished in the O-H region of Raman spectra recorded primarily in the microprobe mode.

The magnetic resonance spectra of I_β -rich celluloses correlate well with a wood-type x-ray diffraction pattern having decreased lateral dimensions and lower degree of orientation. This correlation is true for all specimens investigated except for one particular alga, *Laminaria japonica*. This alga has an x-ray diffractogram pattern and a Raman spectrum of a wood-type cellulose, but the ^{13}C NMR spectrum shows a distinct cellulose I_α .^{10,87} Because of this exception to the otherwise consistent division between I_α -rich bacterial-type cellulose on one hand, and I_β -rich wood-type cellulose on the other hand, it is not possible to conclude from x-ray diffraction and Raman spectroscopy anything about the ratio of I_α to I_β in the bacterial celluloses produced in the presence of the additives. However, the changes in the x-ray diffraction patterns and Raman spectra that did occur upon introduction of the additives suggest that a change in the I_α -to- I_β ratio may have taken place.

The Raman spectra of the bacterial cellulose samples were compared in order to base any conclusion of the I_α -to- I_β ratio on the hydrogen bonding

patterns. The high frequency regions ($3000\text{--}3700\text{ cm}^{-1}$) of the Raman spectra of the control bacterial cellulose and of celluloses prepared in the presence of additives were expanded. It was not possible to distinguish any features in these spectra attributable to either of the cellulose I_α or I_β crystalline forms. Reasons could be that the Raman spectra were not recorded in the microprobe mode, or, for such detailed analysis, the amounts of the samples were too small or the spectra quality was inferior.

CELLULOSE AGGREGATION ALTERATIONS RELATED TO THE ADDITIVE STRUCTURES

The results from the x-ray diffraction and Raman spectroscopy could be divided into three groups: 1. control cellulose, 2. CMC- and mannan-influenced celluloses, and 3. xylan- and xyloglucan-influenced celluloses. This suggests that the additives interacted with the bacterial cellulose in two different ways. The xyloglucan did not have functional groups, and the xylan had a low degree of substitution of uronic acids as functional groups ($DS \approx 0.12$).⁷¹ Hence, the conformations of xyloglucan and xylan were similar to the cellulose conformation, and it was possible for xyloglucan and xylan to co-crystallize with the cellulose. One mechanism could be by molecular replacement in the crystalline lattice when xylan or xyloglucan were present during the aggregation of nascent cellulose. This would create a defect structure within the cellulose lattice.

The additives CMC and mannan were less similar to cellulose than xylan and xyloglucan. CMC had extended functional groups in the form of charged carboxymethyl side-chains which would prevent any closer interaction with the cellulose aggregation. In terms of conformational dissimilarities of the sugar moieties, the mannose unit in mannan was the least similar of the sugars

in the additive backbones to the glucose unit in cellulose. This is due to the axial hydroxyl group at C2 in mannose instead of an equatorial position as in glucose and xylose. Another possible reason for the weak interaction between mannan and cellulose was the relatively low molecular-weight of the mannan fraction used in this study. The molecular weight of the mannan was the lowest of the additives studied.

As a result of their conformation, CMC and mannan lowered the degree of crystallinity of the bacterial cellulose and decreased the crystallite sizes. Xylan and xyloglucan decreased the degree of crystallinity and, more important, probably blended intimately with the cellulose during its aggregation and changed the cellulose lattice structure.

The presence of mannan during cellulose aggregation decreased the crystallite sizes and the fibril widths by approximately the same amounts as the presence of xylan or xyloglucan. However, the aggregation pattern was not changed as much by the presence of mannan as by the presence of xylan or xyloglucan. The mannan molecules may have been capable of interacting with the cellulose molecules during the aggregation and thereby decreased the crystallite and fibril sizes. The dissimilarities of the cellulose and mannan backbones may have prevented further association with additional cellulose molecules and limited the changes of the cellulose crystalline lattice.

The effects of the different additives were similar but not identical. The additives resemble different hemicelluloses that are associated with different layers of the cell walls. It is likely that the hemicelluloses in cell walls of higher plants interact, as selective moderators in a manner similar to what has been shown in the results of this study, with the

aggregation of cellulose as it is deposited in the cell walls.

POLYMER CHEMISTRY OF ADDITIVE SOLUTIONS

The sorption and reaction behavior of the additives could be a function of the polymer chemistry of the solutions. One interpretation of the results could be that the additives were merely precipitating on the cellulose and were not incorporated in the cellulose lattice. The solubility of β -(1-4)-linked polysaccharides depends on factors such as the molecular weight, carbohydrate composition, and substitution pattern. Lower molecular-weight polysaccharides are more readily dissolved than higher molecular-weight fractions. Polysaccharide backbones consisting of hexoses, rather than pentoses, are stiffer and, hence, less soluble. The polysaccharide solubility is increased considerably if the backbone is substituted compared with an unsubstituted polysaccharide such as cellulose.

The relative importance of these factors on the actual solubility of a polysaccharide is difficult to quantify, which makes the relative solubilities of the additives used in this thesis hard to predict because the additives differ in several aspects. The mannan has a low molecular weight (higher solubility) but is unsubstituted (lower solubility); the xylan backbone is less rigid (higher solubility) and this additive has uronic acid substituents (higher solubility); the xyloglucan has a very high molecular weight (lower solubility) but also a high degree of side chains (higher solubility); the CMC has a relatively high molecular weight (lower solubility) and charged functional groups (higher solubility).

All additives were water-soluble and were dissolved in concentrations up

to 0.8% in the incubation solutions for electron microscopy specimens. The dissolution rates of the additives were quite different. By empirical observations, xylan appeared to have the highest rate of dissolution, followed by CMC, mannan, and xyloglucan. The xyloglucan never showed any signs of precipitation but required storage at +2-4°C for approximately 12 hr to dissolve. The ease of dissolution did not seem to correlate with the approximate order of disrupting power on the cellulose lattice. Xylan and xyloglucan were the most effective, followed by mannan and then CMC. This observation in addition to the fact that the extracted cellulose samples were prepared from incubation solutions containing 0.1% additive ruled out the possibility that the additives were precipitating.

A dissolved molecule of the additives can take on different conformations, such as a sphere or rod. The difference in conformation of the additives in solution may have influenced their interaction with cellulose. The higher molecular-weight additives are more likely to be in a coiled spherical or rod-shaped form, which is less likely to be able to interact with a cellulose molecule. However, in this case, xyloglucan had the highest molecular weight, in addition to a strong effect on the cellulose aggregation pattern. This result strongly suggests that the conformation of the additives in solution did not influence their interactions with cellulose.

EFFECT OF ISOLATION PROCEDURES ON THE CELLULOSE AGGREGATION PATTERNS

As the bacterial celluloses produced in the presence of additives were extracted with sodium hydroxide solutions of increasing strength, the appearance of the x-ray diffractograms and Raman spectra changed. These changes were more pronounced in cellulose produced in the presence of xylan

and xyloglucan than in the control sample of cellulose and celluloses produced in the presence of CMC and mannan. The extraction series of celluloses produced in the presence of xylan is represented by the x-ray diffractograms, Figure 17, and Raman spectra, Figure 18. Comparable results from the other additives can be found in Appendix B and C.

The pattern of aggregation of the molecules in a cellulosic material provides a basis for the physical properties of a material. Properties such as extensibility and tensile strength are related to the nature and degree of crystallinity and the crystallite orientation of a cellulose fiber.^{88,89} Therefore, if the aggregation pattern, or tertiary structure, of a cellulose changes, it is expected that the physical properties of this material also will change. The differences between the diffractograms (Figure 17) and the spectra (Figure 18) indicate that the properties of the celluloses would indeed be different depending on what procedure was used to prepare the cellulose. If we go back to the quotation by Preston⁷ referred to in the Introduction, which stated that removal of noncellulosics would only sharpen the x-ray arcs, the point could be made that photographs, instead of diffractograms, of x-ray diffractions such as those in Figure 17 would probably show the same effect described by Preston.

The discussion presented here of the influence of isolation procedures on the cellulose structure is far from complete but does show evidence of an influence. If the underlying phenomena that determine the tertiary structures of cellulose can be understood, the properties of cellulosic materials may be intentionally altered.

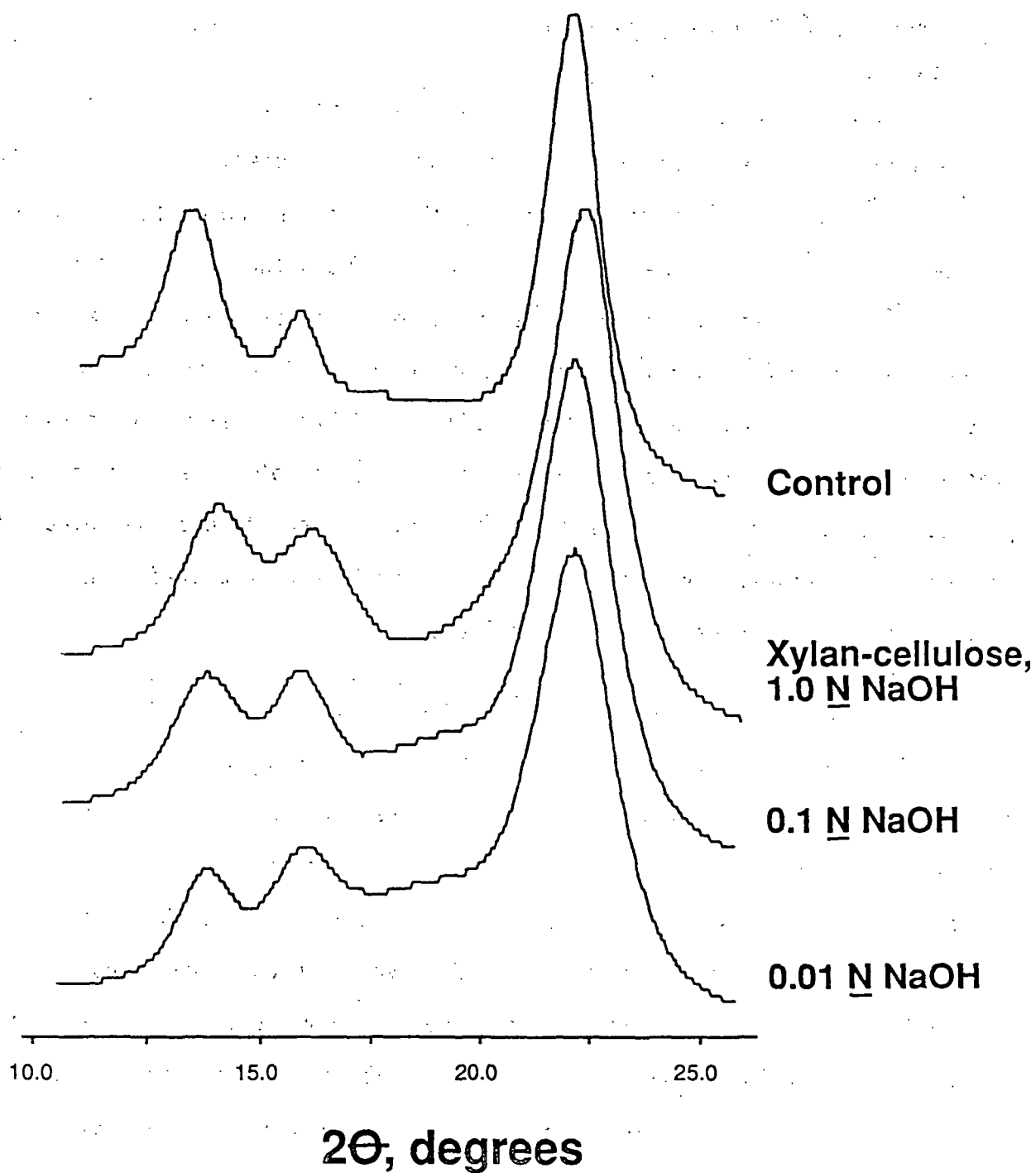


Figure 17. X-ray diffractograms of control cellulose after the last extraction and xylan-celluloses after each extraction step.

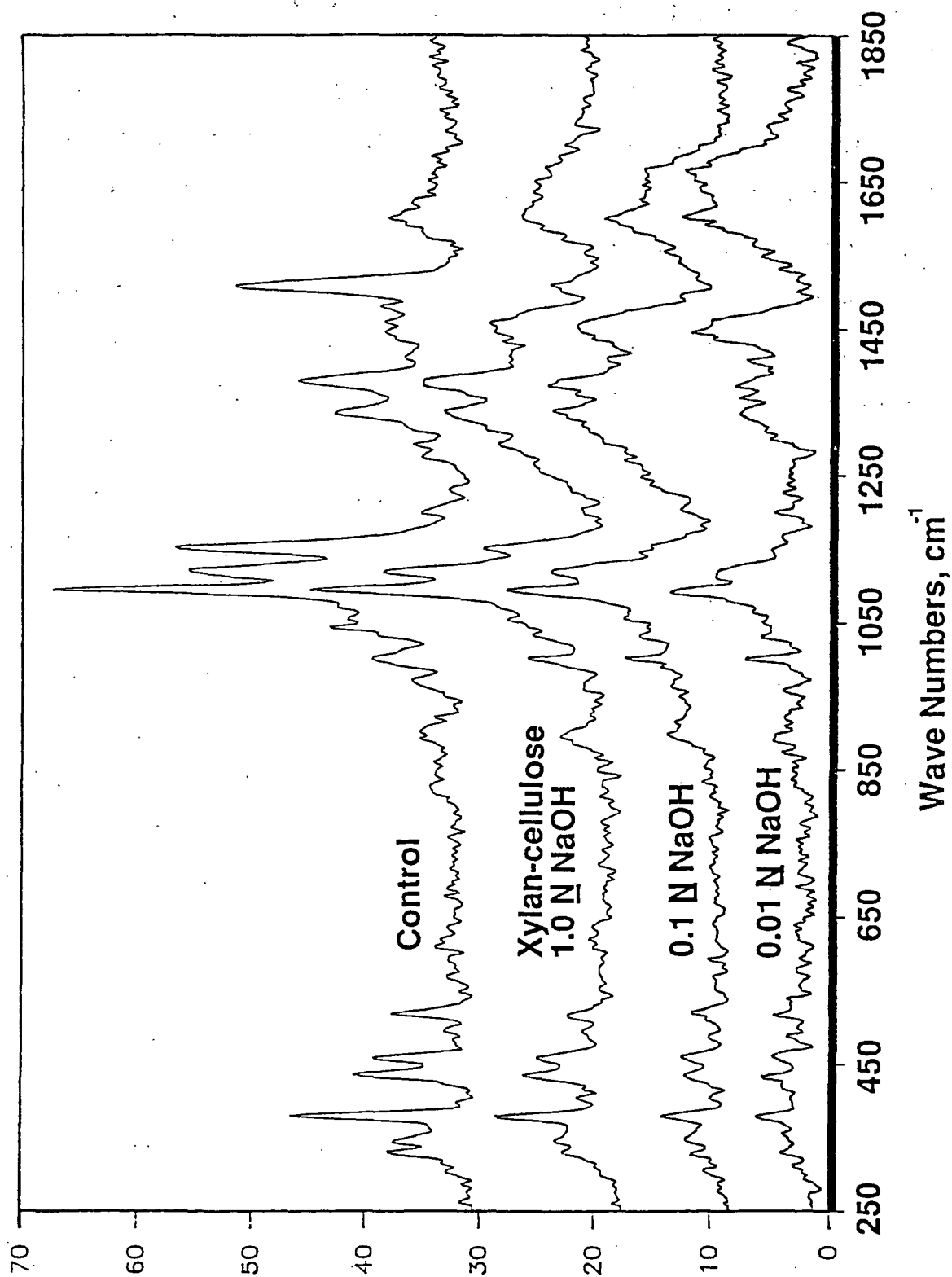


Figure 18. Raman spectra of control cellulose after the last extraction and xylan-celluloses after each extraction step.

ADDITIVES USED IN THIS STUDY AND INTERACTIONS IN CELL WALLS

There are obviously many differences between the additives used in this study and the polysaccharides that can be found in the plant cell walls. One difference is the origins of the mannan and xyloglucan, which were ivory nuts and tamarind seeds, respectively, instead of plant cell walls. Mannan in ivory nuts and xyloglucan in tamarind seeds function as storage reserve polysaccharides rather than being involved in structural reinforcement of the plants. There is a striking difference between the difficulty with which primary wall xyloglucan can be isolated compared with the ease of isolating xyloglucan from tamarind seeds. The xyloglucan in primary cell walls is probably strongly associated with the cellulose there, whereas cellulose is not present in the seeds.

The polysaccharides from seeds and primary walls are structurally different. Mannan from ivory nuts is a homopolymer. In plant cell walls, mannan occurs as a copolymer in the form of galactoglucomannan or glucomannan. The structural differences between xyloglucans from seeds and primary walls are small relative to the differences of the mannans. Xyloglucan in seeds is a β -(1 \rightarrow 4)-glucan with xylose side chains, either single or with a terminal galactose. Primary cell-wall xyloglucan has the same type of backbone as seed xyloglucan. The side chains often have terminal fucose units in addition to the terminal galactose units. The ratios of sugar units are slightly different in xyloglucans from seeds and primary walls, but essentially the same.

Another difference is that the mannan and xylan used in this study was of lower molecular weight than would be present in plant cell walls; the

difference was especially large in the case of the mannan. The reason is that the additives had to be water-soluble to be used with the resting cell method for producing bacterial cellulose. However, the presence of this low molecular weight xylan had a strong effect on the aggregation pattern of cellulose and the presence of the mannan a more moderate effect. These effects are expected to be stronger if a xylan or mannan of higher DP is used.

Clayton and Phelps²⁹ compared the rates of sorption of a glucomannan (from white spruce) and a xylan (from white birch) and found that the sorption rate of the glucomannan was about twice as high as the sorption rate of the xylan. Xylan was expected to have a higher sorption than the glucomannan because of the conformational similarities of the positions of the hydroxyl groups with glucose in cellulose. The xylan had a lower degree of polymerization than the glucomannan, which also led to the expectation of higher sorption.

The authors suggested that the reason for the faster sorption of the glucomannan is that it may not contain uronic acid groups, overriding such factors as lower DP and conformational similarity. Stephen⁶¹, on the other hand, suggested that, whereas the unsubstituted portions of the xylan molecule can associate with cellulose chains, the absence of a primary alcohol group greatly diminishes the capacity of xylan chains to join with each other or with other polysaccharides. Mora *et al.*³⁰ found that the xylan-xylan interactions were stronger than the cellulose-xylan interactions. The reason for this discrepancy may be that the xylans referred to are of different sources and, therefore, have slightly different structure.

The results of the present study showed that the ivory nut mannan

fraction used here had a lower degree of influence on the cellulose structure than the birch xylan. As before, the mannan backbone instead of a glucomannan backbone or the low molecular weight may explain the different results.

In comparing the interactions of xylan and xyloglucan with cellulose, Molinarolo²⁷ found the maximum specific sorption of xyloglucan to be less than half of the sorption of a glucuronoarabinoxylan. On the other hand, Hayashi *et al.*²⁵ found that xyloglucan sorption was decreased to half with a xylan also present in the system but in a 10-fold excess. In this thesis, the influences of xylan and xyloglucan were similar, which could indicate similar magnitudes of interactions with cellulose. One needs to be careful in making these comparisons because most studies in the literature are based on sorption by mature cellulose whereas the influence on the aggregation of nascent cellulose was studied in this thesis.

PROFILE FITTING OF X-RAY DIFFRACTOGRAMS

The profile fitting program was developed to fit x-ray diffractograms of inorganic material or simpler diffractograms of polymers, and is less suitable for complex patterns such as those of cellulose or of samples containing material with lower crystallinity. The limitation in decreasing the fitting step size gave rather crude peak profiles. The x-ray diffractograms of bacterial celluloses before the alkaline extractions had substantial background of amorphous material, and the profile fitting of these diffractograms gave less reproducible results than the diffractograms recorded after later extractions.

The goodness of an individual peak fit was given by an estimated

standard deviation (σ). Values of 1.0-1.5 for σ were considered acceptable by the software producer. In this thesis, the peak fits had σ -values ranging from 0.467 to 0.692 which indicated satisfactory fittings. The overall fitting goodness depended primarily on that the number of fitted peaks represented the physical situation. No statistical test of the overall fitting was performed by the profile fitting program, but the goodness could be estimated from the match of the fitted total profile with the experimental diffractogram and from the magnitude of the residual data. The residual data were calculated from the raw data minus the sum of all fitted profiles and the background.

The fittings of the outer peaks in the diffractograms (101 and 002) were less variable than the fittings of the middle peaks in the diffractograms (10 $\bar{1}$ and amorphous). A possible reason for this is that the fitting of the middle peaks has error contributions from two sides. Different sensitivities of the peaks to chemical treatments can also contribute to this phenomenon. The small sample sizes in this study resulted in diffractograms with low signal-to-noise ratios which also may have contributed to a less accurate fitting.

RAMAN BANDS AT 1152 AND 1506 cm^{-1}

The Raman spectra of the bacterial celluloses after the last extraction with 1.0 N NaOH had increased intensities at 1152 and 1506 cm^{-1} (1152 and 1510 cm^{-1} in the spectrum of xylan-cellulose). The 1152-band, but not the 1506-band, is normally present at a much lower intensity in the Raman spectrum of cellulose I. The intensities of the 1506-band were of increasing magnitude in the spectra of xylan-, xyloglucan-, mannan-, CMC-, and control cellulose. The intensity of the 1152-band correlated with the intensity of the 1506-band.

The unknown bands may have originated in the bacterial cells which were not removed completely from the cellulose samples. The alkaline extractions in this study were performed at room temperature. However, to remove proteins from wood celluloses, boiling in alkali is required. Boiling a bacterial cellulose pellicle in 1% NaOH removed the cell material and did not result in increased intensities at 1152 and 1506 cm^{-1} . It is possible that the extraction with 1.0 N NaOH degraded the bacterial cells, but did not fully remove the degradation products.

The weights of the cellulose samples after the last extraction were about one mg and increased in the following order: control-, mannan-, CMC-, xylan-, and xyloglucan-cellulose - approximately opposite to the order of increasing intensities of the unknown bands. The smaller samples were more difficult to collect after washing, and less likely to be thoroughly washed. This would suggest that the unknown bands were from some compounds that were not washed off the cellulose products.

The sharpness of the unknown bands suggests they originate from an isolated functional group in an organic molecule, or from an inorganic source. If not from the bacterial cells, the unknown bands may be from a contaminant present in the sodium hydroxide or on the glassware used.

CONCLUSIONS

Bacterial cellulose was produced by nondividing cells in a system such that polysaccharides added to the growth medium interacted with the cellulose during its aggregation. The cellulose produced in the absence of and in the presence of polysaccharides consisted of cellulose I as the predominant polymorph, with subtle differences in the aggregation patterns. These differences were found in the widths, intensity ratios, and positions of the x-ray diffractogram peaks, and in the widths and resolution of the Raman bands. These differences indicate that the presence of additives decreased the degrees of crystallinity and orientation, and changed the unit cell dimensions of the cellulose. The cellulose produced in the presence of additives had narrower fibril widths than the controls, revealed *via* transmission electron microscopy. The narrower fibrils agreed with the widths of cellulose fibrils reported for higher plants.

The additives influenced the cellulose aggregation in different ways by their presence. The presence of CMC slightly decreased the crystallite sizes and fibril widths. The presence of xylan or xyloglucan caused a larger decrease of the crystallite sizes and fibril widths, and also caused a change in the aggregation patterns. The presence of mannan decreased the crystallite sizes approximately as much as the presence of xylan or xyloglucan. However, the cellulose aggregation patterns were not as strongly altered by the presence of mannan as by the presence of xylan or xyloglucan. It was concluded that xylan and xyloglucan were capable of incorporating into the cellulose crystalline lattice because their backbones were relatively similar to the cellulose backbone. Mannan were capable of associating with the

aggregating cellulose but the greater dissimilarities between the mannan and cellulose prevented further association with subsequently aggregating cellulose, thereby causing decreased crystallite and fibril lateral dimensions but limiting the changes of the cellulose crystalline lattice.

The presence of xylan or xyloglucan changed the aggregation pattern of the bacterial cellulose to resemble the type of aggregation pattern found in celluloses from higher plants. As a result of these observations, polysaccharides in the plant cell walls are proposed to participate, in ways similar to the effects found in this study, in determining the aggregation patterns of celluloses in higher plants. Results from earlier studies^{62,63} indicate that different types of hemicelluloses are present in different proportions in each cell wall layer. This study indicates that hemicelluloses in the cell walls of higher plants may participate as selective moderators which determine different modes of aggregation of cellulose during the biogenesis of the separate plant cell-wall layers.

The procedure for isolation of a cellulose from hemicellulose, lignin, and other wood components, is one factor which determines the pattern of aggregation of the particular cellulose, and, thus, the nature and properties of a cellulosic material.

RECOMMENDATIONS

The presence of polysaccharide additives during aggregation of cellulose may have an impact on the ratio of the cellulose crystalline forms I_α and I_β , as determined by solid state ^{13}C NMR spectroscopy. A positive conclusion about this impact could not be drawn on the basis of the x-ray diffraction and Raman spectroscopy results in this study. A further investigation of the ratio of cellulose I_α to I_β of the bacterial celluloses produced in the presence of hemicelluloses would be valuable. The procedure for cellulose production from resting cells would have to be modified or multiplied to produce enough material for analysis with solid state ^{13}C NMR.

The hydrogen bonding pattern of the samples could reveal the ratio of I_α to I_β if the Raman spectra would be recorded on oriented samples. This could be accomplished by drying the celluloses under tension to get oriented samples, and then recording Raman spectra in the microprobe mode with the electric vector of the light parallel (0°) to the fibril axis.

The synergistic effects of a mixture of hemicelluloses on the cellulose aggregation pattern is another interesting area to investigate further. This would more truly represent the situation in a plant cell wall where the hemicelluloses are not present one at a time with the cellulose. It is possible that the interactions with cellulose are stronger when mixtures of hemicelluloses are used.

ACKNOWLEDGEMENTS

I sincerely thank Dr. Rajai Atalla, Dr. Norm Thompson, Dr. Terry Conners, and Dr. Morris Johnson, the members of the thesis advisory committee, for their guidance, contributions, and encouragement throughout the course of this thesis.

The financial support of this research by The Gunnar and Lillian Nicholson Graduate Fellowship and Faculty Exchange Fund, and the Institute of Paper Science and Technology and its member companies is gratefully acknowledged.

Many of the staff, faculty, and students at the Institute have contributed to this investigation with their advice and assistance for which I am very grateful. Special thanks are in order to Becky Whitmore and Clark Woitkovich for their help with the Raman spectrometer and x-ray diffractometer, and to Dr. Sue Molinarolo who generously provided the xyloglucan.

I thank Dr. Candace Haigler and Dr. Moshe Benziman for valuable discussions regarding preparation of bacterial cellulose. The gift of bacterial culture from Dr. Haigler is highly appreciated.

While working on this thesis, my life was made easier by the help from many wonderful people. Fellow students at the Institute have supplied plenty of encouragement, great company, and challenging discussions. Lots of thanks to Beth, Bob, and Pat, who helped me through the last year in Appleton. I also thank the U.S.D.A. Forest Products Laboratory for letting me use the

facilities in Madison, and John and John for their help.

I thank my family back home for their encouragement which kept coming so regularly in a stamped envelope. Finally, I thank my husband Allan for his support and patience during the completion of this thesis.

LITERATURE CITED

1. Ben-Hayyim, G. and Ohad, I., J. Cell Biol. 25:191-207 (1965).
2. Haigler, C.H.; Brown, R.M., Jr.; Benziman, M., Science 210:903-6 (1980).
3. Brown, R.M., Jr.; Haigler, C.H.; Cooper, K., Science, 218:1141-42 (1982).
4. Haigler, C.H.; White, A.R.; Brown, R.M., Jr.; Cooper, K.M., J. Cell Biology 94:64-69 (1982).
5. Kai, A.; Koseki, T., Chemistry Letters, The Chemistry Society of Japan, pp. 607-10 (1985).
6. Mullis, R.H.; Thompson, N.S.; Parham, R.A., Planta (Berl.) 132:241-48 (1976).
7. Preston, R.D. The Physical Biology of Plant Cell Walls, Chapman and Hall, London, 1974, p. 170.
8. Atalla, R.H., in "Cellulose: Structural and Functional Aspects", (J.F. Kennedy, G.O. Phillips and P.A. Williams, eds.) Ellis Horwood, in press.
9. Atalla, R.H., J. Appl. Polym. Sci.: Appl. Polym. Symp. 37:295-301 (1983).
10. Atalla, R.H.; VanderHart, D.L., in "Cellulose and Wood, Chemistry and Technology", Proc. 10th Cellulose Conf. (C. Schuerch, ed.) Wiley Interscience, John Wiley & Sons, New York, 1989, pp. 169-88.
11. Asai, T, Acetic Acid Bacteria, Classification and Biochemical Activities. University Park Press, Baltimore 1968.
12. Pasteur, L., Etudes sur le vinaigre, Paris, 1868.
13. Brown, A.J., J. Chem. Soc. 49:432-39 (1886), 51:643 (1887).
14. Zaar, K., Cytobiologie 16:1-15 (1977).
15. Brown, R.M., Jr.; Willison, J.H.M.; Richardson, C.L., Proc. Natl. Acad. Sci. USA 73(12):4565-69 (1976).
16. Zaar, K., J. Cell Biology 80:773-77 (March, 1979).
17. Schramm, M.; Hestrin, S., J. Gen. Microbiol. 11:123-9 (1954).
18. Williams, W.S.; Cannon, R.E., Appl. Environm. Microbiol. 55(10):2448-52 (1989).
19. Haigler, C.H., Dept. Biol. Sci., Texas Tech. Univ., Lubbock, TX, Personal communication, 1988.

20. Allen, R.L.M., Colour Chemistry, Thomas Nelson and Sons Ltd., London, 1971. p. 278-79.
21. Venkataraman, K., The Analytical Chemistry of Synthetic Dyes, Wiley-Interscience Publication, New York, 1977. p. 7.
22. Haigler, C.H.; Chanzy, H. J. Ultrastructure and Molecular Structure Research 98:299-311 (1988).
23. Kai, A., Makromol. Chem., Rapid Commun. 5(6):307-10 (1984).
24. Haigler, C.H.; Benziman, M., in "Cellulose and Other Natural Polymer Systems: Structure, Biogenesis and Degradation" (Brown, R.M., Jr., ed.) Plenum, New York, 1982. pp. 273-297.
25. Hayashi, T.; Marsden, M.P.F.; Delmer, D.P., Plant Physiol. 83:384-89 (1987).
26. Valent, B.S.; Albersheim, P., Plant Physiol. 54:105-8 (1974).
27. Molinarolo, S.L. Sorption of Xyloglucan onto Cellulose Fibers. Doctoral Dissertation. Appleton, WI, The Institute of Paper Chemistry, 1989.
28. Walker, E.F., Tappi 48(5):298-303 (1965).
29. Clayton, D.W.; Phelps, G.R., J. Polym. Sci.: Part C 11:197-220 (1965).
30. Mora, F.; Ruel, K.; Comtat, J.; Joseleau, J.-P., Holzforschung 40:85-91 (1986).
31. Most, D.S., Tappi 40(9):705-712 (1957).
32. Laffend, K.B.; Swenson, H.A., Tappi 51(3):118-122 (1968).
33. Russo, V.A.; Thode, E.F., Tappi 43(3):209-18 (1960).
34. Dugal, H.S.; Swanson, J.W., Tappi 55(9):1362-1367 (1972).
35. Blackwell, J; Kurz, D.; Su, M.-Y.; Lee, D.M., in "Structures of Cellulose" (R.H. Atalla, ed.) ACS Symp. Ser. No. 340, Am. Chem. Soc., Washington, DC, 1987, pp. 199-213.
36. Simon, I.; Scheraga, H.A.; Manley, R.St.J., Macromolecules 21:983-990 (1988).
37. Simon, I.; Glasser, L.; Scheraga, H.A.; Manley, R.St.J., Macromolecules 21:990-998 (1988).
38. Sarko, A., in "Cellulose Structure, Modification and Hydrolysis" (R.A. Young and R.M. Rowell, eds.) John Wiley & Sons, New York, 1986, pp. 29-49.
39. Hayashi, J.; Kon, H.; Takai, M.; Hatano, M.; Nozawa, T., in "Structures of Cellulose" (R.H. Atalla, ed.) ACS Symp. Ser. No. 340, Am. Chem. Soc.,

IPC19 . 001 BM 24OCT88
 MANNON, 176-3/120MG/D2O-NAOD
 13C, 91MHZ

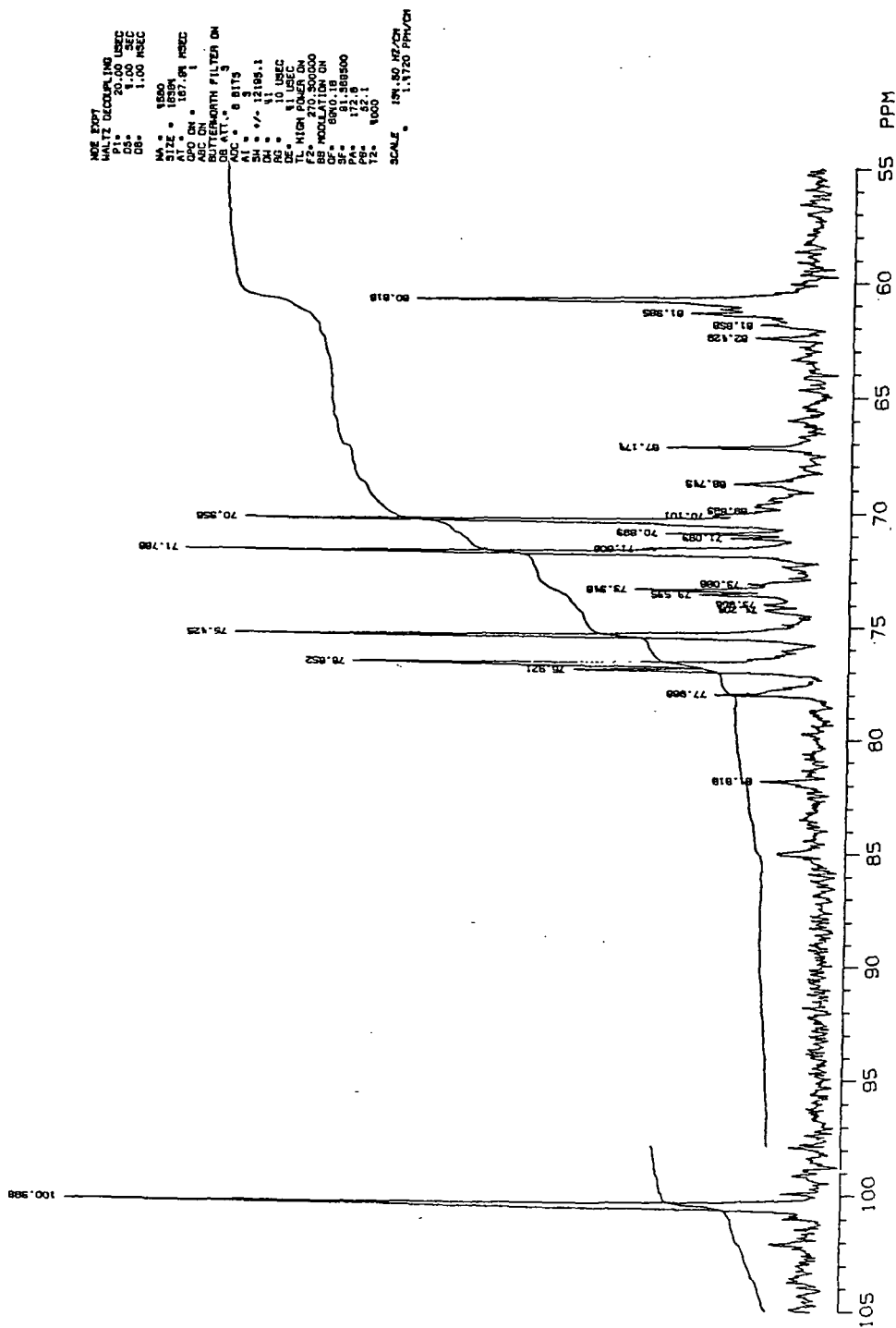


Figure 19. ^{13}C NMR spectrum of mannan.

Washington, DC, 1987, pp. 135-50.

40. Atalla, R.H., in "Structures of Cellulose" (R.H. Atalla, ed.) ACS Symp. Ser. No. 340, Am. Chem. Soc., Washington, DC, 1987, pp. 1-14.

41. French, A.D.; Roughead, W.A.; Miller, D.P., in "Structures of Cellulose" (R.H. Atalla, ed.) ACS Symp. Ser. No. 340, Am. Chem. Soc., Washington, DC, 1987, pp. 15-37.

42. Miller, D.P., Tappi Int. Dissolving Pulps Conf. 1987, pp. 177-80.

43. Atalla, R.H., Appl. Polym. Symp. 28:659-69 (1976).

44. Isogai, A.; Ishizu, A.; Nakano, J.; Atalla, R.H., in "Structures of Cellulose" (R.H. Atalla, ed.) ACS Symp. Ser. No. 340, Am. Chem. Soc., Washington, DC, 1987, pp. 292-301.

45. Atalla, R.H., in "Industrial Polysaccharides, Biomedical and Biotechnological Advances", Proceedings of the 3rd International Workshop, (V. Crescenzi, I.C.M. Dea, S. Paoletti, S.S. Stivala and I.W. Sutherland, eds.) Gordon and Breach Science Publishers, in press.

46. Marrinan, H.J.; Mann, J., J. Polym. Sci. 21:301-11 (1956).

47. Atalla, R.H.; VanderHart, D.L., Science 223:283-85 (1984).

48. VanderHart, D.L.; Atalla, R.H., Macromolecules 17:1465-72 (1984).

49. Horii, F.; Yamamoto, H.; Kitamaru, R.; Tanahashi, M.; Higushi, T., Macromolecules 20:2946-49 (1987).

50. Hirai, A.; Horii, F.; Kitamaru, R., Macromolecules 20:1440-42 (1987).

51. Chanzy, H.; Henrissat, B.; Vincendon, M.; Tanner, S.F.; Belton, P.S., Carbohydrate Research, 160: 1-11 (1987).

52. Thompson, N.S., Appleton, WI, Personal communication, 1989.

53. Kooiman, P., Recueil Des Travaux Chimiques Des Pays-Bas 80:840-865 (1961).

54. Hayashi, T.; MacLachlan, G., in "Cellulose Structure, Modification and Hydrolysis" (R.A. Young and R.M. Rowell, eds.) John Wiley & Sons, New York, 1986, pp. 67-76.

55. Hayashi, T.; MacLachlan, G., Plant Physiol. 75:596-604 (1984).

56. Hayashi, T.; Delmer, D.P., Carbohydrate Res. 181:273-77 (1988).

57. Talmadge, K.W.; Keegstra, K.; Bauer, W.D.; Albersheim, P., Plant Physiol. 51:158-73 (1973).

58. Nealey, L.T. The Isolation, Characterization, and Biological Testing of Xyloglucan from Suspension Cultured Loblolly Pine Cell Spent Medium. Doctoral

Dissertation. Appleton, WI, The Institute of Paper Chemistry, 1987.

59. Hayashi, T.; Wong, Y.-S.; MacIachlan, G., *Plant Physiol.* 75:605-10 (1984).

60. Fry, S.C., *Planta* 169:443-453 (1986).

61. Stephen, A.M., in "The Polysaccharides" (G.O. Aspinall, ed.) Academic Press, New York, 1983, Vol. 2, pp. 97-193.

62. Sjöström, E., *Wood Chemistry, Fundamentals and Applications*, Academic Press, New York, 1971.

63. Byers, E.M. An Autoradiographic Study of the Hemicellulose Distribution in the Walls of *Pinus resinosa* Tracheids. Doctoral Dissertation. Appleton, WI, The Institute of Paper Chemistry, 1989.

64. Aspinall, G.O.; Hirst, E.L.; Percival, E.G.V.; and Williamson, I.R., *J. Chem. Soc.* pp. 3184-88 (1953).

65. Aspinall, G.O.; Rashbrook, R.B.; Kessler, G., *J. Chem. Soc.* pp. 215-21 (1958).

66. Timell, T.E., *Can. J. Chem.* 35:333-38 (1957).

67. Hercules Inc. Wilmington, Delaware, Cellulose gum, 1968.

68. Thiem, J.; Sievers, A.; Karl, H., *J. Chromat.* 130:305-13 (1977).

69. Henderson, M.E. Mechanisms of Alkaline Glycosidic Bond Cleavage in 1,5-Anhydro-4-O- β -Mannopyranosyl-D-Mannitol. Doctoral Dissertation. Appleton, WI, The Institute of Paper Chemistry, 1986. pp. 67-68.

70. Borchardt, L.G.; Piper, C.V. *TAPPI* 53(2):257-60 (1970).

71. Duckert, L.; Byers, E.; Thompson, N.S., *Cellulose Chem. Technol.* 22(1):29-37 (1988).

72. Hestrin, S., in "Methods in Carbohydrate Chemistry" (Whistler, ed.) Vol. III, Acad. Press, New York, 1963. pp. 4-9.

73. Haigler, C.H. Alteration of Cellulose Assembly in *Acetobacter xylinum* by Fluorescent Brightening Agents, Direct Dyes, and Cellulose Derivatives. Doctoral Dissertation. Chapel Hill, North Carolina, The University of North Carolina at Chapel Hill, 1982.

74. Benziman, M., Dept. Biol. Chem., Inst. Life Sciences, The Hebrew University of Jerusalem, Israel, Personal communication, 1986 and 1988.

75. Sandford, P.A.; Baird, J., in "The Polysaccharides" (G.O. Aspinall, ed.) Academic Press, New York, 1983, Vol. 2, pp. 411-490.

76. Philips Electronic Instruments, Inc. Instructions for Profile Fitting. Publication no. 4835.015.13900, Philips, Mahwah, NJ, June 1987.

77. Woitkovich, C.P., Institute of Paper Science and Technology, Atlanta, GA, Personal communication, 1989.
78. Hayat, M.A. Basic Techniques for Transmission Electron Microscopy, Academic Press, Orlando, 1986. pp. 266-70.
79. Frei, E.; Preston, R.D. Proc. Roy. Soc. B. 169:127-45 (1968).
80. Gast, J.C. A Nuclear Magnetic Resonance Study of the Glycosidic Linkage of the Xylo- and Cello-Oligosaccharides. Doctoral Dissertation. Appleton, WI, The Institute of Paper Chemistry, 1983.
81. Gorin, P.A.J., Can. J. Chem. 51:2375-83 (1973).
82. Isogai, A., Dept. Forest Products, Fac. Agriculture, Univ. Tokyo, Japan, Unpublished work, 1989.
83. Wiley, J.H. Raman Spectra of Celluloses. Doctoral Dissertation. Appleton, WI, The Institute of Paper Chemistry, 1986.
84. Boylston, E.K.; Hebert, J.J., J. Appl. Polym. Sci. 25(9):2105-7 (1980).
85. Wiley, J.H.; Atalla, R.H., Carbohydrate Research 160:113-29 (1987).
86. Harada, H.; Goto, T., in "Cellulose and Other Natural Polymer Systems: Structure, Biogenesis and Degradation" (Brown, R.M., Jr., ed.) Plenum, New York, 1982. pp. 383-401.
87. Hackney, J.M., U.S.D.A. Forest Products Laboratory, Madison, WI, Personal communication, 1989.
88. Ward, K., Jr., Textile Res. J. 20(6):363-72 (1950).
89. Howsmon, J.A.; Sisson, W.A., in "Cellulose and Cellulose Derivatives" (E. Ott, H.M. Spurlin, and M.W. Grafflin, eds.) Interscience Publishers, New York, 1954. Part I(IVB), pp. 231-347.

APPENDIX A
LIQUID STATE ^{13}C NMR SPECTRA

Table 14. ^{13}C NMR spectrum of mannan.

Position (ppm)	Intensity	Assignment ^{80,81}
60.818	strong	C6int
61.385		
61.858	weak	
62.429		
67.174	med-str	C4nred
68.743	weak	
69.893	weak	
70.101	weak	
70.356	strong	C2int
70.893		
71.093	weak	
71.608		
71.786	strong	C3int
73.086	weak	
73.348	weak	
73.535		
73.966	weak	
74.204	weak	
75.425	strong	C5int
76.652	strong	C4int
76.921	med-str	
77.966		
81.819	weak	
100.398	strong	C1int

int = internal carbohydrate moiety
nred = nonreducing end group

Table 15. ^{13}C NMR spectrum of xylan.

Position (ppm)	Intensity	Assignment ⁸⁰
59.586	medium	α -C5red
63.033	strong	C5int+ β -C5
71.328	medium	C4nred
72.067	med-str	
72.885	strong	C2int or C3int
74.305	strong	C3int or C2int
75.854	strong	C4int+ β C4
82.368	medium	
97.399	weak	β -C1red
100.822	weak	
101.910	strong	C1int+C1nred
176.766	medium	-COO ⁻

red = reducing end group

int = internal carbohydrate moiety

nred = nonreducing end group

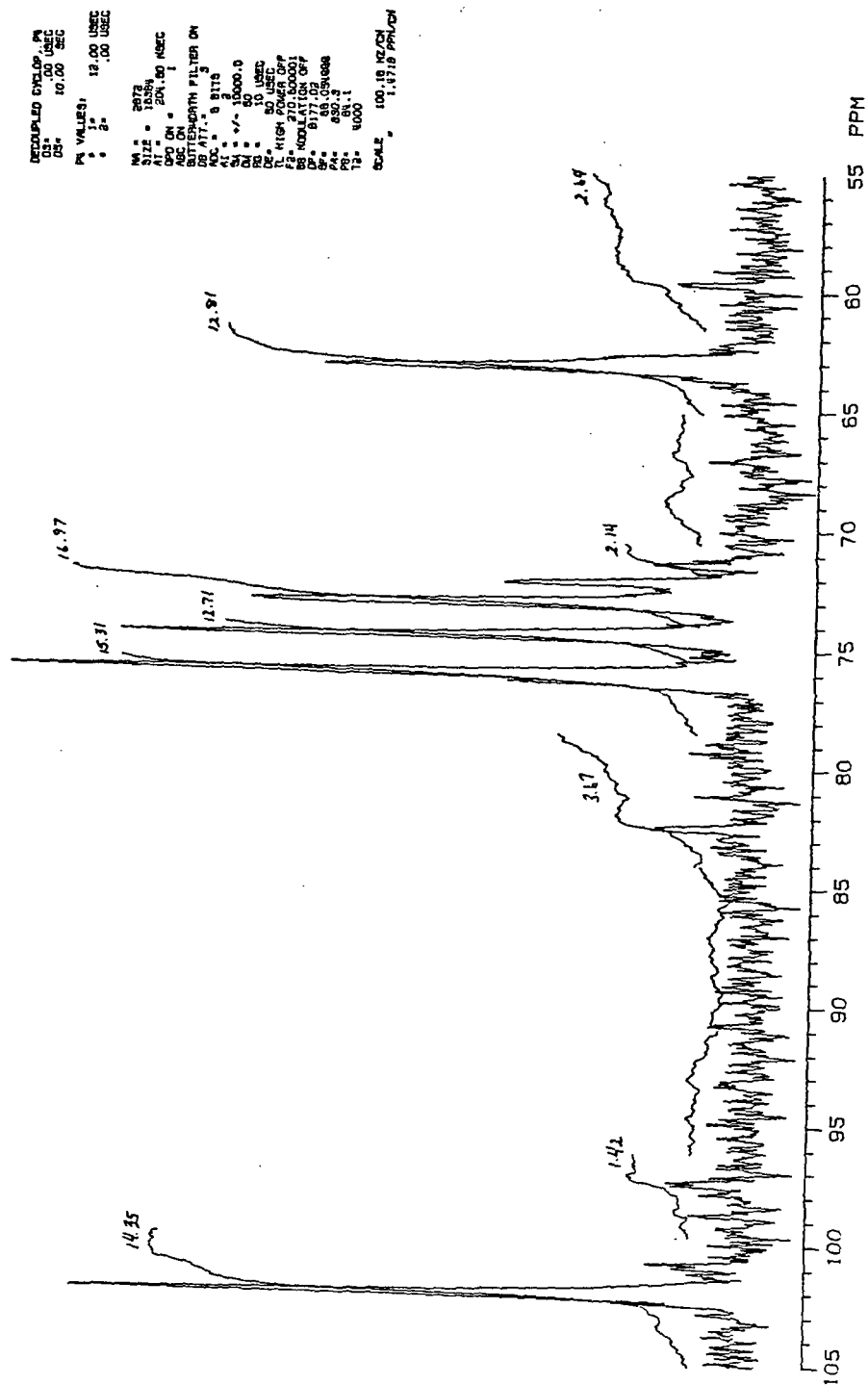


Figure 20. ^{13}C NMR spectrum of xylan.

APPENDIX B

X-RAY DIFFRACTOGRAMS AND PROFILE FITTING RESULTS

Table 16. X-ray diffractograms in this Appendix.

Diffractogram	Sample
Figure 21. Control cellulose	
ABX987.RD	before alkaline extractions
AB1074.RD	after 0.01 <u>N</u> NaOH extraction
AB1154.RD	after 0.1 <u>N</u> NaOH extraction
AB1194.RD	after 1.0 <u>N</u> NaOH extraction
Figure 22. Cellulose produced in CMC	
ACM981.RD	before alkaline extractions
CM1071.RD	after 0.01 <u>N</u> NaOH extraction
CM1151.RD	after 0.1 <u>N</u> NaOH extraction
CM1191.RD	after 1.0 <u>N</u> NaOH extraction
Figure 23. Cellulose produced in mannan	
NMA989.RD	before alkaline extractions
MA1075.RD	after 0.01 <u>N</u> NaOH extraction
MA1155.RD	after 0.1 <u>N</u> NaOH extraction
MA1195.RD	after 1.0 <u>N</u> NaOH extraction
Figure 24. Cellulose produced in xylan	
AXY985.RD	before alkaline extractions
XY1073.RD	after 0.01 <u>N</u> NaOH extraction
XY1153.RD	after 0.1 <u>N</u> NaOH extraction
XY1193.RD	after 1.0 <u>N</u> NaOH extraction
Figure 25. Cellulose produced in xyloglucan	
AXG983.RD	before alkaline extractions
XG1072.RD	after 0.01 <u>N</u> NaOH extraction
XG1152.RD	after 0.1 <u>N</u> NaOH extraction
XG1192.RD	after 1.0 <u>N</u> NaOH extraction

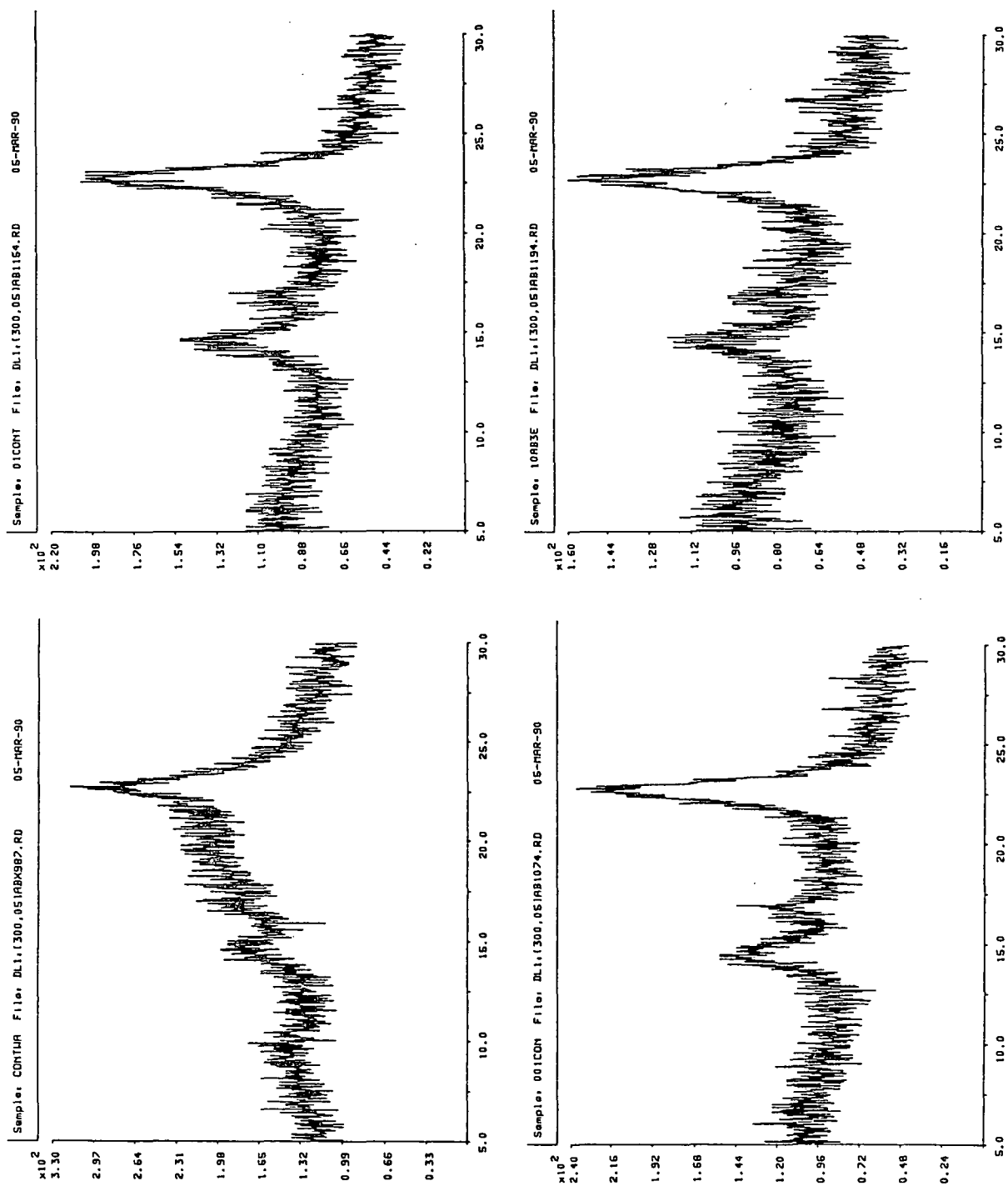


Figure 21. X-ray diffractograms of control celluloses.

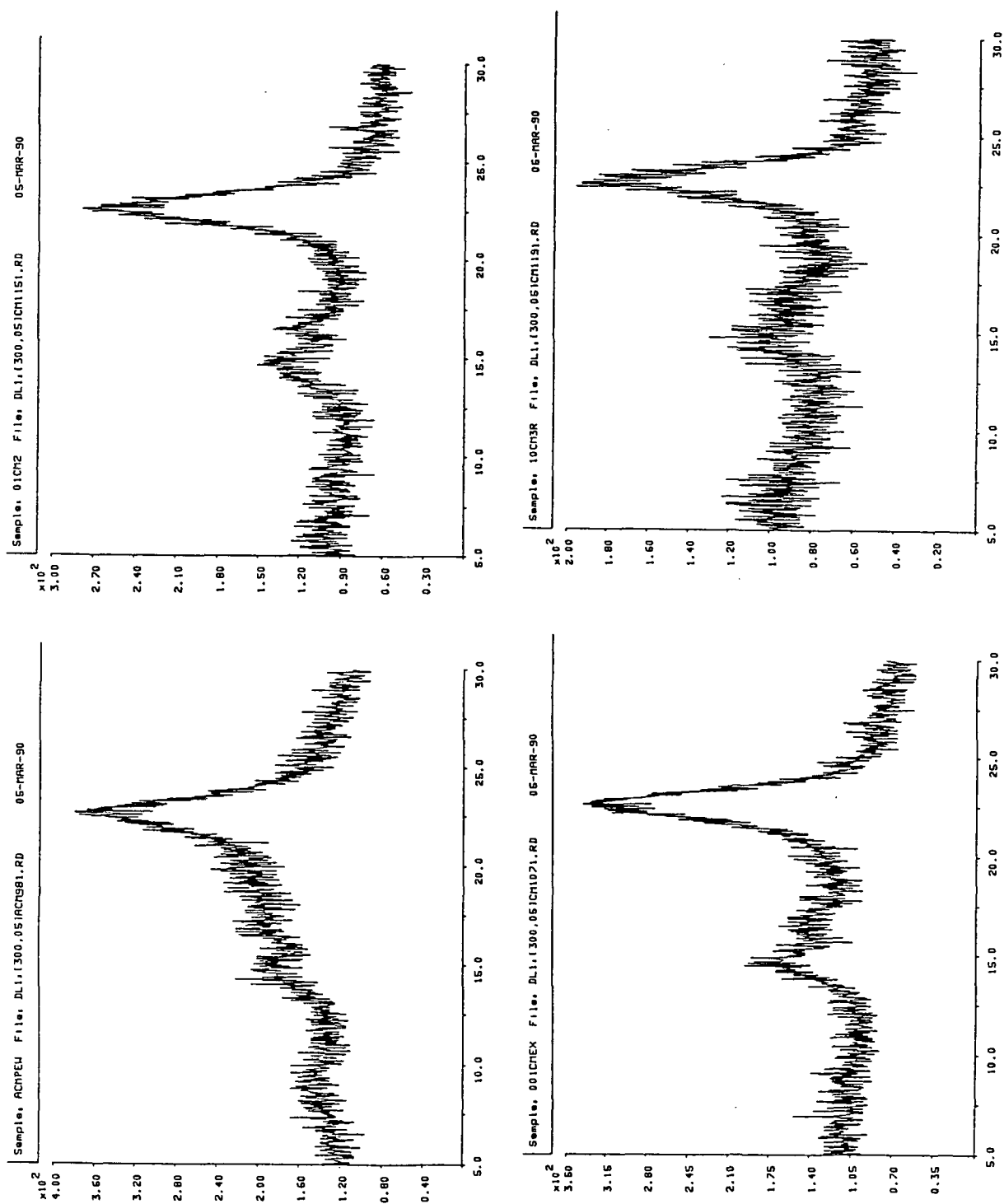


Figure 22. X-ray diffractograms of CMC-celluloses.

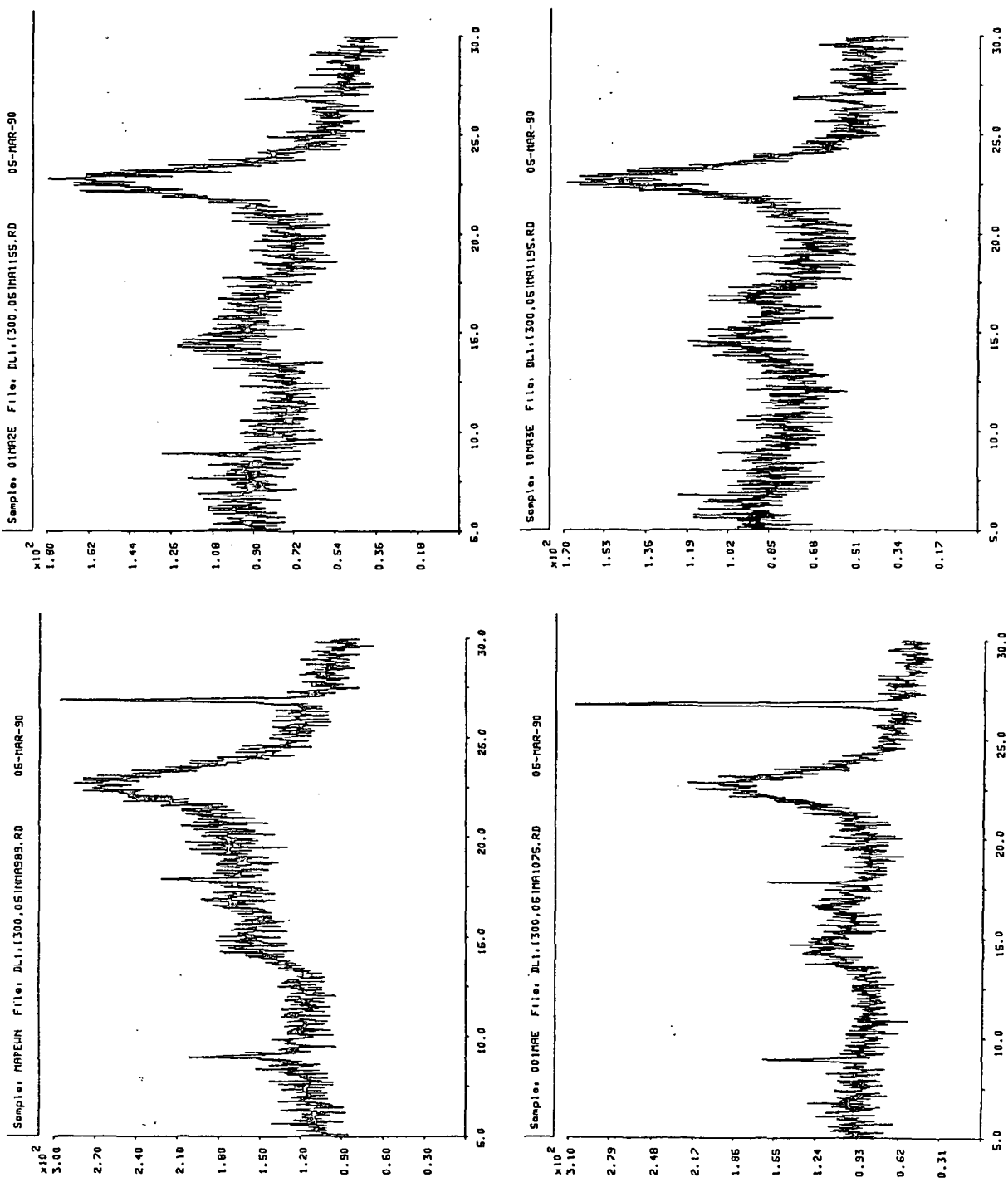


Figure 23. X-ray diffractograms of mannan-celluloses.

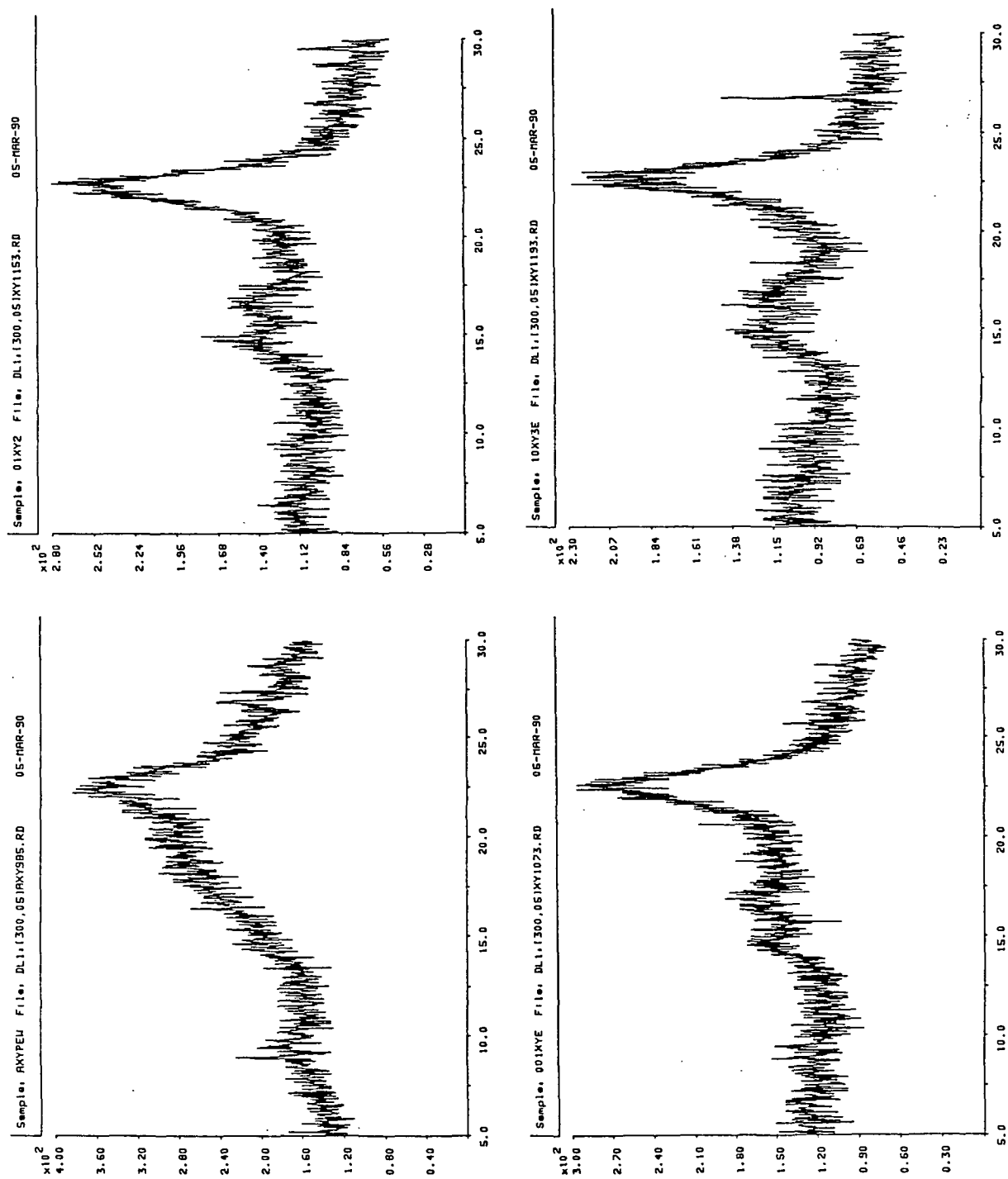


Figure 24. X-ray diffractograms of xylan-celluloses.

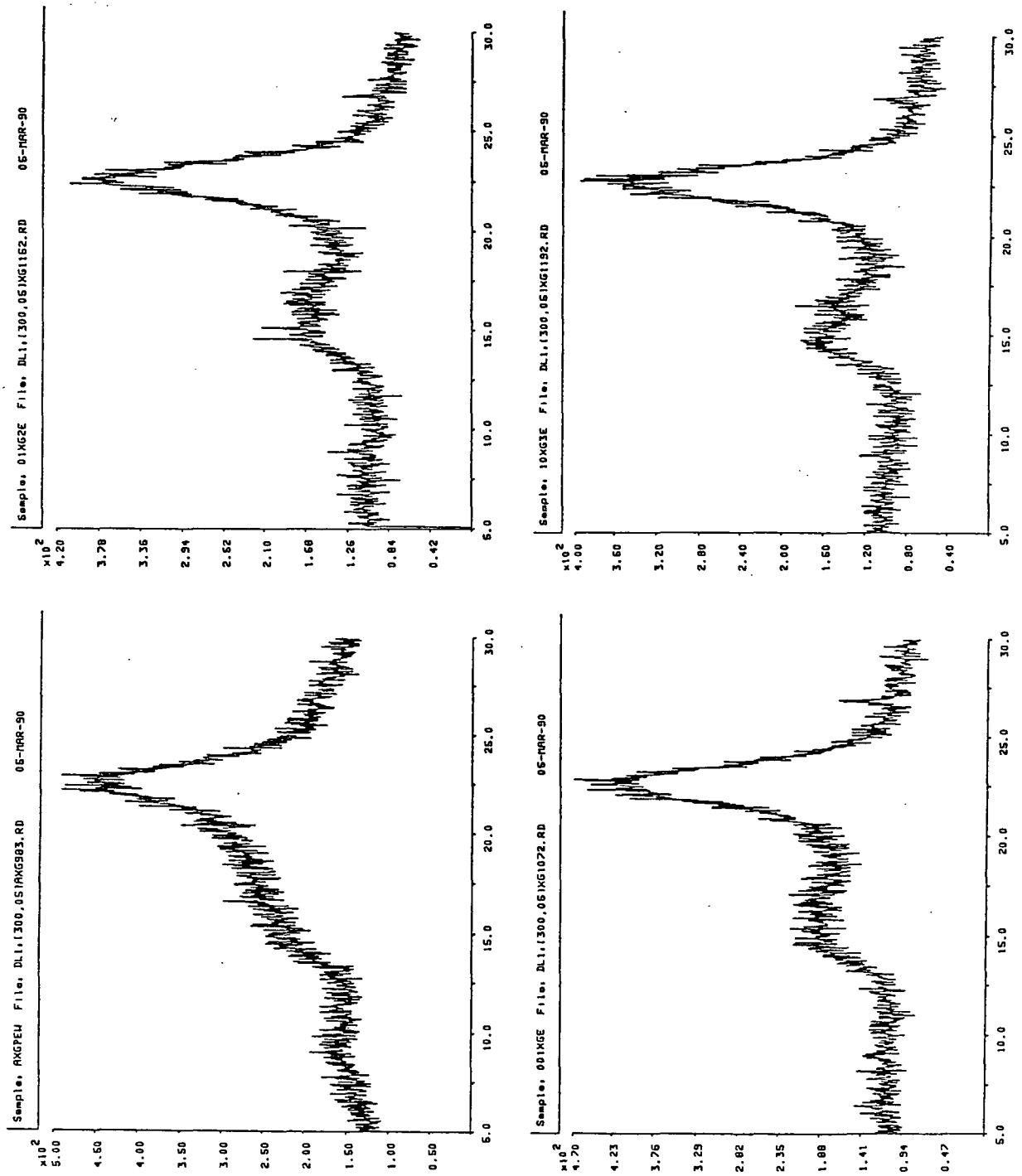
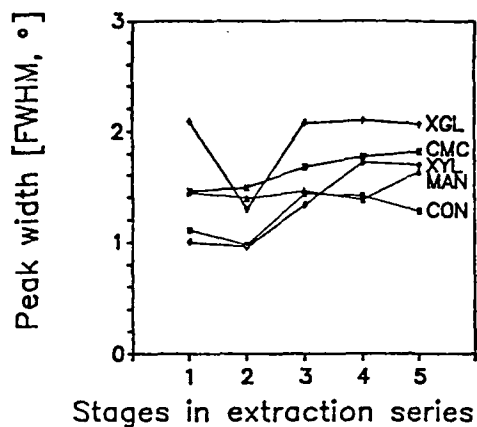
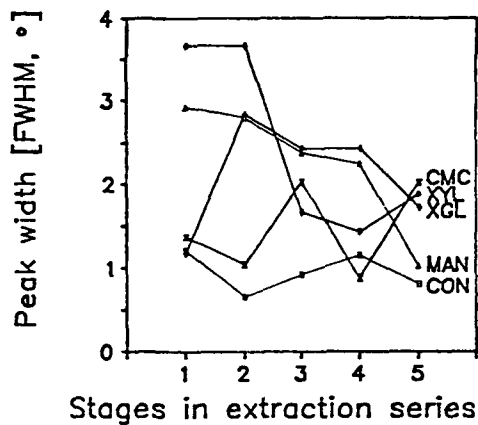


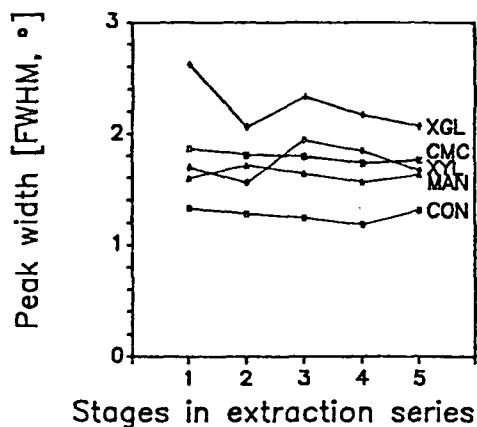
Figure 25. X-ray diffractograms of xyloglucan-celluloses.



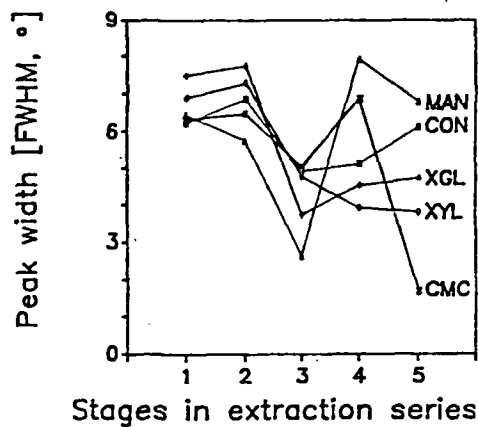
PEAK: (101)



PEAK: (101̄)



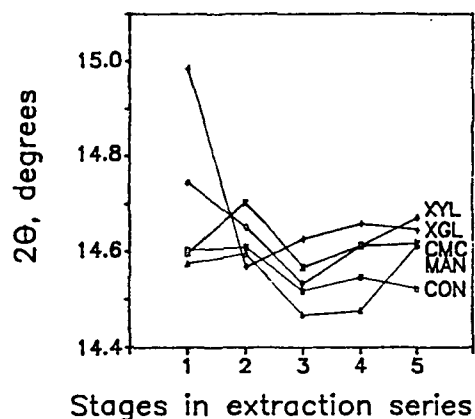
PEAK: (002)



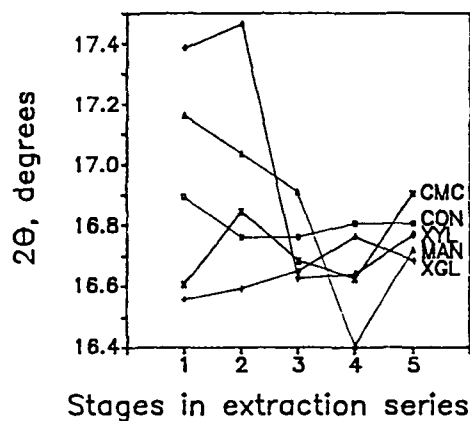
PEAK: AMORPHOUS

Stages in extraction series: 1. Starting material; 2. Water extraction; 3. 0.01 N NaOH; 4. 0.1 N NaOH; 5. 1.0 N NaOH.

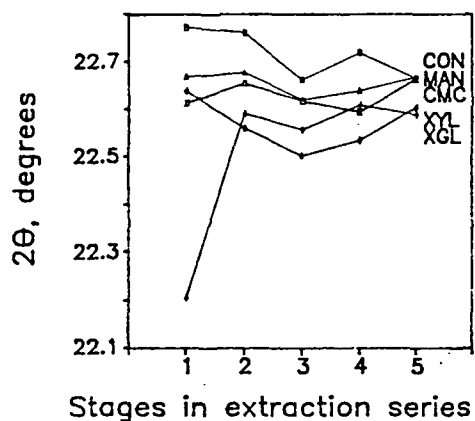
Figure 26. Peak width at half maximum of fitted x-ray peaks.



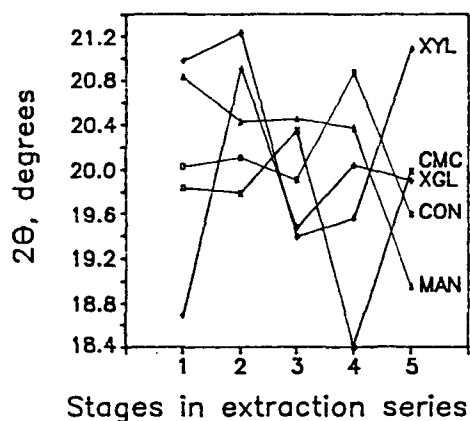
PEAK: (101)



PEAK: (101̄)



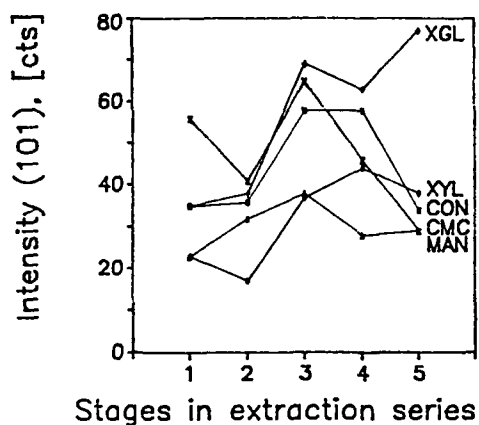
PEAK: (002)



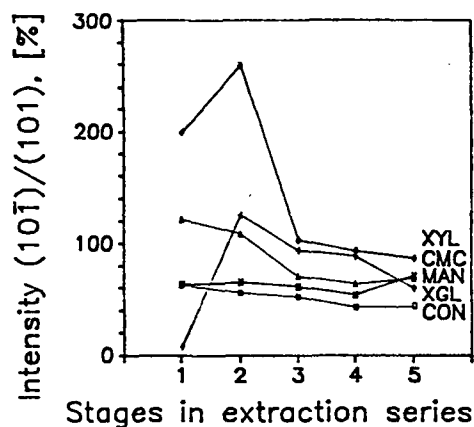
PEAK: AMORPHOUS

Stages in extraction series: 1. Starting material; 2. Water extraction; 3. 0.01 N NaOH; 4. 0.1 N NaOH; 5. 1.0 N NaOH.

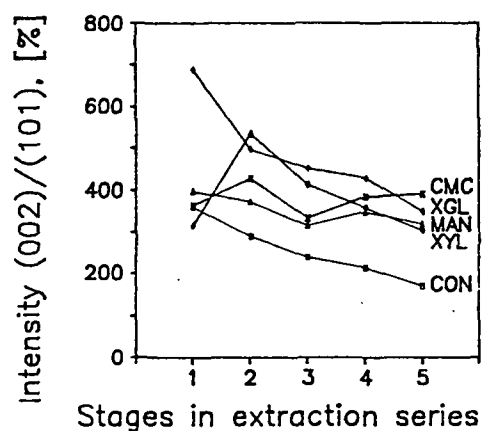
Figure 27. Peak positions of fitted x-ray peaks.



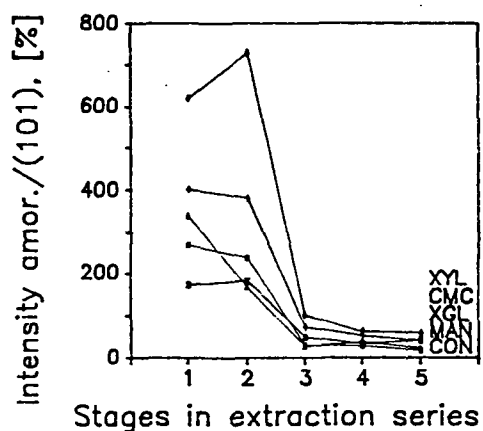
PEAK: (101)



PEAK: (101)



PEAK: (002)



PEAK: AMORPHOUS

Stages in extraction series: 1. Starting material; 2. Water extraction; 3. 0.01 N NaOH; 4. 0.1 N NaOH; 5. 1.0 N NaOH.

Figure 28. Peak intensities of fitted x-ray peaks.

APPENDIX C
RAMAN SPECTRA

Table 17. Raman spectra of the following samples in this Appendix.

Figure 29. Control cellulose

3875-98-7	before alkaline extractions
3875-107-4	after 0.01 <u>N</u> NaOH extraction
3875-115-4	after 0.1 <u>N</u> NaOH extraction
3875-119-4	after 1.0 <u>N</u> NaOH extraction

Figure 30. Cellulose produced in CMC

3875-98-1	before alkaline extractions
3875-107-1	after 0.01 <u>N</u> NaOH extraction
3875-115-1	after 0.1 <u>N</u> NaOH extraction
3875-119-1	after 1.0 <u>N</u> NaOH extraction

Figure 31. Cellulose produced in mannan

3875-98-9	before alkaline extractions
3875-107-5	after 0.01 <u>N</u> NaOH extraction
3875-115-5	after 0.1 <u>N</u> NaOH extraction
3875-119-5	after 1.0 <u>N</u> NaOH extraction

Figure 32. Cellulose produced in xylan

3875-98-5	before alkaline extractions
3875-107-3	after 0.01 <u>N</u> NaOH extraction
3875-115-3	after 0.1 <u>N</u> NaOH extraction
3875-119-3	after 1.0 <u>N</u> NaOH extraction

Figure 33. Cellulose produced in xyloglucan

3875-98-3	before alkaline extractions
3875-107-2	after 0.01 <u>N</u> NaOH extraction
3875-115-2	after 0.1 <u>N</u> NaOH extraction
3875-119-2	after 1.0 <u>N</u> NaOH extraction

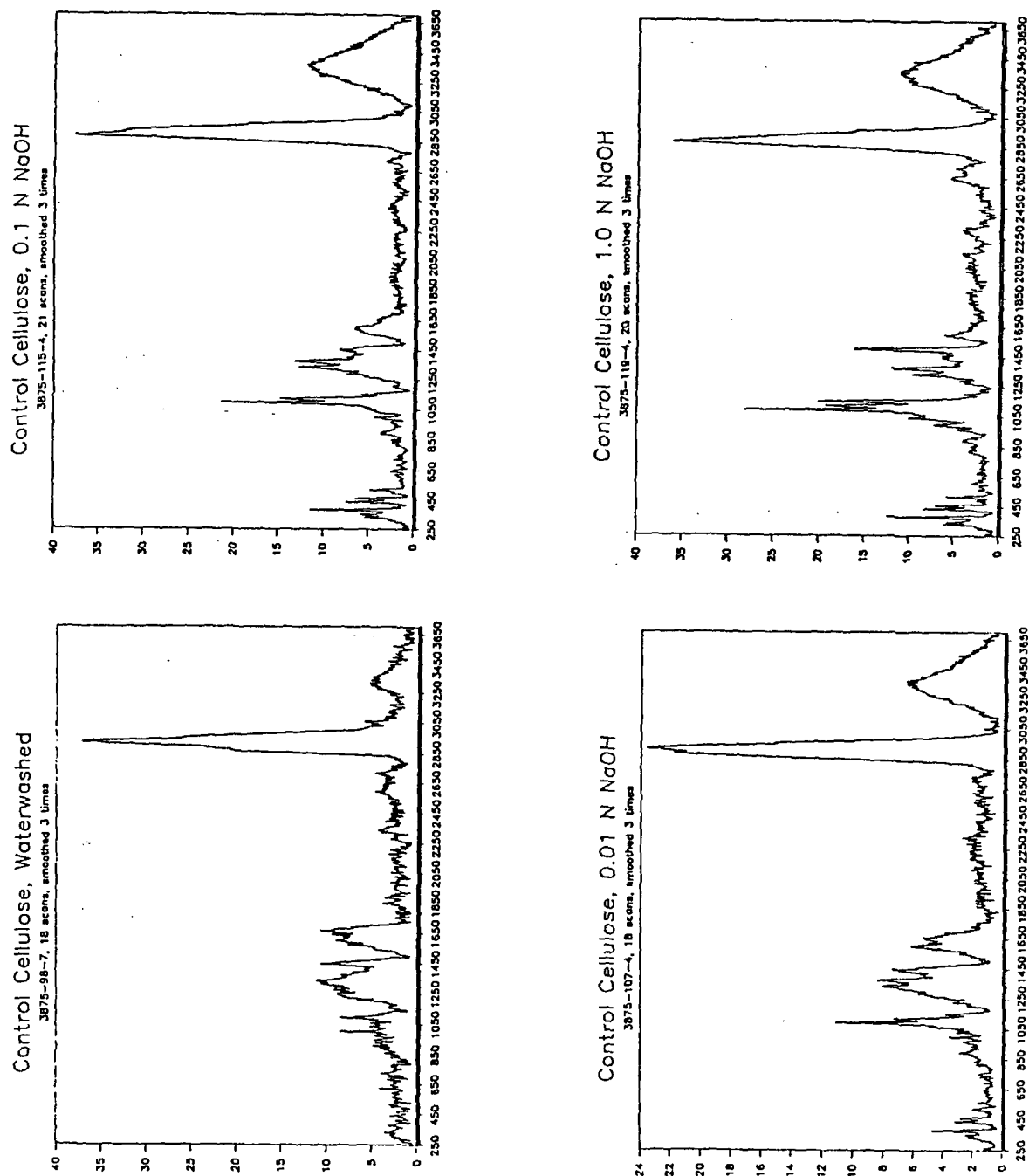


Figure 29. Raman spectra of control celluloses.

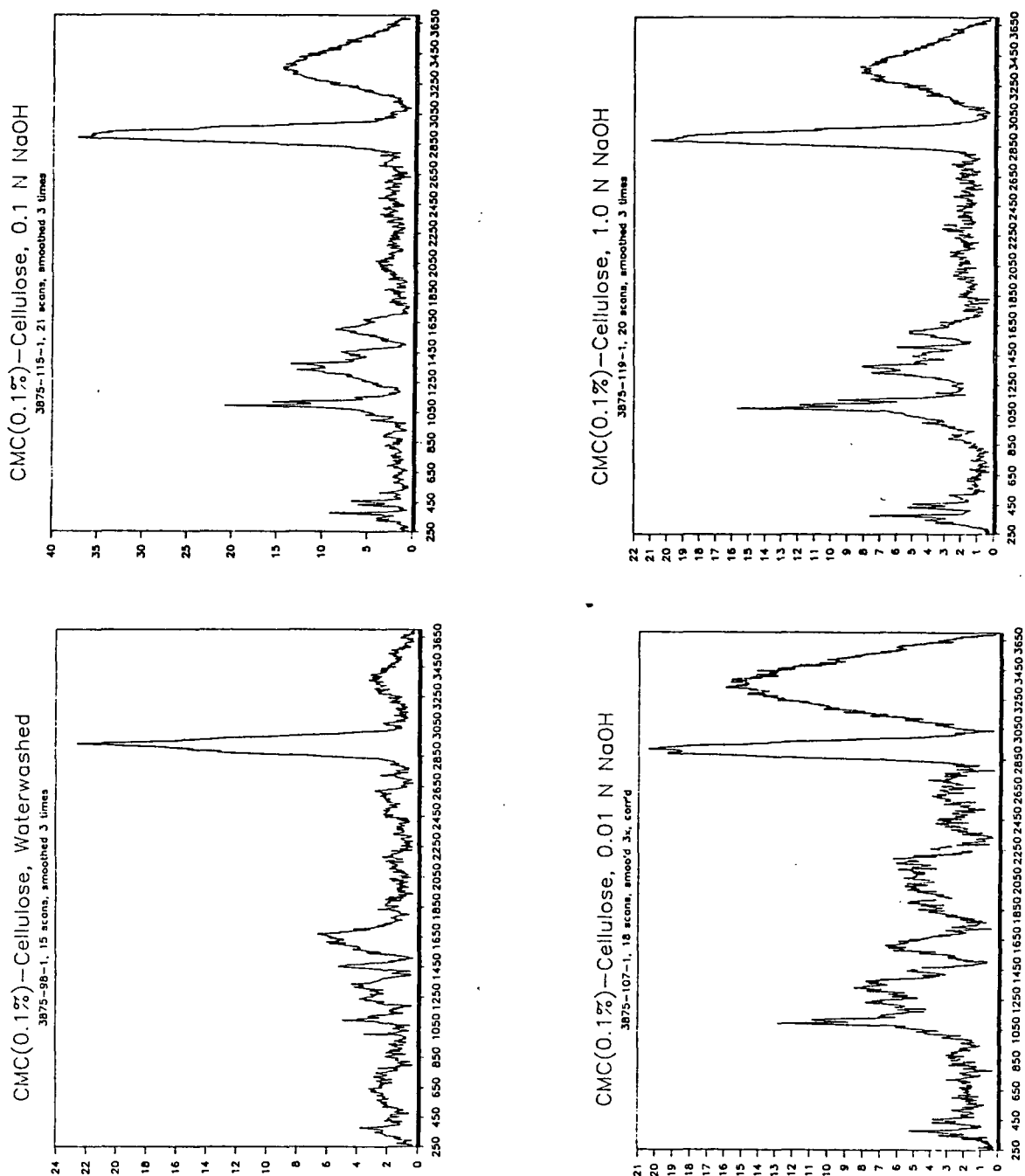


Figure 30. Raman spectra of CMC-celluloses.

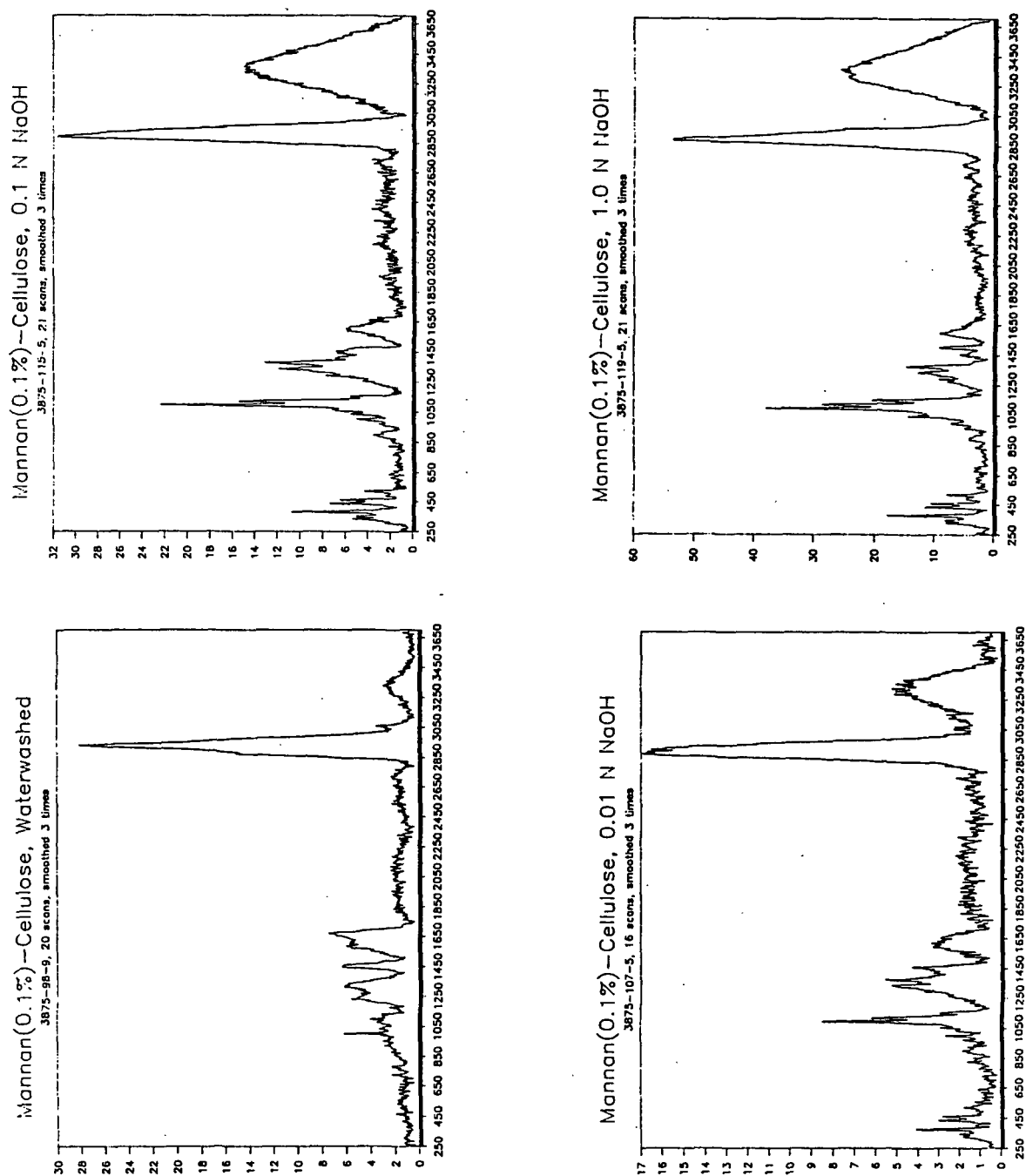


Figure 31. Raman spectra of mannan-celluloses.

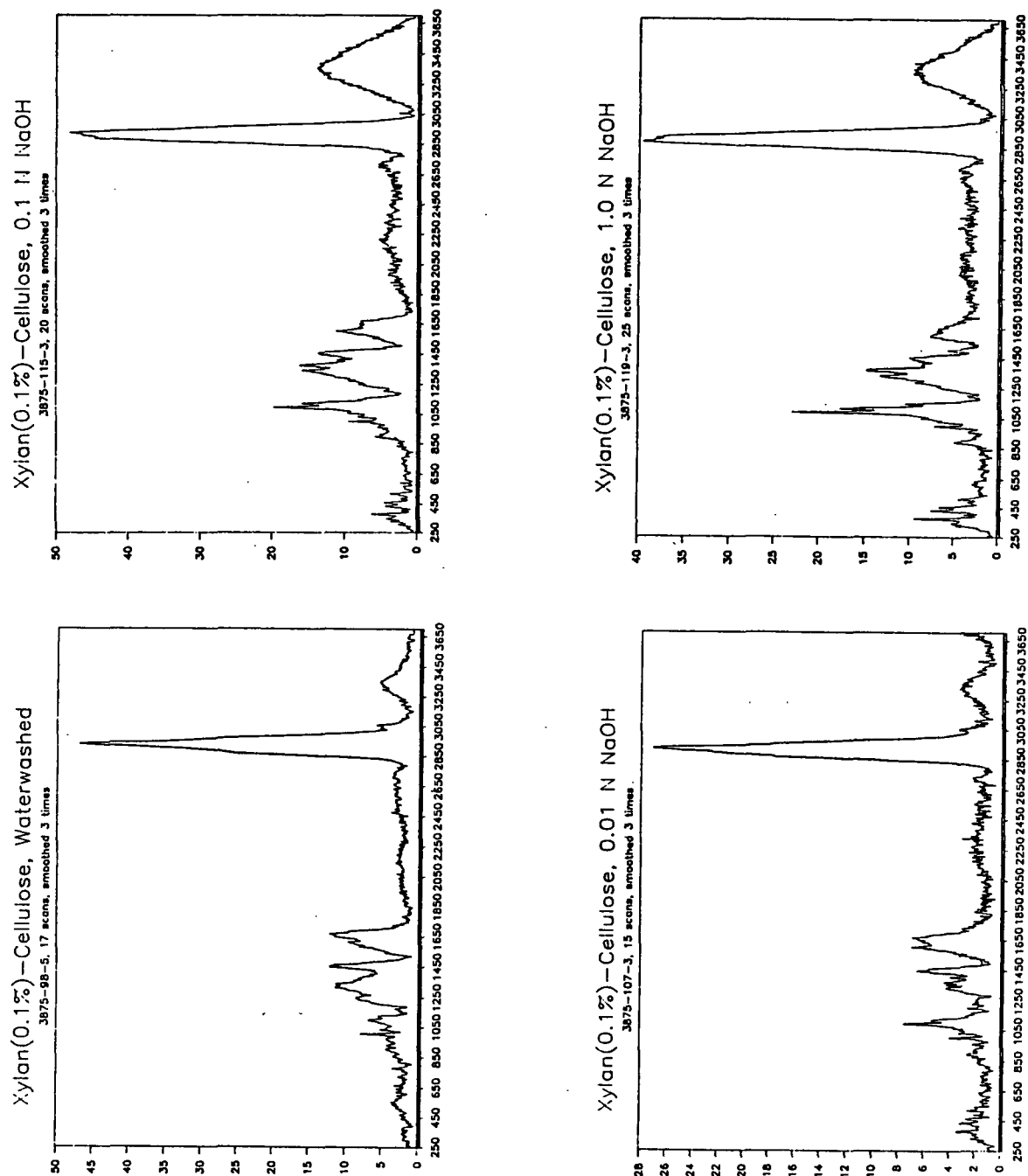


Figure 32. Raman spectra of xylan-celluloses.

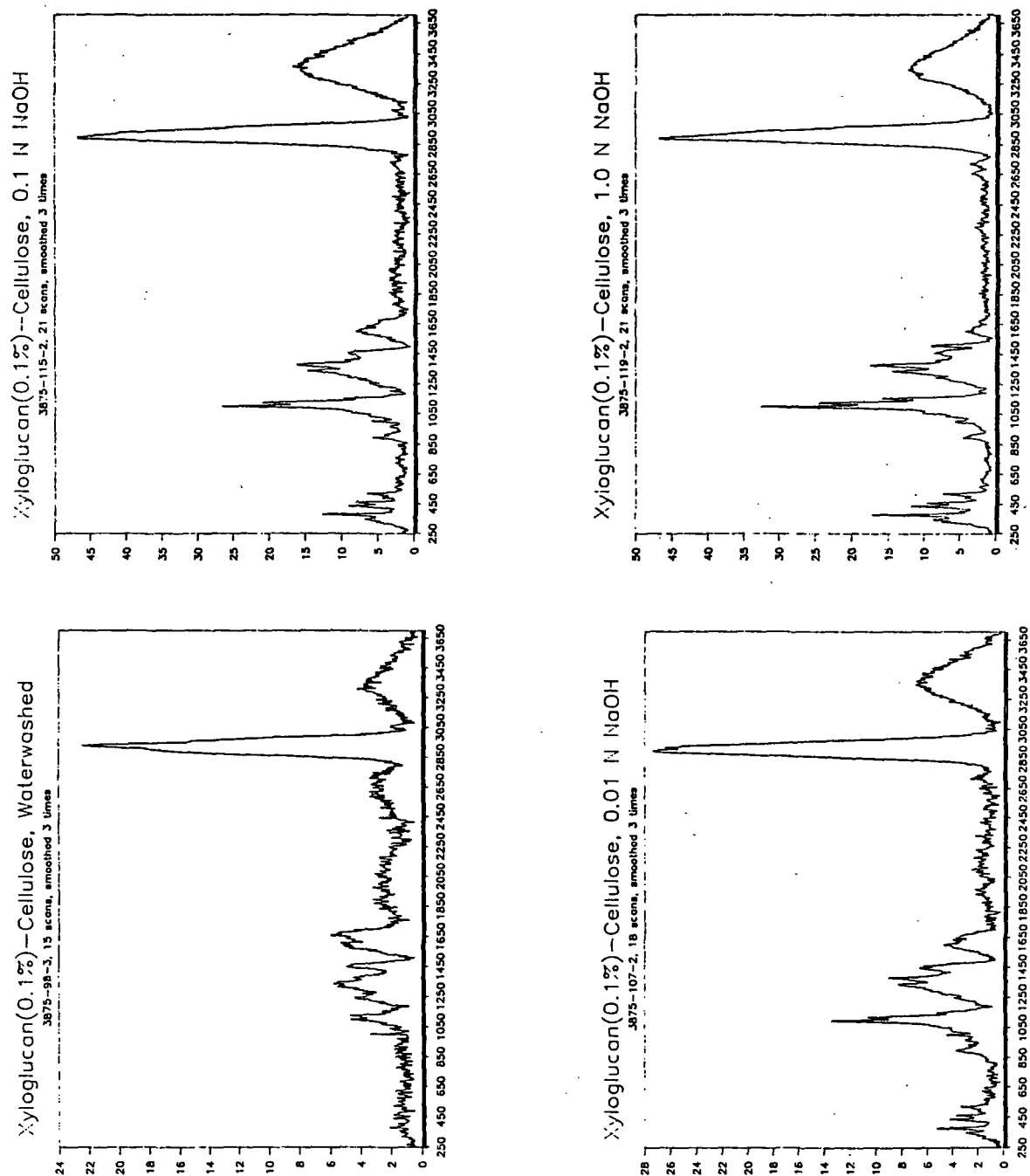


Figure 33. Raman spectra of xyloglucan-celluloses.

APPENDIX D

CONFORMATIONAL COMPONENT RESOLUTION OF RAMAN SPECTRA

COMPUTER PROGRAM USED FOR RESOLUTION OF RAMAN SPECTRA (From ref. 77)

```
5   REM Analysis of Raman spectrum for the composition of kI, kII, and k0.
6   REM Filename: ANA3COMP.BAS
10  DIM DTA(7500)
20  K = 0
30  L = 0
40  M = 0
50  N = 0
60  O = 0
70  P = 0
80  Q = 0
90  Q1 = 0
100 Q2 = 0
110 REM
120 OPEN "I",#1,"kI.prn"
140 FOR I = 0 TO 500
160 INPUT #1,DTA(I)
170 NEXT I
180 CLOSE #1
200 OPEN "I",#2,"kII.prn"
210 FOR I = 2048 TO 2548
220 INPUT #2,DTA(I)
230 NEXT I
240 CLOSE #2
300 OPEN "I",#3,"k0.prn"
310 FOR I = 4096 TO 4596
320 INPUT #3,DTA(I)
330 NEXT I
340 CLOSE #3
400 OPEN "I",#4,"unknown.prn"
410 FOR I = 6144 TO 6644
420 INPUT #4,DTA(I)
430 NEXT I
440 CLOSE #4
500 REM
510 REM
1110 FOR I = 0 TO 300
1120 A = DTA(I)
1130 B = DTA(I+2048)
1140 C = DTA(I+4096)
1150 Y = DTA(I+6144)
1160 D = A*A
1170 E = B*B
1180 F = C*C
1190 G = A*B
1200 H = A*C
1210 J = B*C
1220 J1 = A*Y
```

```

1230 J2 = B*Y
1240 J3 = C*Y
1250 K = K+D
1260 L = L+E
1270 M = M + F
1280 N = N + G
1290 O = O + H
1300 P = P + J
1310 Q = Q + J1
1320 Q1 = Q1 + J2
1330 Q2 = Q2 + J3
1340 NEXT I
1350 A1 = (L*M)-P*P
1360 A2 = (K*M)-O*O
1370 A3 = (K*L)-N*N
1380 A4 = (O*P)-(M*N)
1390 A5 = (N*P)-(L*O)
1400 A6 = (N*O)-(K*P)
1410 R = (K*L*M)+(2*N*O*P)-(P*P)*K-(O*O)*L-(N*N)*M
1420 S1 = (A1*Q)+(A4*Q1)+(A5*Q2)
1430 X1 = S1/R
1440 S2 = (A4*Q)+(A2*Q1)+(A6*Q2)
1450 X2 = S2/R
1460 S3 = (A5*Q)+(A6*Q1)+(A3*Q2)
1470 X3 = S3/R
1480 U = 0
1490 FOR I = 0 TO 300
1500 A = DTA(I)
1510 B = DTA(I+2048)
1520 C = DTA(I+4096)
1530 Y = DTA(I+6144)
1540 T = (Y-(X1*A)-(X2*B)-(X3*C))
1550 T1 = T*T
1560 U = U + T1
1570 NEXT I
1580 X1 = INT ((X1*1000)+.5)/1000
1590 X2 = INT ((X2*1000)+.5)/1000
1600 X3 = INT ((X3*1000)+.5)/1000
1610 V = (U/298)^.5
1620 W = ((A1/R)^.5)*V*1.96
1630 W1 = ((A2/R)^.5)*V*1.96
1635 W2 = ((A3/R)^.5)*V*1.96
1640 W = INT ((W*1000)+.5)/1000
1650 W1 = INT ((W1*1000)+.5)/1000
1660 W2 = INT ((W2*1000)+.5)/1000
1670 PRINT "KI = ";X1;"+";W
1680 PRINT "KII = ";X2;"+";W1
1690 PRINT "K0 = ";X3;"+";W2
1693 TOTAL = X1 + X2 + X3
1695 PRINT "TOTAL: ";TOTAL
1697 PRINT "SUM OF SQUARED ERRORS: ";U
1700 END

```

Table 18. Conformational components of bacterial celluloses.

	CON	CMC	MAN	XYL	XGL
k_I 0.01 <u>N</u>	0.73±0.05	0.38±0.04	0.59±0.04	0.38±0.04	0.44±0.04
k_I 0.1 <u>N</u>	0.77±0.03	0.69±0.04	0.67±0.02	0.51±0.04	0.51±0.03
k_I 1.0 <u>N</u>	0.73±0.02	0.58±0.03	0.56±0.02	0.50±0.02	0.58±0.02
k_{II} 0.01 <u>N</u>	-.07±0.16	0.06±0.15	-.23±0.14	0.11±0.15	-.10±0.12
k_{II} 0.1 <u>N</u>	0.04±0.11	-.12±0.12	-.06±0.08	0.16±0.13	0.03±0.09
k_{II} 1.0 <u>N</u>	-.05±0.08	-.01±0.09	-.02±0.08	-.06±0.08	0.09±0.06
k_0 0.01 <u>N</u>	0.31±0.15	0.53±0.14	0.62±0.13	0.43±0.15	0.62±0.12
k_0 0.1 <u>N</u>	0.17±0.10	0.41±0.12	0.37±0.08	0.30±0.12	0.45±0.09
k_0 1.0 <u>N</u>	0.32±0.07	0.43±0.08	0.43±0.07	0.55±0.07	0.33±0.06

CON: Control cellulose without additive; CMC: Cellulose produced with CMC; MAN: Cellulose produced with mannan; XYL: Cellulose produced with xylan; XGL: Cellulose produced with xyloglucan.

APPENDIX E
PHOTOMICROGRAPHS OF BACTERIAL CELLULOSE RIBBONS

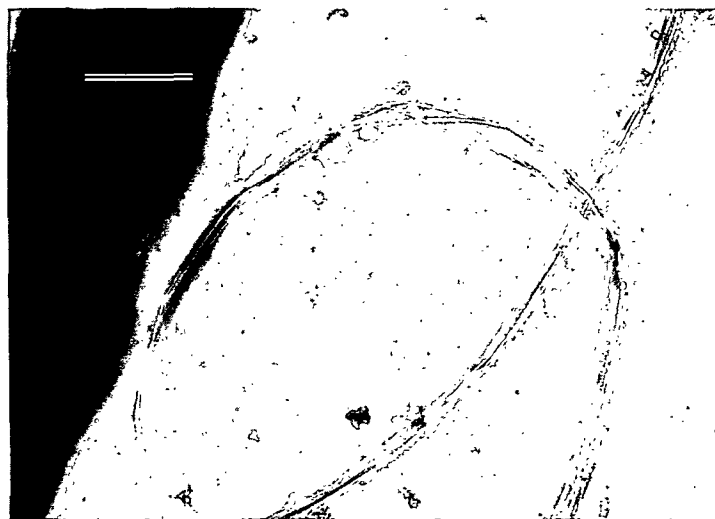


Figure 34. Photomicrographs of control cellulose; no. 2412, 2535, and 2538; scale bar: $0.3\mu\text{m}$, $\times 48,000$.

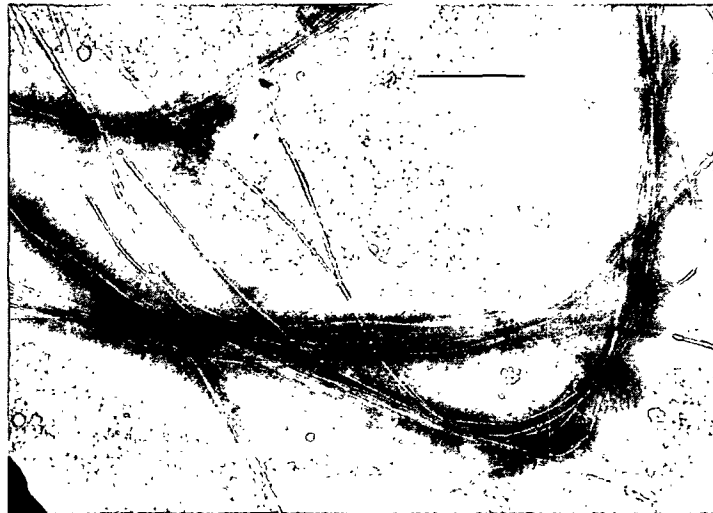


Figure 35. Photomicrographs of CMC-cellulose; no. 2441 and 2443: 0.8% CMC, no. 2446: 0.4% CMC; scale bar: $0.3\mu\text{m}$, X48,000.

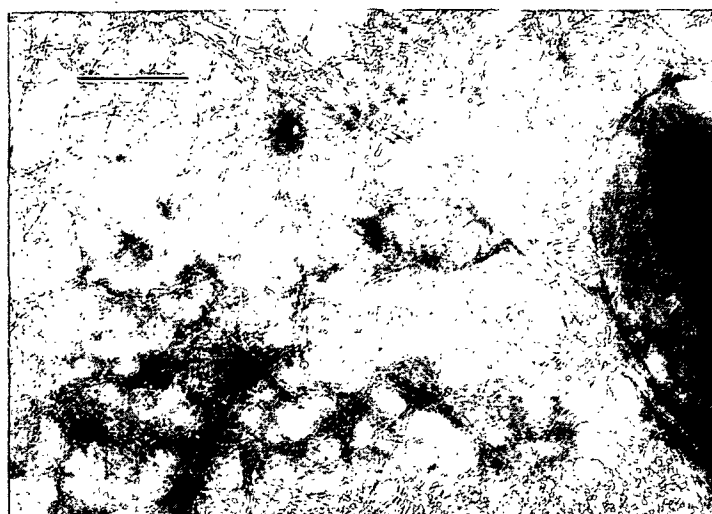


Figure 36. Photomicrographs of mannan-cellulose; no. 2489: 0.8% mannan, no. 2492: 0.4% mannan, and no. 2494: 0.1% mannan; scale bar: $0.3\mu\text{m}$, X72,000.



Figure 37. Photomicrographs of xylan-cellulose; no. 2452: 0.8% xylan, scale bar: 0.4 μm , X36,000; no. 2457: 0.4% xylan, and no. 2465: 0.1% xylan, scale bar: 0.3 μm , X48,000.

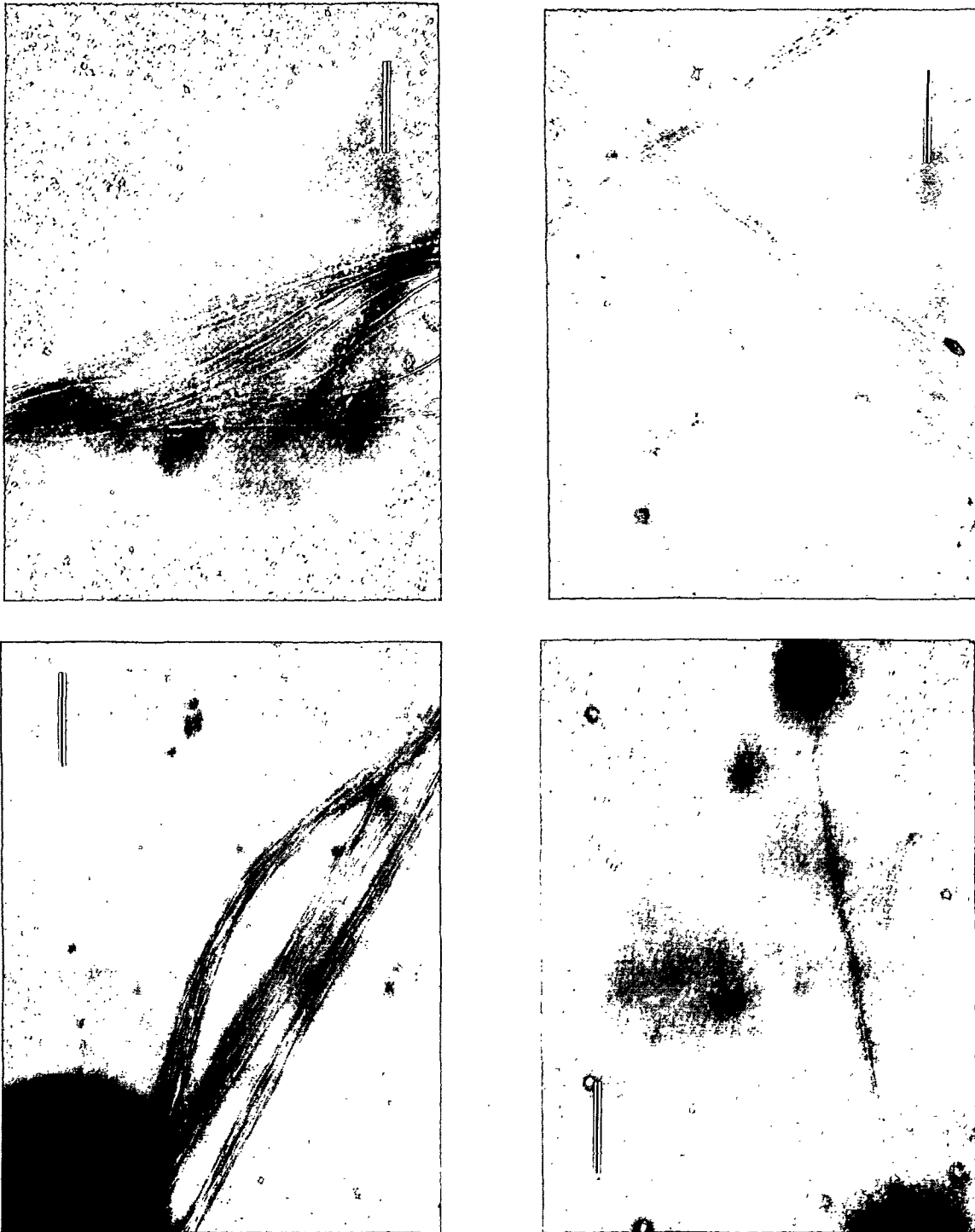


Figure 38. Photomicrographs of xyloglucan-cellulose; no. 2507 and 2509: 0.8% xyloglucan, no. 2514 and 2524: 0.1% xyloglucan; scale bar: 0.3 μm , X48,000.